N83 10520

Large-Area Silicon Sheet Task

A.D. Morrison, Chairman

Presentations were made by seven contractors and by JPL on silicon (Si) sheet efforts and related work.

Westinghouse Electric Corp. reviewed progress on the Si dendritic-web growth contract. A set of new computer models was used successfully to define a growth system configuration that was then built and used to grow web with lower thermally generated stress than has any configuration previously developed by empirical means.

Mobil Tyco Solar Energy Corp., which is conducting research on the edge-defined film-fed growth (EFG) method of making Si ribbon, reported that a significant increase in cell efficiency was demonstrated in large areas (50 cm^2) of ribbon grown at high speed (3.5 cm/min). The best cells gave 11.7% efficiency (AM1 and AR coated), just short of this year's goal of 12%.

In the Semix Inc. semicrystalline cast Si program, a technique was developed to determine base resistivity and carrier lifetime in semicrystalline wafers. Also, 100-cm^2 cells of 13.5% efficiency (AMI) were made in limited quantities.

Kayex Corp., which has just completed its effort on advanced Czochralski Si ingot growth, reviewed achievements since contract inception. These included automated growth of 150 kg of 15-cm-dia ingot material per crucible, with after-growth yields of greater than 90% at throughputs of 1.5 kg/h.

Cornell University reported on scanning transmission electron microscopy (STEM) and microprobe investigations of processed EFG ribbon. The following process-induced changes in the defect structure (as compared to unprocessed EFG ribbon) were noted:

(1) Processing introduces regularly spaced, sub-boundary-like dislocation arrays in the bulk (base section) of the material.

(2) Some (but not all) of the dislocation nodes in these networks act as nucleation centers for small ($d < 100$ Angstrom) precipitates.

(3) Large precipitates ($d \approx 1$ μm) are formed in the bulk of the material.

The chemical composition of the large precipitates was studied by non-dispersive X-ray analysis in a JEOL 200 CX STEM and by dispersive analysis (for C) in a JEOL 733 Superprobe. Elements identified were Ti, Fe, W, Mo, Cl, Ca and C. None of these elements were found in the matrix. It appears that the precipitates act as gettering centers for impurities. Cl is traceable to the Cl bakeout of the graphite dies.

The structural arrangement and the electrical activity of dislocations at or close to the central twin plane in processed material was studied by electron-beam induced current (EBIC) microscopy on a shallow-bevel specimen.

The majority of the dislocations in the twin plane are regularly spaced and mostly straight arrays of dislocation of like sign, accommodating a tilt component. Dislocation density in the twin plane is high, and the dislocations are effective recombination centers. Inspection of straight sections under higher magnification shows that the electrical activity varies along the dislocation, possibly due to precipitates (TEM will be carried out after completion of EBIC to clarify this point). Temperature-dependent EBIC is being carried out in order to determine the electronic energy levels associated with the various sections.

JPL in-house research program results were presented on the electrical and structural properties of grain boundaries in silicon, particularly those concerning electrical and enhanced diffusion along the grain boundaries.

Temperature-dependence measurements of zero-bias conductance, a photoconductivity technique, and deep-level transient spectroscopy (DLTS) were developed to investigate potential barrier, carrier recombination velocity, and electronic states, respectively. The studies of potential barrier have revealed that considerable variation in the activation energy along grain boundaries often exists, presumably due to variation of local disorders; the activation energy usually increases with annealing temperature, and the potential barrier decreases with increasing light intensity. The recombination velocity measurements show that the velocity increases with boundary state density and light intensity. The preliminary result from the DLTS experiments indicates a trend: the density of states generally increases with the distance from the edges of the band gap. However, the details vary considerably from sample to sample, a result that can be attributed to local variation of disorders.

A grooving and staining technique, secondary ion mass spectroscopy, and EBIC measurements in scanning electron microscopy were used to study enhanced diffusion of phosphorus at grain boundaries in polycrystalline silicon. The results shows that the enhanced diffusion occurs only at high-order grain boundaries having high carrier recombination and the depth of the enhanced diffusion varies drastically from boundary to boundary, making any quantitative measurement difficult unless the boundary can be characterized well.

The University of Illinois at Chicago is studying the fundamental mechanisms of abrasion and wear and the deformation of Si by a diamond in various fluid environments. The abrasion rates and depths of damage of <100> and <111> p-type Si in three fluid environments (acetone, ethanol, and water) were determined, and the surface deformation mechanism was found to change when the fluid was varied.

Applied Solar Energy Corp. presented results on the efficiency of solar cells made from EFG ribbon and Semix Inc. material. For EFG material, a baseline process was applied to ribbons grown with or without CO_2 in the ambient. In general, cells made from EFG ribbon grown in CO_2 performed better. However, the results from both groups were lower than those reported previously.

For the Semix material, work continued on Ingot 5848-13C. High-efficiency processes were applied and the results were presented. A series of more severe gettering schedules was performed on identified portions of the ingot. It was shown that short-circuit current improved with gettering up to a limiting value (which was still below that of the control cell). Light-biased diffusion length measurements showed that there was a negative light-biased effect (the minority carrier diffusion length decreased) that limited the improvement of short-circuit current in the more severely gettered cells. Also, the baseline process was applied to 10 x 10-cm Semix wafers randomly selected (not from a single ingot).

LARGE-AREA SILICON SHEET TASK

ORIGINAL PAGE IS
OF POOR QUALITY

ADVANCED DENDRITIC WEB GROWTH DEVELOPMENT

WESTINGHOUSE ELECTRIC CORP.

Technology Single crystal rib... growth	Report Date 04/21/82
Approach Silicon dendritic web growth **Contractor** Westinghouse Electric Corp. Research & Development Center JPL Contract 955843 **Goals** • Develop computer models for characterizing and understanding web growth • Develop experimental web growth machine for use with models • Demonstrate melt-replenished steady-state web growth • Demonstrate 25 cm^2/minute web growth rate • Demonstrate 5 cm web growth width	**Status** • First generation computer models developed and verified • Experimental web growth machine completed and operational • Melt-replenished steady-state web growth demonstrated at intermediate growth rate of 7 cm^2/min • Web growth rate of 27 cm^2/minute demonstrated under transient conditions • Growth width To 5 cm demonstrated

Program Emphasis

- Deformation Is Major Limitation Of Ribbon Width And Throughput Rate
- Deformation Is Correlated To Thermally Generated Stress
- Computer Models Provide Understanding Of Web Growth And Thermal Requirements For Stress Reduction And Optimized Throughput

Principal Activity

- **Develop Computer Models For Web Growth**
- **Develop Experimental Web Growth Machine Capable Of Automated, Melt-Replenished, Steady-State Growth**
- **Utilize Computer Models And Experimental Growth Machine For Development Of Advanced Web Growth**

Computer Models to Characterize Web Growth

- **Compute Web Temperature Distribution Generated By A Specified Growth Configuration**
- **Compute Thermal Stress Generated By A Specified Web Temperature Distribution**
- **Compute The Critical Buckling Conditions For A Specified Thermal Stress**

Application of Computer Models

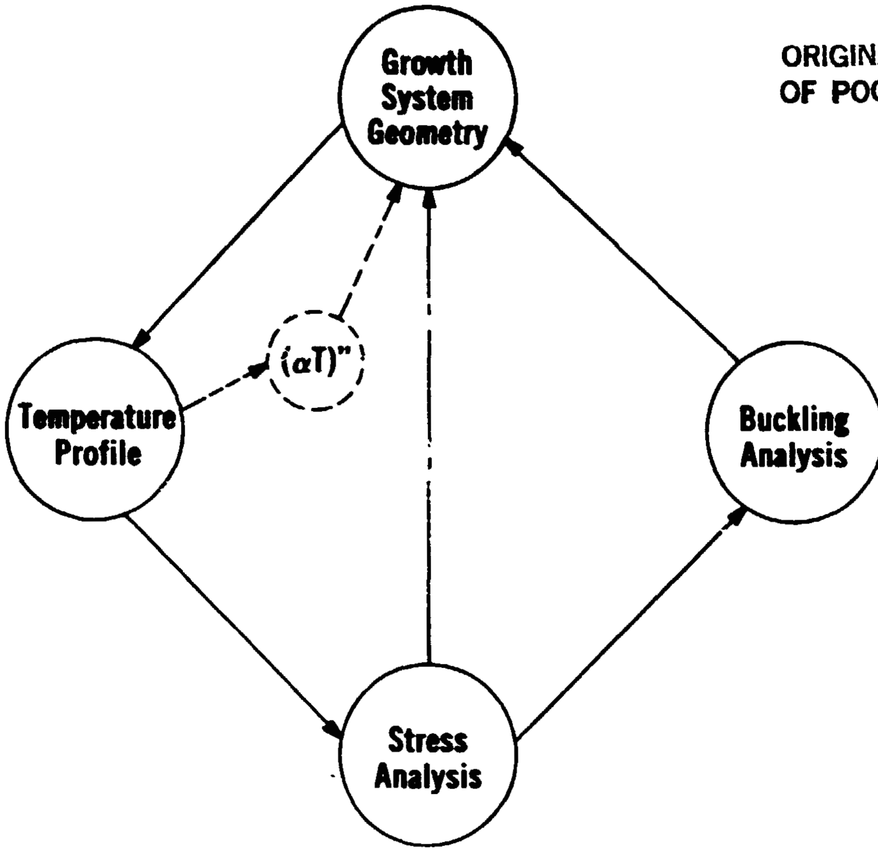

Status of Computer Models

- **Web Temperature Model Has Been Expanded To Be More Definative And Has Been Verified As Adequate For Next Generation Of Increased Web Throughput**
- **Thermal Stress Model Is Complete And Verified**
- **Critical Buckling Model Is Complete And Verified**

Viewing Regions From a Point on the Web

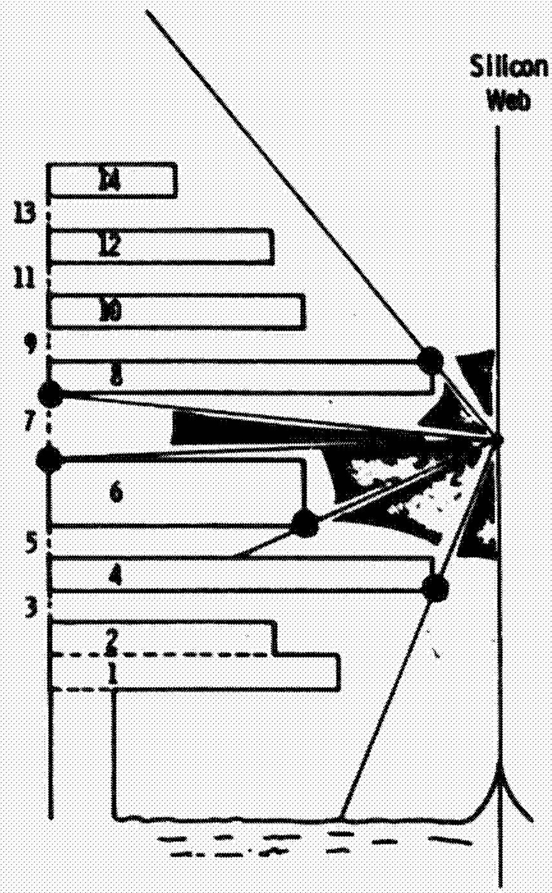

Steady-State Web Growth Is Necessary

- **For Process Analysis, Understanding And Improvement**
- **For Subsequent Process Standardization**

Experimental Web Growth Machine Provides Basic Requirements for Automated Steady-State Growth:

- **Flat Temperature Profile In Growth Region Of Melt**
- **Controlled Constant Temperature**
- **Controlled Constant Melt Level**
- **Controlled Constant Thickness**
- **Controlled Constant Width**

Dendritic Web Experimental Sheet Growth Unit (ESGU)

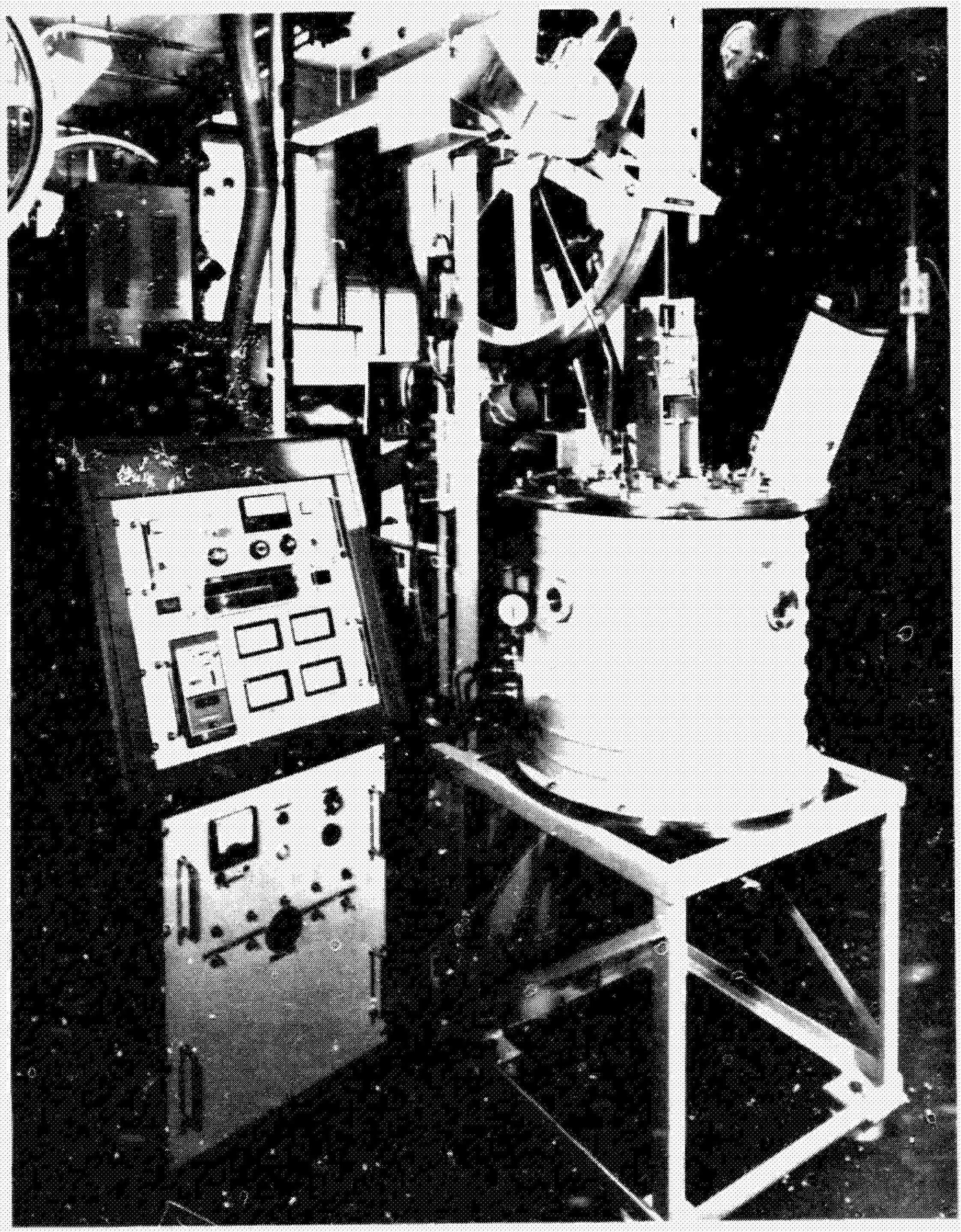

Combined Use of Models and Experimental Web Growth

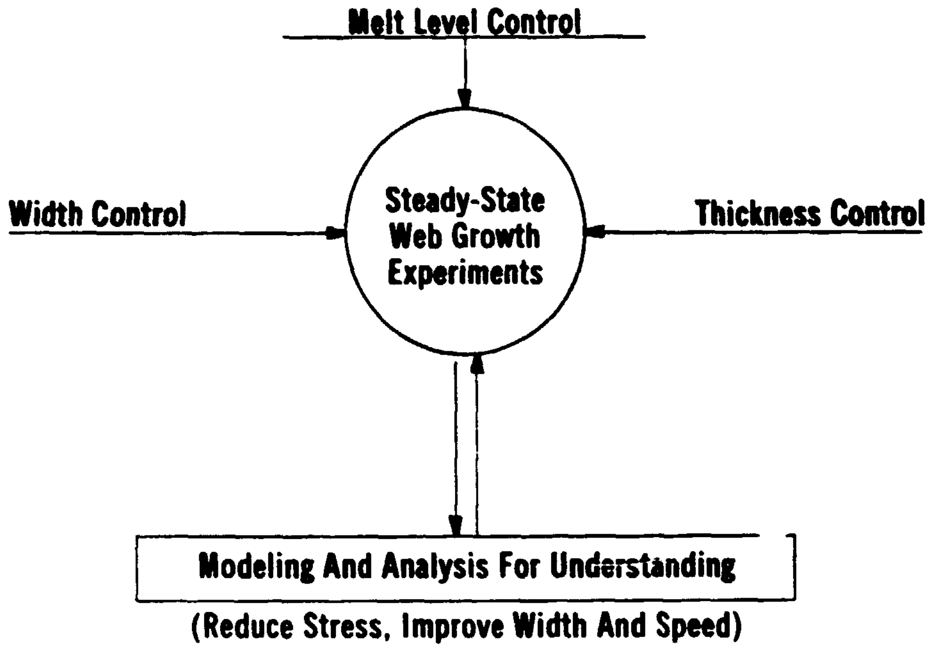

Results of First Use of Models

- **In First Application Models Were Verified By Comparison With A Previously Characterized Growth Configuration. The Model Identified System Limitations And Suggested Modifications Which Resulted In Width Increase Of 25% (To 5 cm)**
- **Automated Steady-State Web Growth Achieved At Intermediate Rate (7 cm^2/minute)**
- **Use Of Models Proven As Route For Understanding And Improvement Of Web Growth**

Problems and Concerns

- **Present** - **None. Understanding And Improvement Of Process Proceeding As Planned**
- **Future** - **Availability Of Low-Cost Polysilicon In Pellet Form**

Summary

- **Computer Models Of Web Growth Completed And Verified**
- **Experimental Web Growth Machine Proven In Automated Steady-State Growth**
- **Web Growth Improved By Application Of Models**

LARGE-AREA SILICON SHEET TASK

ORIGINAL PAGE IS
OF POOR QUALITY

EDGE-DEFINED FILM-FED GROWTH

MOBIL TYCO SOLAR ENERGY CORP.

TECHNOLOGY	REPORT DATE
LARGE AREA SILICON SHEET BY EFG	4/21/82
APPROACH MULTIPLE GROWTH OF 10 CM WIDE SILICON RIBBON AT 4 CM/MINUTE. **CONTRACTOR** MOBIL TYCO SOLAR ENERGY CORPORATION **GOALS** • REDUCE STRESS AND IMPROVE FLATNESS OF RIBBON GROWN AT 4 CM/MINUTE AND 200 μM THICKNESS. • DEMONSTRATE 12% CELL EFFICIENCY ON LARGE AREAS (50 CM^2) FOR RIBBON GROWN IN HIGH SPEED SYSTEM. • DESIGN, CONSTRUCT AND OPERATE NEW MULTIPLE RIBBON FURNACE FOR GROWTH OF FOUR 10 CM WIDE RIBBONS.	**STATUS** • CARTRIDGE DESIGN CHANGES HAVE REDUCED RIBBON STRESS AND BUCKLING LEVELS FOR 200 μM THICK RIBBON TO LEVEL WHERE FABRICATION OF LARGE AREA CELLS IS POSSIBLE. • LARGE AREA (50 CM^2) CELLS OF 11.7% (AM1 AND AR COATED) HAVE BEEN ACHIEVED FOR RIBBON GROWN IN HIGH SPEED SYSTEM (AT 3.5 CM/MINUTE). • NEW MULTIPLE RIBBON FURNACE HAS BEEN BUILT AND TESTED (OPERATION HAS BEEN SET ASIDE DUE TO REDUCTION OF PROGRAM).

Progress in Stress Studies

- INFLUENCE OF CARTRIDGE COMPONENT DESIGN ON STRESS AND BUCKLING LEVELS IN 10 CM WIDE RIBBON HAS BEEN IDENTIFIED:
  - TEMPERATURE FIELDS IN LINEAR COOLING PLATES OF SEVERAL DIFFERENT DESIGNS HAVE BEEN MEASURED.
  - IMPROVED FLATNESS WAS ACHIEVED IN 200 μM THICK RIBBON GROWN WITH A MODIFIED DESIGN CARTRIDGE.
  - CHANGE IN HORIZONTAL ISOTHERM SHAPE IS PROBABLE CAUSE FOR REDUCED STRESS AND BUCKLING LEVELS.

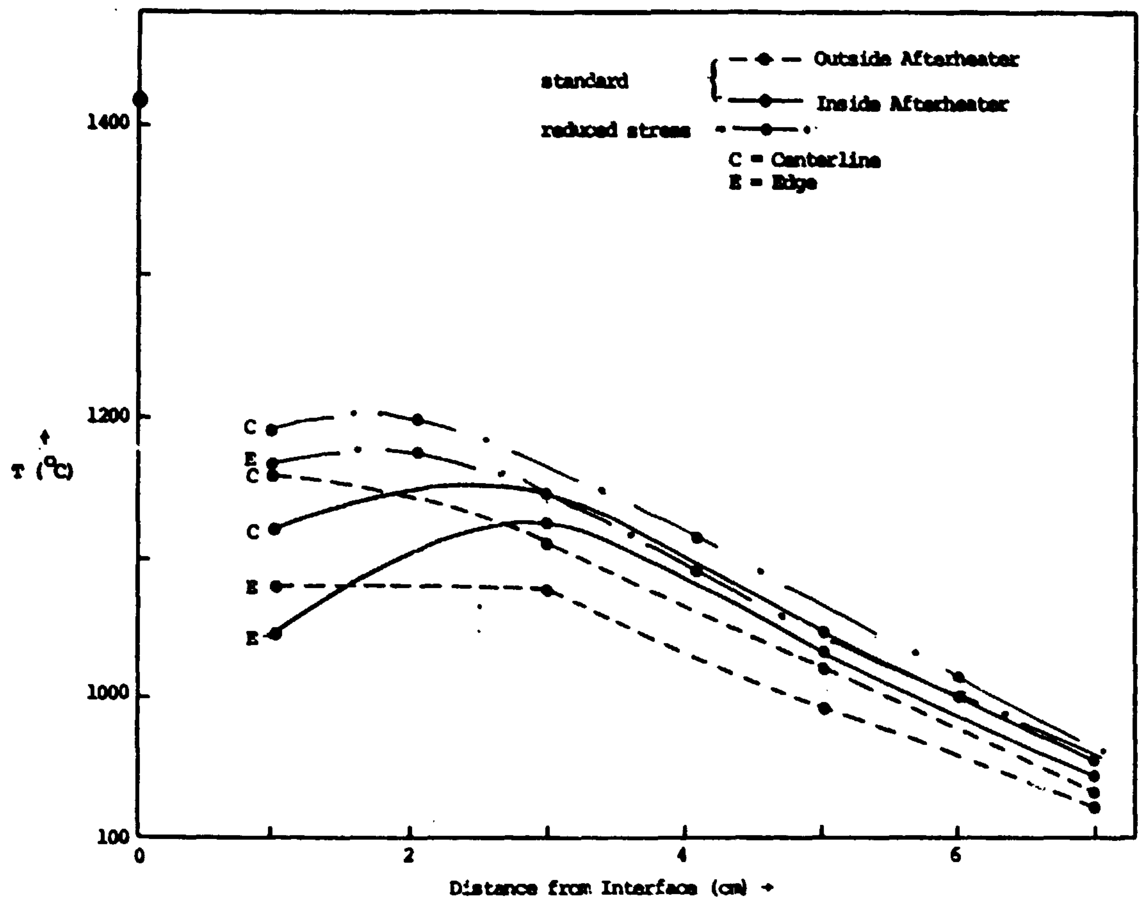

Comparison of center and edge temperature profiles in 10 cm cartridge linear cooling plates.

Stress Studies: Plans

- CAPABILITY IS NEEDED TO PREDICT: (I) MOVING RIBBON TEMPERATURE PROFILES GIVEN SYSTEM COMPONENT TEMPERATURES AND GEOMETRY, AND (II) STRESS DISTRIBUTIONS AND BUCKLING THRESHOLDS FROM RIBBON TEMPERATURE FIELDS.
- EMPIRICAL APPROACH WILL: (I) GUIDE THEORETICAL STUDIES AND ESTABLISH BOUNDARY CONDITIONS FOR MODELING, AND (II) ARRIVE AT REDUCED STRESS GROWTH CONFIGURATIONS THAT ARE COMPATIBLE WITH ACCEPTABLE GROWTH CONDITIONS AT 4 CM/MIN.

IMPORTANT TO SYNTHESIZE OUT OF THIS APPROACH A SYSTEM THAT WILL PRODUCE 200 μM THICK RIBBON AT 4 CM/MIN WITH SUFFICIENTLY LOW STRESS AND FLATNESS TO MEET DEMANDS IN YIELD AREA.

Progress in Quality Improvement

- SIGNIFICANT IMPROVEMENT IN CELL EFFICIENCY OF HIGH SPEED GROWN RIBBON TO 11-12% HAS BEEN ACHIEVED.
  - AMBIENT CONTROL HAS PROVEN TO BE VERY IMPORTANT PARAMETER IN OBTAINING CONSISTENT ELECTRONIC QUALITY RIBBON.
  - RIBBON EXIT GAS SEAL, MORE UNIFORM INTERFACE GAS CONTROL SYSTEMS IMPLEMENTED SUCCESSFULLY.

SPV Diffusion Length Data for 10 cm Wide Ribbon Grown with Stretched Cartridge in Machine 17. Bulk Melt Doping was 4 Ω-cm for All Runs.

Run No. and Segment	M.Z. Argon Flow Rate (ℓ/minute)	Cartridge Gas Composition	Cartridge Gas Flow Rate (ℓ/minute)	Gas Seal	Speed (cm/minute)	L_D (μm)
17-199-1A	10	argon	1.5	no	3.0 - 3.2	23.0
-1C					3.8	35.0
17-200-1A	6	argon	1.0	no	3.5	33.0
-1D		0.45% CO_2 + 45 ppm O_2	1.8		3.8 - 3.9	43.0
17-201-1B	6	argon	1.0	yes	3.3	33.0
-1D	3				3.3 - 3.4	30.0
17-202-1A	3	argon	1.0	yes	3.5 - 3.6	43.0
-1B	2				3.8	39.0
-1C	2				3.8	52.0
-1D	0				3.8	36.0
17-203-1A	6	argon	1.0	yes	3.3	41.0
-1C		0.17% CO_2 + 18 ppm O_2	1.2		3.5	45.0
17-204-1A	6	argon	1.0	yes	3.5	49.0
-1C		0.29% CO_2 + 29 ppm O_2	1.4		3.5	36.0
17-205-1B	6	0.17% CO_2 + 17 ppm O_2	1.2	yes	3.5	45.4

Solar Cell Data for Phosphine Processed Large Area (50 cm^2)
Solar Cells Made from 10 cm Wide Ribbons.
100 mW/cm^2, Xenon Light, 28°C, AR Coated.

Run No.	Growth Ambient	Speed (cm/min)	Average Resistivity (Ω-cm)	Diffusion Length (μm)	Cell Parameters J_{sc} (mA/cm^2)	V_{oc} (V)	FF	η (%)	Mean η (%)
17-143	0.2% CO_2	2.5	1.5	27	26.5	0.523	0.608	8.4	9.6
					26.5	0.531	0.705	9.9	
					27.7	0.534	0.677	10.0	
					26.2	0.530	0.699	9.7	
					28.6	0.538	0.634	9.7	
					26.2	0.529	0.717	9.9	
					26.6	0.533	0.896	9.9	
17-174	Quartz in melt	3.5	1.0	35	25.3	0.527	0.667	8.9	9.4
					26.7	0.534	0.697	9.9	
17-175	0.3% CO_2 + 30 ppm O_2	3.5	1.0	36	26.8	0.539	0.735	10.6	10.3
					27.7	0.545	0.706	10.7	
					26.1	0.537	0.720	10.1	
					27.5	0.547	0.641	9.7	
17-178	1% CO_2 + 100 ppm O_2	3.5	1.0	34	26.4	0.518	0.696	9.5	9.1
					26.2	0.517	0.642	8.7	
17-181	0.23% CO_2 + 23 ppm O_2	3.5	4.0	43	29.0	0.525	0.603	9.2	10.0
					28.8	0.522	0.713	10.7	
17-204	Stretched cartridge with gas seal 0.29% CO_2 + 29 ppm O_2	3.5	4.0	36	29.1	0.547	0.726	11.6	11.1
					28.3	0.530	0.629	9.5	
					29.7	0.541	0.688	11.1	
					29.3	0.546	0.732	11.7	
					29.8	0.537	0.704	11.3	
					30.5	0.542	0.669	11.1	
					29.8	0.546	0.716	11.7	

ORIGINAL PAGE IS
OF POOR QUALITY

EFG Ribbon Quality: Status

- HIGH SPEED GROWN RIBBON EFFICIENCIES AT 11-12% ARE STILL BELOW BEST EFG RIBBON AVAILABLE, WITH PARTICULAR SHORTFALL IN V_{OC} AND FF.

- ISSUES TO SETTLE:
  - WHAT ARE UNDERLYING MATERIAL QUALITY DEFICIENCIES?
  - CAN THIN RIBBON, PROCESSED WITH IMPROVED GETTERING AND BSF SCHEMES, ACHIEVE GOALS ON PRESENT MATERIAL?

Annealing Studies

- HIGH TEMPERATURE HEAT TREATMENTS (800-1100°C) IN NITROGEN AND OXYGEN AMBIENTS LEAD TO CONSISTENT DEGRADATION OF (DARK) SPV DIFFUSION LENGTHS INDEPENDENTLY OF GROWTH CONDITIONS, INTERSTITIAL OXYGEN LEVEL OF RIBBON (CO_2 ON OR OFF, OR QUARTZ IN THE MELT).

- PH_3 TREATMENT DURING ANNEAL CAN IMPROVE DARK DIFFUSION LENGTH <u>AND</u> APPEARS TO BE NECESSARY TO PRODUCE LIGHT ENHANCEMENT.

Schottky Barrier SPV Diffusion Length Measurements Before and After Heat Treatment of 10 cm Wide Ribbon in an Oxygen Ambient.

Heat Treatment	Growth Run	Growth Ambient	No. of Sample Pairs	Diffusion Length L_B Before Heat Treat. $\bar{x}$ (μm)	s (μm)	$s/\bar{x}$	Diffusion Length L_A After Heat Treat. $\bar{x}$ (μm)	s (μm)	$s/\bar{x}$	Ratio (L_A/L_B) $\bar{x}$ (μm)	s (μm)	$s/\bar{x}$
5 hrs at 800°C in O_2. Sister sample measurement.	CZ	-	3				83.4	5.42	0.06			
	17-117	argon	8	43.9	21.0	0.48	33.3	7.94	0.24	0.78	0.64	0.65
			7	48.7	17.5	0.40	34.3	7.97	0.23	0.78	0.28	0.36
	17-166	quartz in melt	8	48.2	21.3	0.44	35.5	15.8	0.44	0.77	0.30	0.39
	16-258	0.425 ℓ/min of 1% CO_2	8	51.7	19.4	0.38	39.5	7.32	0.19	0.88	0.40	0.45
50 mins at 900°C in O_2. Sister sample measurement.	CZ	-	3				73.7	15.3	0.21			
	17-117	argon	8	40.6	16.0	0.39	21.6	8.36	0.39	0.57	0.25	0.43
	17-166	quartz in melt	8	45.7	25.5	0.57	30.1	13.1	0.44	0.82	0.65	0.79
			7	51.0	25.4	0.50	29.0	13.8	0.48	0.60	0.24	0.39
	16-259	0.425 ℓ/min of 1% CO_2	8	45.4	10.9	0.24	28.9	8.71	0.30	0.65	0.14	0.22
7.5 hrs at 900°C in O_2. Sister sample measurement.	CZ	-	4	111.0	5.29	0.05	32.6	2.79	0.09	0.294	0.025	0.086
	17-148	argon	6	30.7	8.8	0.29	17.0	9.89	0.58	0.57	0.27	0.48
	17-147	quartz in melt	6	37.2	13.9	0.37	15.7	14.3	0.91	0.41	0.36	0.87

$\bar{x}$ = mean value; s = standard deviation.

Schottky Barrier SPV Diffusion Length Measurements Before and After PH_3 Diffusion for 10 cm Wide Ribbon.

Heat Treatment	Growth Run	Growth Ambient	No. of Sample Pairs	Diffusion Length L_B Before Heat Treat. $\bar{x}$ (μm)	s (μm)	$s/\bar{x}$	Diffusion Length L_A After Heat Treat. $\bar{x}$ (μm)	s (μm)	$s/\bar{x}$	Ratio (L_A/L_B) $\bar{x}$ (μm)	s (μm)	$s/\bar{x}$
900°C diffusion: 10 mins O_2/N_2 + 30 mins PH_3 + furnace cool to 650°C in 100 mins. Same sample measurement.	CZ	-	2	155.0	2.12	0.01	146.0	1.13	0.01	0.94	0.02	0.02
	17-142	argon	7	28.3	12.0	0.42	38.8	11.6	0.30	1.43	0.31	0.22
	17-174	quartz in melt	7	31.3	6.86	0.22	27.6	5.76	0.21	0.92	0.32	0.35
	17-175	0.3% CO_2 + 30 ppm O_2	5	37.7	7.12	0.19	37.5	23.1	0.62	1.11	0.95	0.86
			4	40.3	4.80	0.12	27.9	9.69	0.35	0.70	0.23	0.33
800°C diffusion: 1 hr in O_2/N_2 + 1 hr in PH_3 + 4 hrs in O_2/N_2. Sister sample measurement.	CZ	-	3	157.9	6.77	0.04	116.8	7.74	0.07	0.74	0.37	0.10
	17-117	argon	7	26.5	7.92	0.30	34.9	12.4	0.36	1.40	0.57	0.41
	17-175	0.3% CO_2 + 30 ppm O_2	6	42.8	11.6	0.27	53.3	10.7	0.20	1.33	0.47	0.36
	17-177	1% CO_2 + 100 ppm O_2	8	43.2	7.49	0.17	43.2	10.8	0.25	1.01	0.24	0.23
	17-174	quartz in melt	7	46.4	15.4	0.33	44.3	15.6	0.35	0.96	0.19	0.20

Status of EFG Multiple-Ribbon Program: Needs

- NEW FURNACE FOR FOUR 10 cm WIDE RIBBONS IS OPERATIONAL WITH AUTOMATIC WIDTH CONTROL AND MELT REPLENISHMENT. WORK TO BE DONE CONCERNS:
  - ESTABLISHING RELIABILITY, LIFETIME FOR FURNACE COMPONENTS IN LONG TERM OPERATION.
  - IMPLEMENTING AMBIENT CONTROL AT LEVEL WHICH ENSURES QUALITY CONSISTENCY.
- FUNDAMENTAL QUESTIONS REGARDING VIABILITY AND COST-EFFECTIVENESS OF FURNACE IN PRODUCTION MODE REMAIN:
  - YIELDS FOR THIN RIBBON MUST BE HIGH: LOW STRESS, FLATNESS AT 150-200 μm THICKNESS, 4 cm/min ARE ABSOLUTE NECESSITY.
  - SIMULTANEOUS ACHIEVEMENT OF HIGH DUTY RATE, CONSISTENT QUALITY, HIGH YIELDS MUST OCCUR.

Problems and Concerns

- STRESS AND NON-FLATNESS IN THIN (200 μm) RIBBON DO NOT PERMIT FABRICATION OF RIBBON GROWN AT HIGHEST SPEEDS (~4 cm/minute) INTO CELLS WITH ACCEPTABLE YIELDS.
- DEMONSTRATE THAT BEST CELL PERFORMANCE LEVELS OF 11-12% ACHIEVED IN SINGLE CARTRIDGE FURNACES CAN BE OBTAINED CONSISTENTLY IN A MULTIPLE RIBBON FURNACE.
- DEMONSTRATE RELIABILITY OF MULTIPLE RIBBON FURNACE OPERATION OVER THE LONG TERM, WITH ACCEPTABLE DUTY RATES, THROUGHPUT AND MATERIAL QUALITY.

LARGE-AREA SILICON SHEET TASK

ORIGINAL PAGE IS
OF POOR QUALITY

SEMICRYSTALLINE PROCESS DEVELOPMENT

SEMIX INC.

TECHNOLOGY	REPORT DATE
LARGE AREA SILICON SHEET	April 22, 1987
APPROACH SEMICRYSTALLINE CRYSTALLIZATION PROCESS DEVELOPMENT AND VERIFICATION **CONTRACTOR** SEMIX INCORPORATED	**STATUS** WORK IS CONTINUING TO DEVELOP AN UNDERSTANDING OF THE BASIC MECHANISMS IN THE CRYSTALLIZATION OF SEMICRYSTALLINE MATERIAL. A TECHNIQUE HAS BEEN DEVELOPED TO DETERMINE BASE RESISTIVITY AND CARRIER LIFETIME IN SEMICRYSTALLINE WAFERS. EXTENSIONS OF THIS TECHNOLOGY ARE BEING PURSUED FOR EVALUATION OF UCP BRICKS. SEMIX HAS ACHIEVED CELLS OF 13.5% EFFICIENCIES IN LIMITED QUANTITIES. WE HAVE COMPLETED THE DESIGN PHASE AND ENTERED THE PROCUREMENT AND CONSTRUCTION PHASE OF A PROTOTYPE 3 UCP SYSTEM CAPABLE OF SOLIDIFYING 42 KILOGRAMS OF SILICON. WE ARE INVESTIGATING THE CRITICAL ELEMENTS NECESSARY TO DEMONSTRATE HIGH THROUGHPUT CAPABILITY.
GOALS INVESTIGATE STRUCTURAL PROPERTIES OF UCP MATERIAL. ASSESS AND DEVELOP TECHNIQUES TO CHARACTERIZE SEMICRYSTALLINE MATERIAL. DEMONSTRATE 14% AMI EFFICIENCY WITH 100 CM^2 SOLAR CELLS. EVALUATE AND INVESTIGATE THE CRITICAL ELEMENTS NECESSARY FOR HIGH THROUGHPUT UCP SYSTEMS.	

Principal Areas of Research

A. FUNDAMENTAL STUDIES OF SEMICRYSTALLINE MATERIAL

B. HIGH EFFICIENCY SEMICRYSTALLINE SOLAR CELLS

C. WAFERING MECHANISMS

Areas of Fundamental Study

CRYSTALLIZATION

INVESTIGATION OF THE ROLE OF MICROSTRUCTURE ON THE PERFORMANCE OF SEMICRYSTALLINE SILICON, MOST NOTABLY THROUGH:

- GRAIN ORIENTATION STUDIES, AND
- INVESTIGATION OF STRUCTURAL INHOMOGENEITIES

CHARACTERIZATION

DEVELOPMENT OF TECHNIQUES FOR THE CHARACTERIZATION OF SEMICRYSTALLINE SILICON FOR BOTH:

- RESISTIVITY
- CARRIER LIFETIME

Crystallization

PURPOSE: TO DETERMINE THE ROLE OF GRAIN VOLUMES AND GRAIN BOUNDARIES ON THE QUALITY OF SEMICRYSTALLINE MATERIAL.

APPROACH: DETERMINATION OF THE RELATIVE ORIENTATION OF NEIGHBORING CRYSTALLITES.

INVESTIGATION OF THE IMPACT OF MICROSTRUCTURAL DEFECTS ON CELL PROPERTIES:

- INDIVIDUAL DISLOCATIONS
- DISLOCATION SUBGRAIN BOUNDARIES

Relative Positions of Grains in Sample Semicrystalline Material

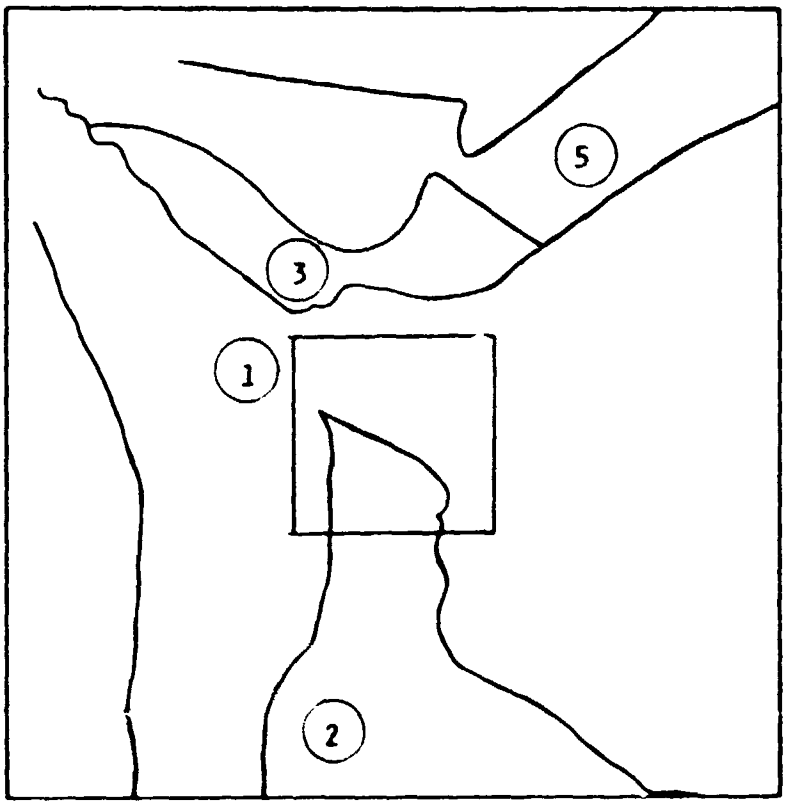

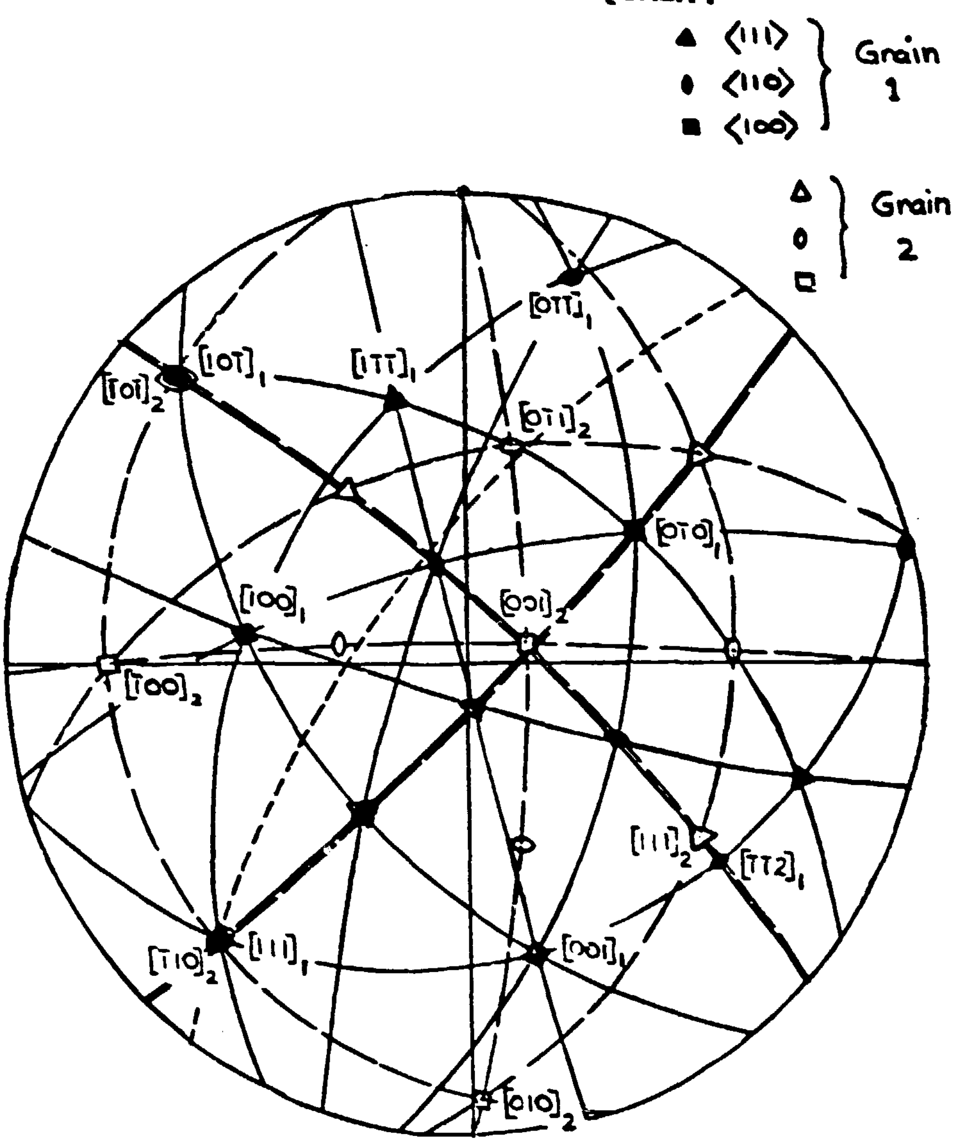

ORIENTATIONS OF GRAINS 1 and 2 IN SAMPLE SEMICRYSTALLINE MATERIAL

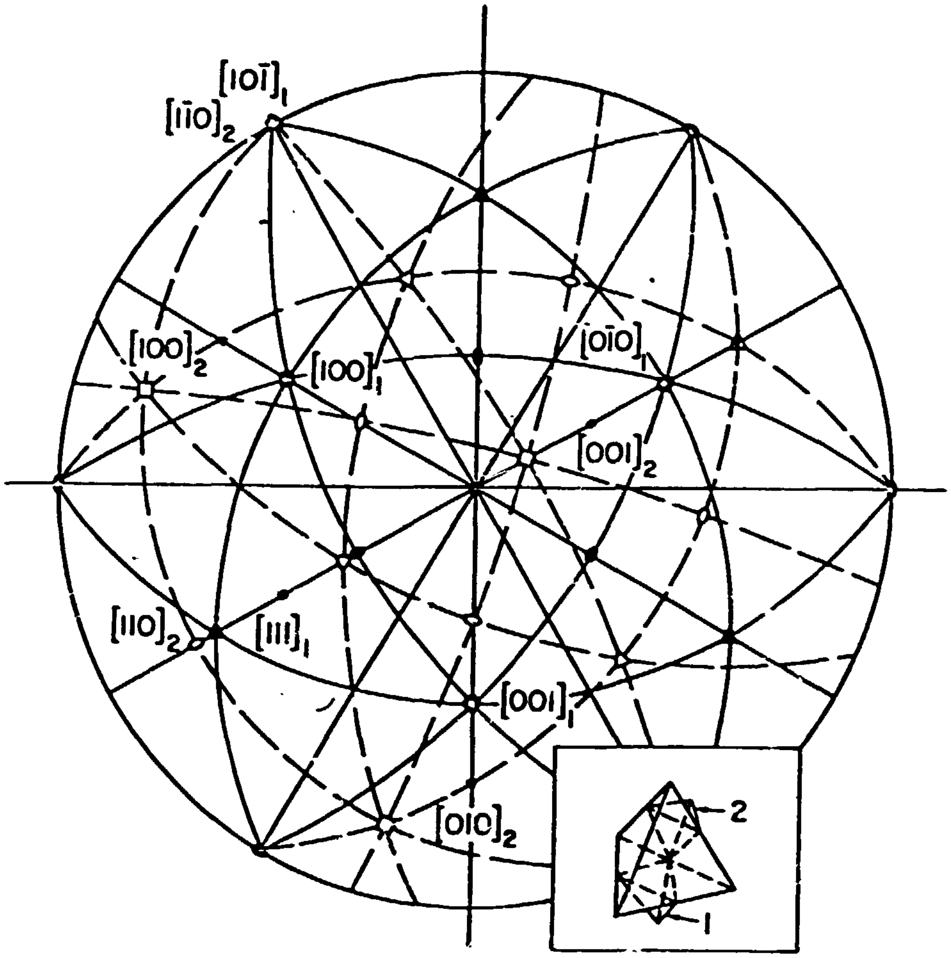

Second Order Orientation Relationship of Grains 1 and 2 in {111} Twin Geometry Relative to a Third Grain

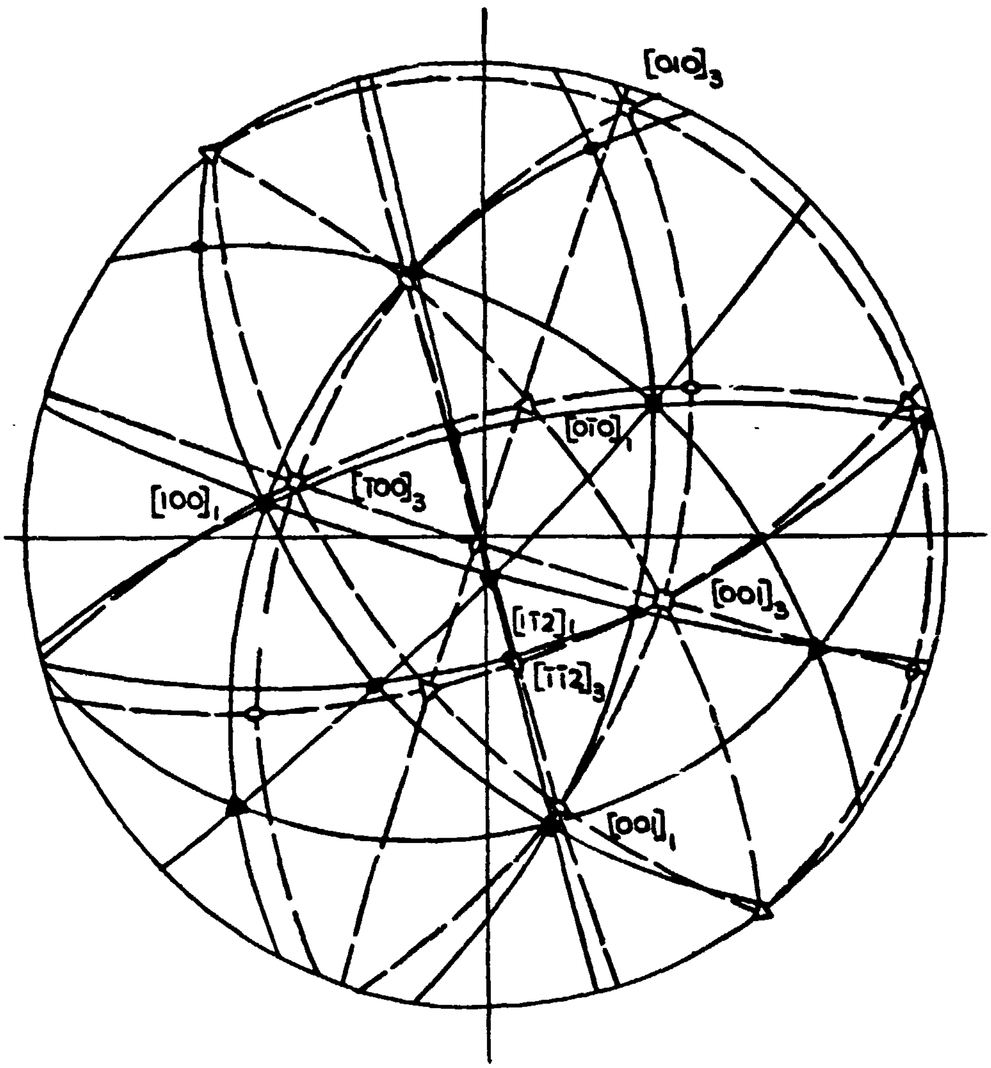

Orientation Relationship for Grains 1 and 3 of 90° Rotation About Nearly Common <112> Axes

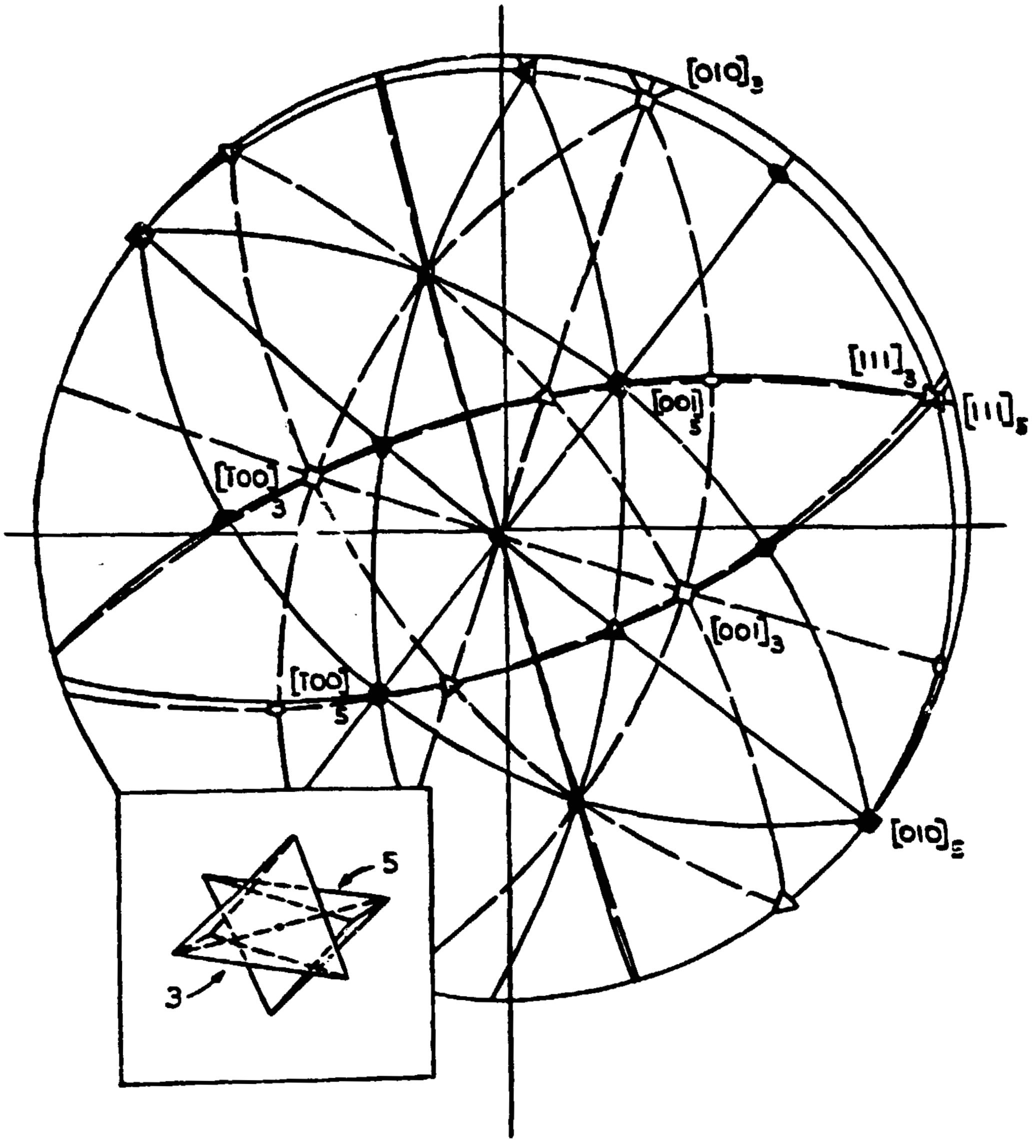

(111) Twin Orientation Relationship of Grains 3 and 5

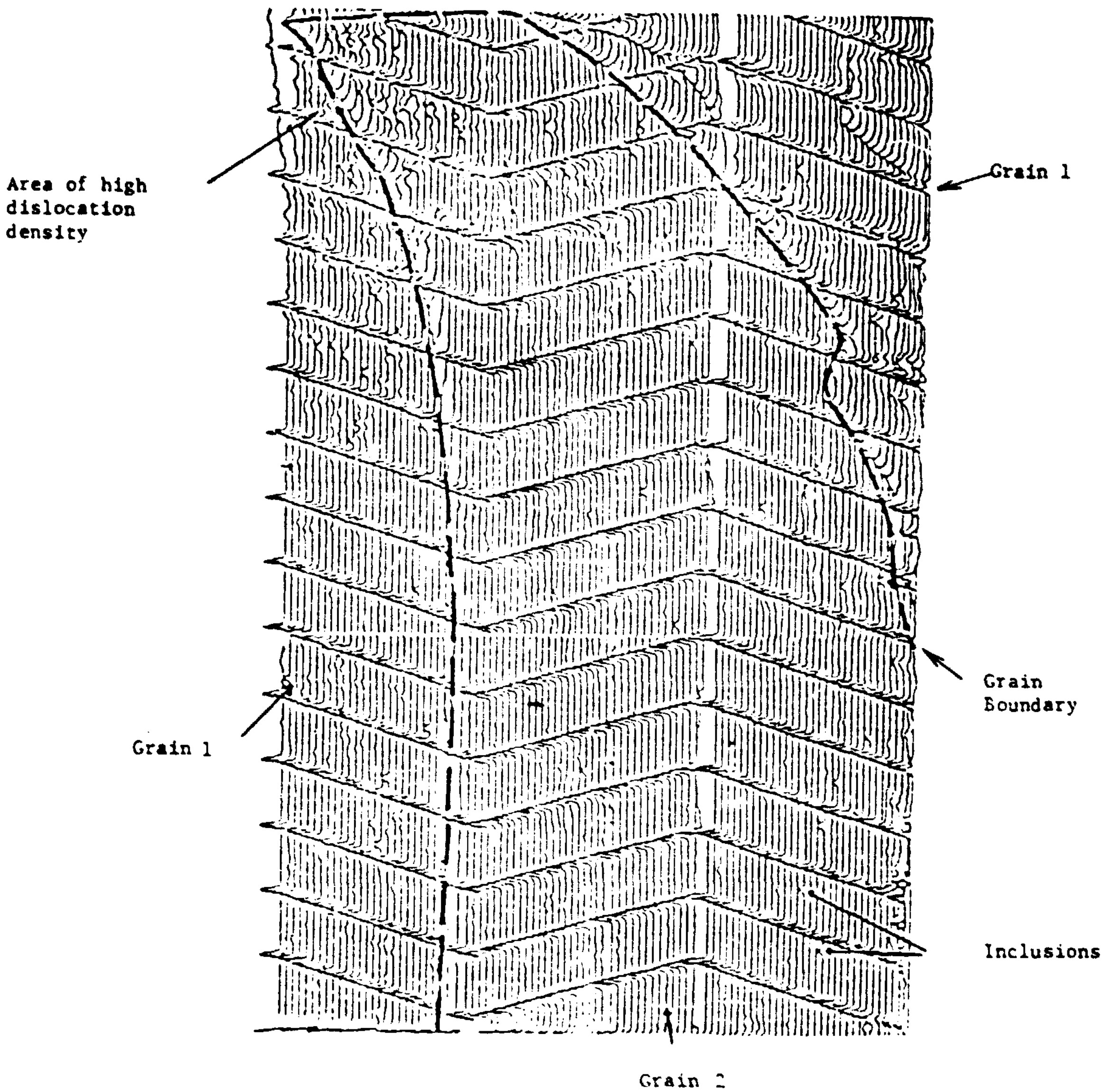

Scanning Photoresponse Pattern of an Area of a 2cm x 2cm 13% AM1 Efficient Cell Showing the Location of the Grain Boundaries and an Area of High Dislocation Density

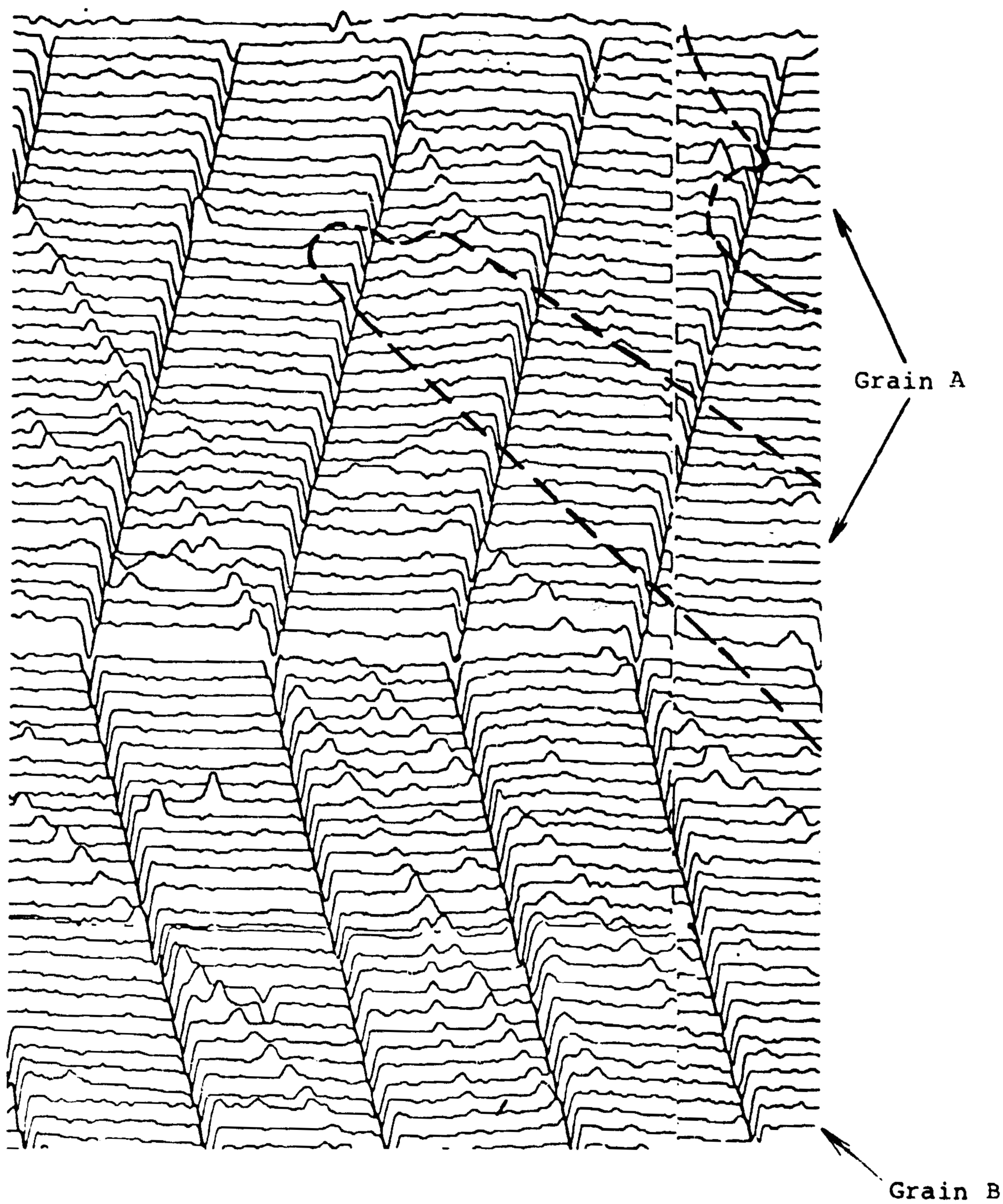

Scanning Photoresponse Pattern of an Area of a 2cm. x 2cm. Cell, No. 4726-C3-4, Including the Location of the Electrically Inactive Grain Boundaries

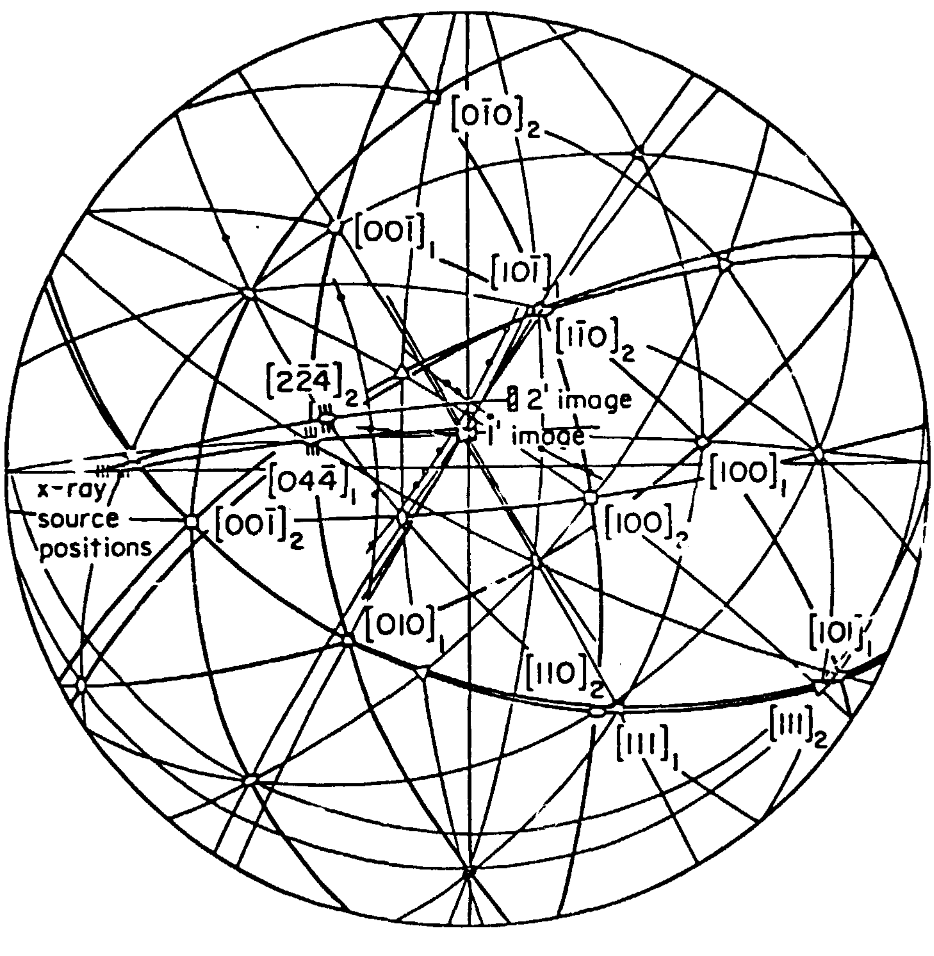

Second Order Twin Relationship of Grains 1 and 2 Oriented to Give $(04\bar{4})_1$ and $(2\bar{2}\bar{4})_2$ Skew Reflections

Conclusions

IN UCP SEMICRYSTALLINE SILICON, MOST GRAIN ORIENTATIONS APPEAR TO BE CRYSTALLOGRAPHICALLY RELATED BY A MULTIPLE ORDER TWINNING RELATIONSHIP, AND MOST GRAIN BOUNDARY INTERFACES ARE CRYSTALLOGRAPHICALLY DETERMINED. AS LONG AS THE CRYSTALLOGRAPHICALLY DETERMINED BOUNDARIES CONTAIN NO DISLOCATIONS, THE BOUNDARIES SHOW NO DELETERIOUS ELECTRICAL BEHAVIOR.

BECAUSE OF THE LARGE GRAIN SIZE OF THIS MATERIAL, AND THE LOW DENSITY OF NON-CRYSTALLOGRAPHICALLY RELATED BOUNDARIES, GRAIN BOUNDARIES HAVE A MINIMAL EFFECT ON THE PHOTOVOLTAIC PROPERTIES OF SEMICRYSTALLINE SILICON.

MINIMIZING INTERNAL GRAIN DEFECTS THEN BECOMES THE KEY TO HIGH WAFER QUALITY.

THE INTERNAL GRAIN ORDER IS AFFECTED BY MANY FACTORS INCLUDING:

- INCLUSIONS
- INDIVIDUAL DISLOCATIONS
- IMPURITIES
- DISLOCATION SUBGRAIN BOUNDARIES

OCCASIONALLY, THE LARGE CRYSTAL WILL DEVELOP A SUBGRAIN DEFECT STRUCTURE. THIS STRUCTURE IS COMPRISED OF NUMEROUS SUBGRAINS THAT HAVE GRAIN DIAMETERS ON THE ORDER OF ONE MILLIMETER OR LESS AND APPEAR TO BE ROTATED BY 5^{o} - 7^{o} ABOUT SPECIFIC CRYSTALLOGRAPHIC DIRECTIONS SUCH AS A $\langle 110 \rangle$ AXIS.

Determination of Lifetimes in Semicrystailine Si

PURPOSE:

DEVELOP A CONTACTLESS TECHNIQUE FOR THE MEASUREMENT OF CARRIER LIFETIMES IN SEMICRYSTALLINE MATERIAL.

UNIQUENESS OF APPROACH:

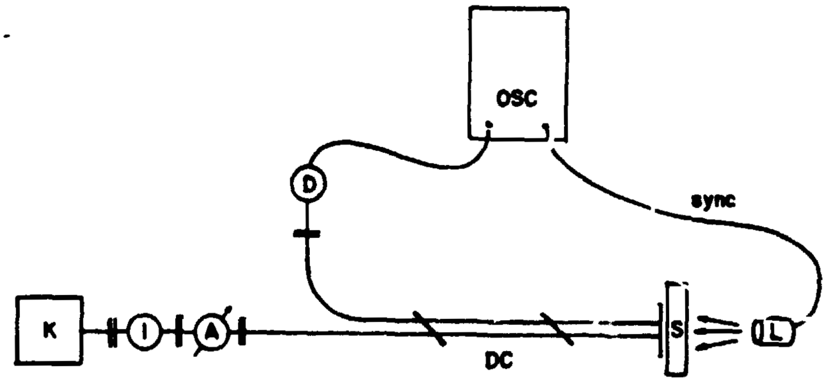

Variation in Measured Response vs Base Resistivity and Sample Thickness

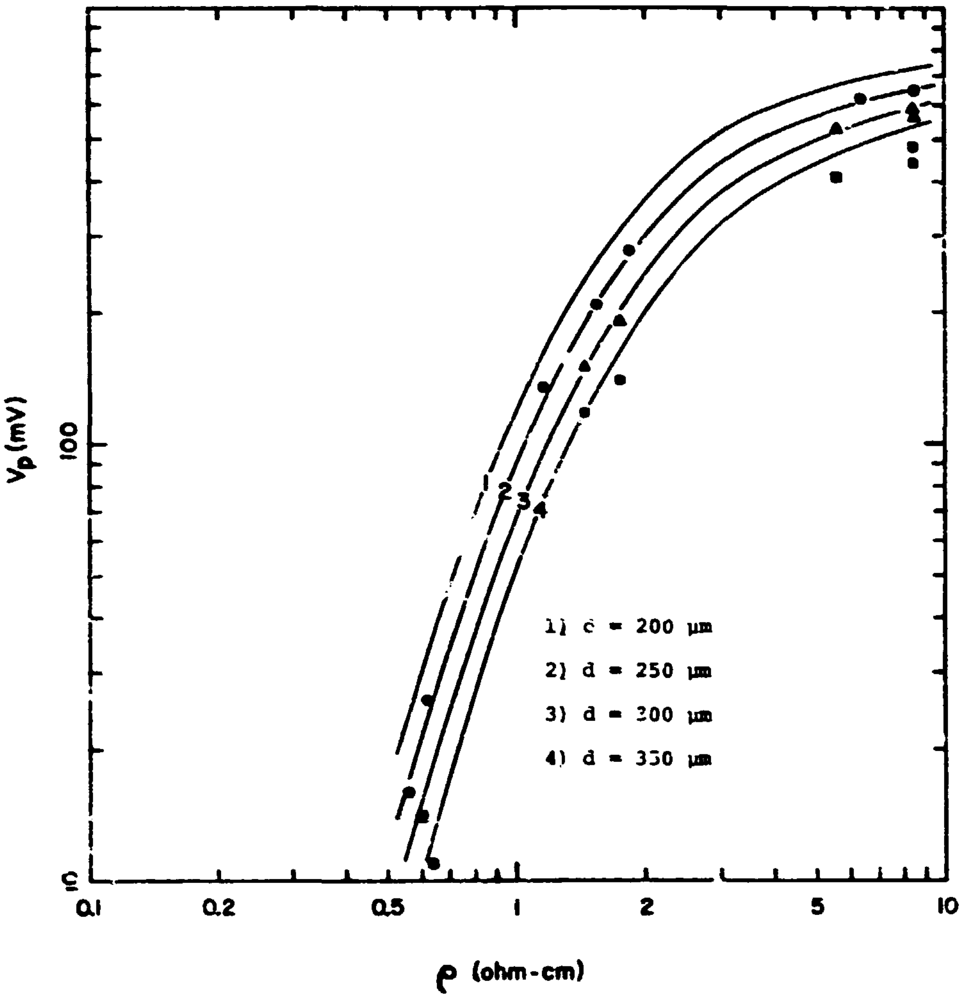

Theoretical Model

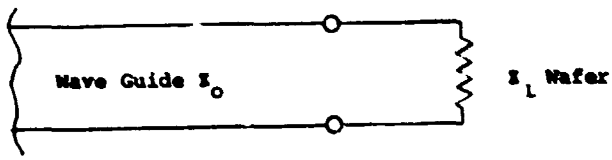

ASSUMPTIONS

- High Conductivity Limit

  $\sigma \gg \omega\epsilon$

- Exponential Carrier Distribution
- No Diffusion of Carriers
- No Surface Recombination Velocity
- Carriers Decay Exponentially with Time

  $N(t) = N_o^* e^{-t/\tau}$

Transmission-Line Model

Carrier Distribution

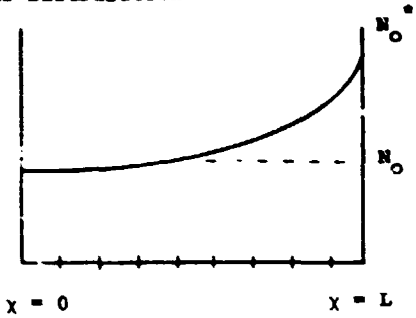

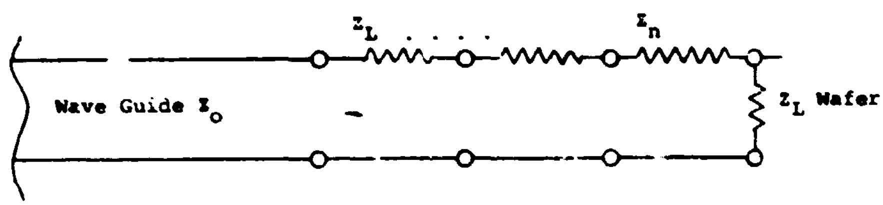

Reflection Coefficient

$$R = \frac{Z_L - Z_o}{Z_L + Z_o} \quad ; \; R \propto N_o + N_o^*$$

Reflected Power

$$P_M = RR^* \propto V_M$$

Normalized Modulation

$$\Delta = \frac{V_M^* - V_M}{V_M}$$

Normalized Modulation Calculated vs Base Resistivity and Sample Thickness

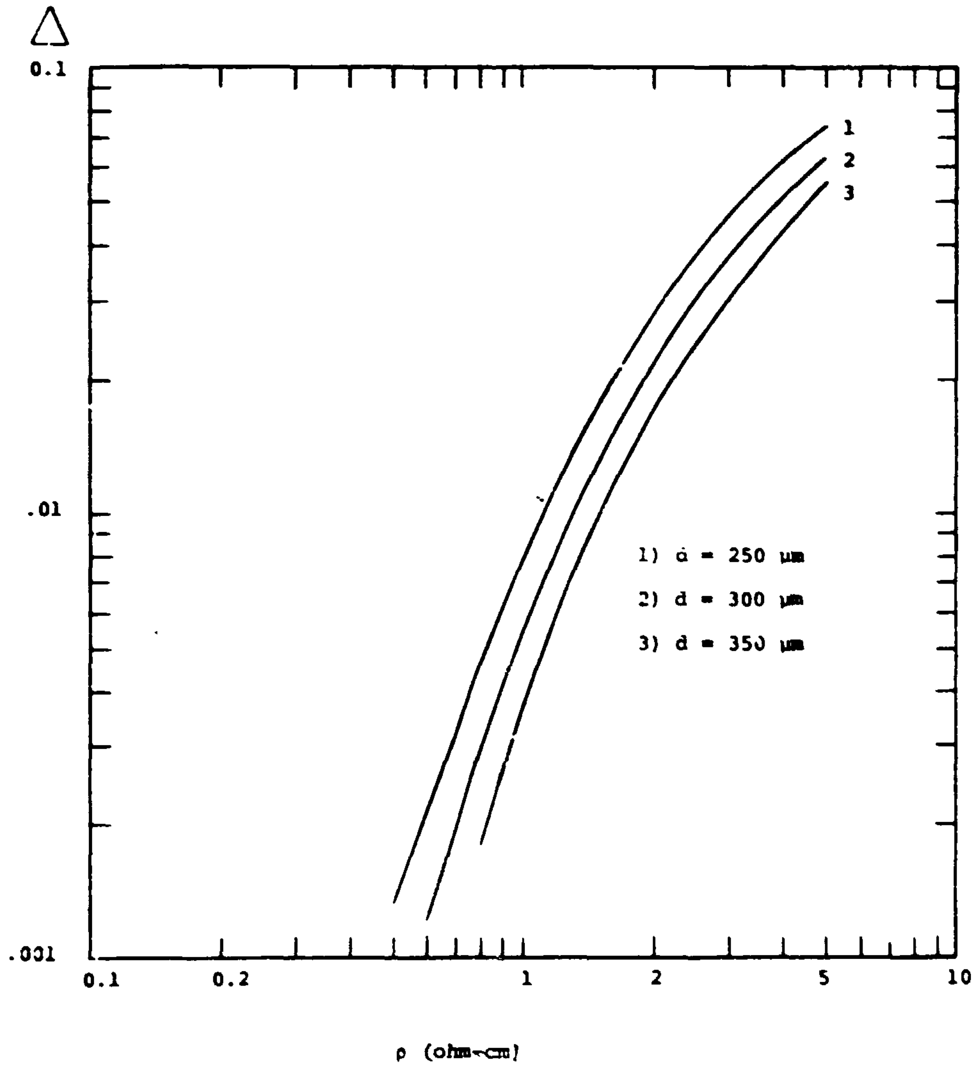

Change in Reflected Power With Time

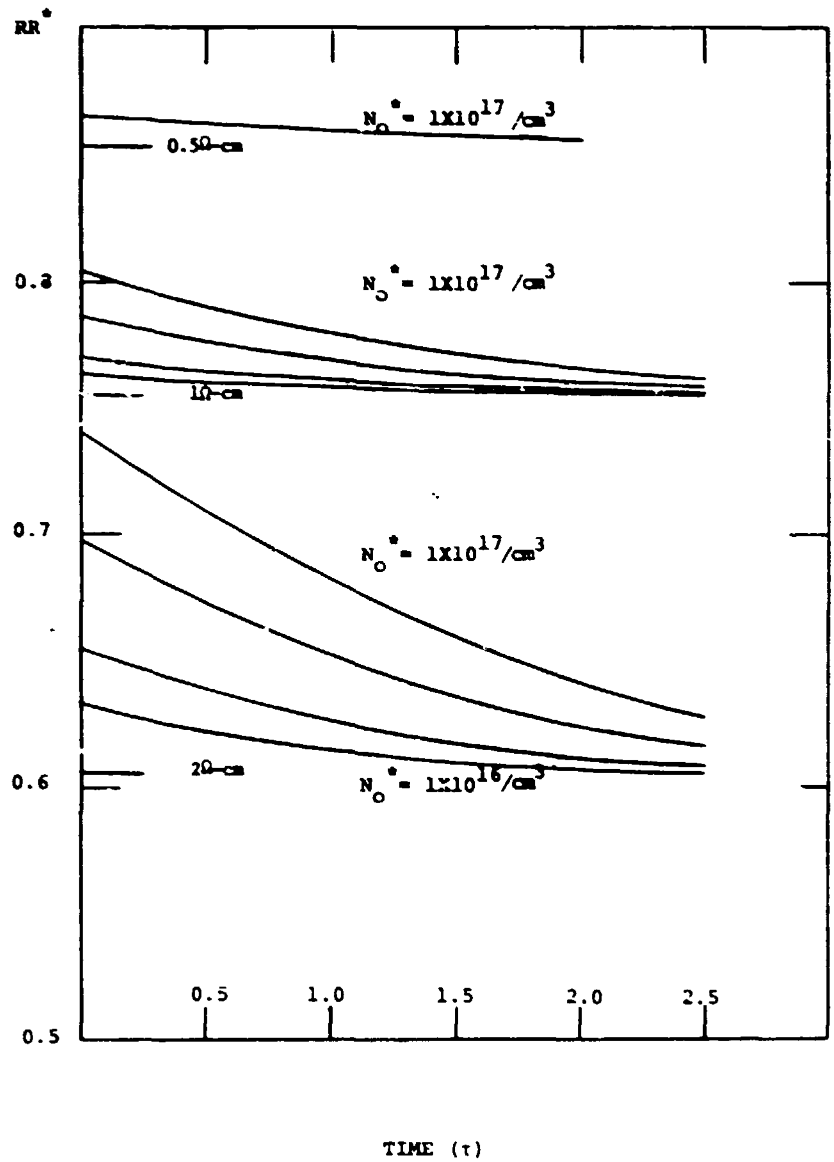

Variation in Measured Decay Time vs Base Resistivity and Generated Carrier Concentration

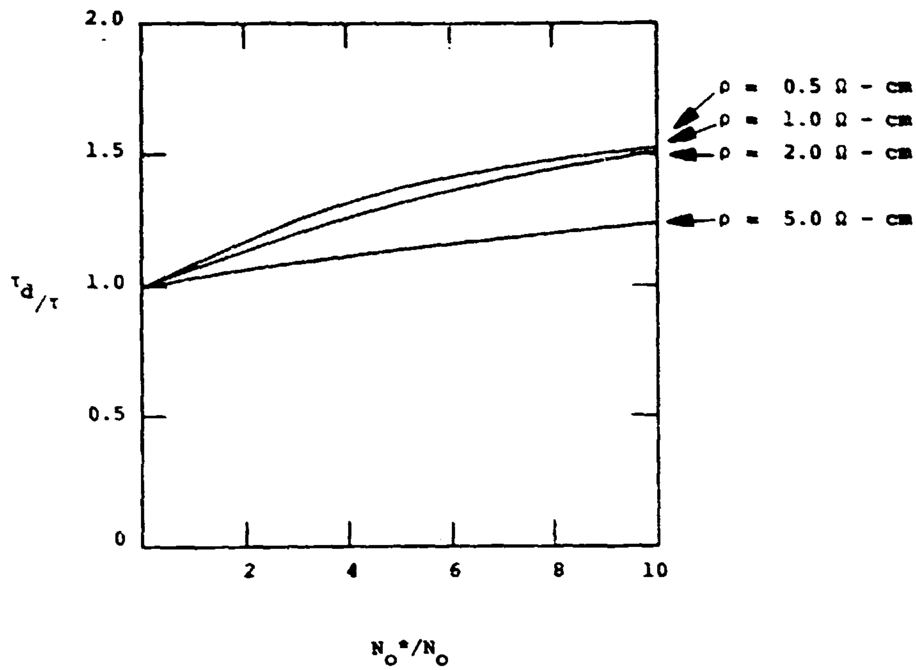

Conclusions

THIS IS A RELIABLE TECHNIQUE FOR THE CHARACTERIZATION OF SEMI-CRYSTALLINE MATERIAL. THE MODEL ACCURATELY PREDICTS THE OBSERVED BEHAVIOR ASSOCIATED WITH CHANGES IN BASE RESISTIVITY AND SUBSTANTIATES THE EMPIRICALLY OBSERVED BEHAVIOR FOR THE PREDICTION OF CARRIER LIFETIMES.

SURFACE PASSIVATION IS NECESSARY TO OBTAIN CONSISTENT AND MEANINGFUL RESULTS.

THE MEASURED DECAY TIME IS SOME MULTIPLE OF THE CARRIER LIFETIME, DEPENDENT UPON THE:

SAMPLE THICKNESS
BASE RESISTIVITY
ILLUMINATION INTENSITY

Wafering Mechanisms

PURPOSE: TO DETERMINE IF THE HSMBS WAFERING TECHNOLOGY IS A VIABLE METHOD FOR THE ECONOMICAL PRODUCTION OF SHEET SILICON FOR PHOTOVOLTAICS.

High-Speed MBS Saw

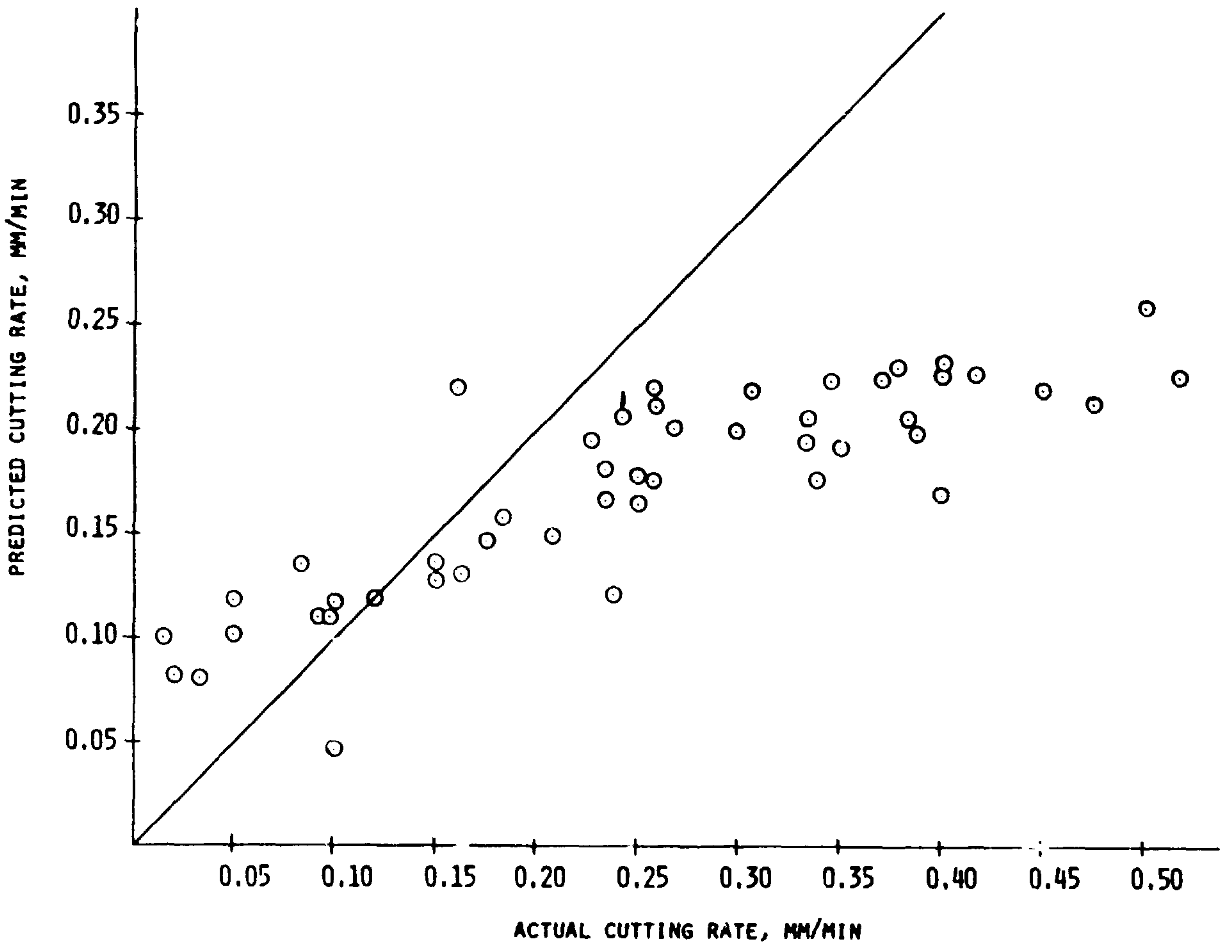

High-Speed MBS Saw: Cutting Rate vs Blade Speed

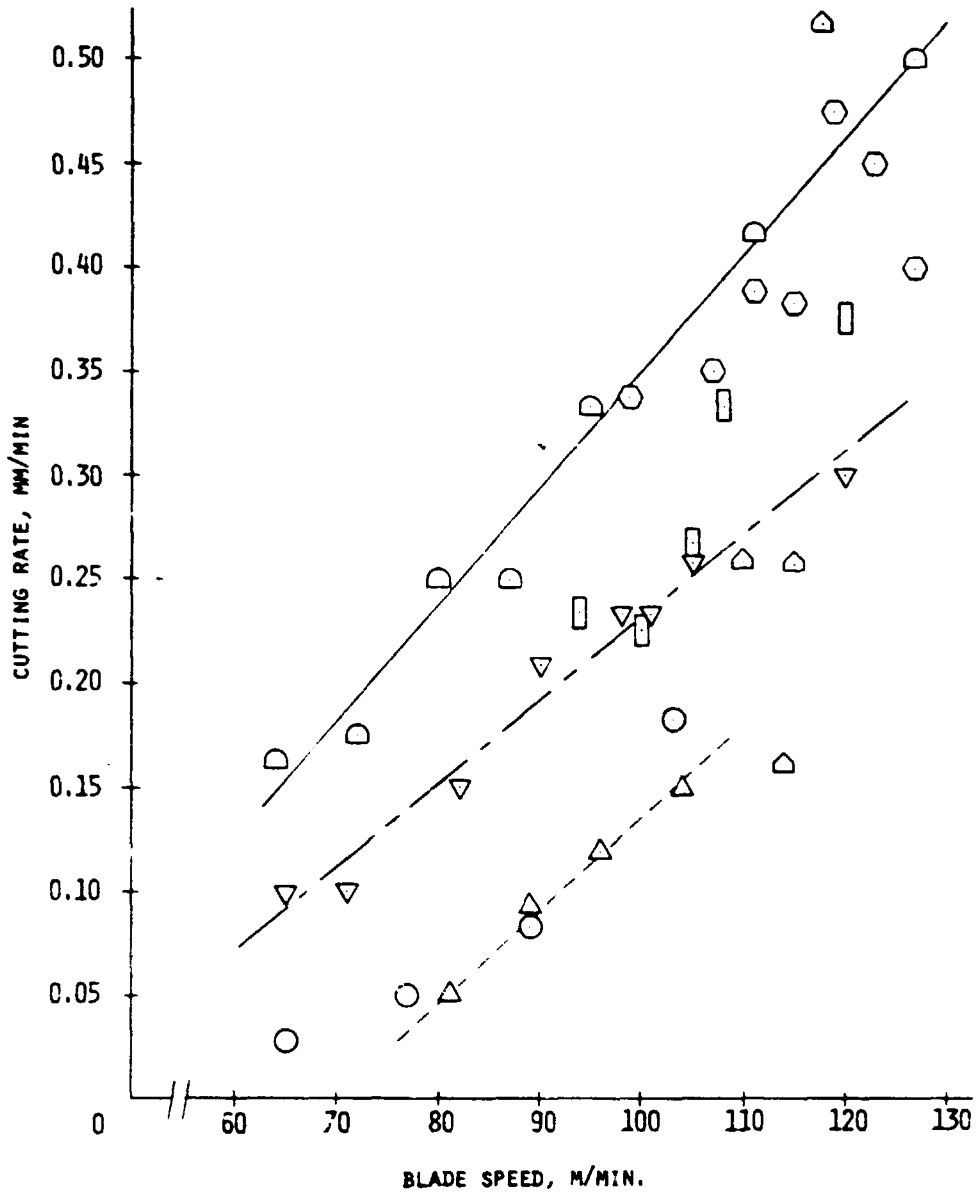

ORIGINAL PAGE IS
OF POOR QUALITY

High-Speed MBS Saw: Average Cutting Rates (Complete Runs Only)

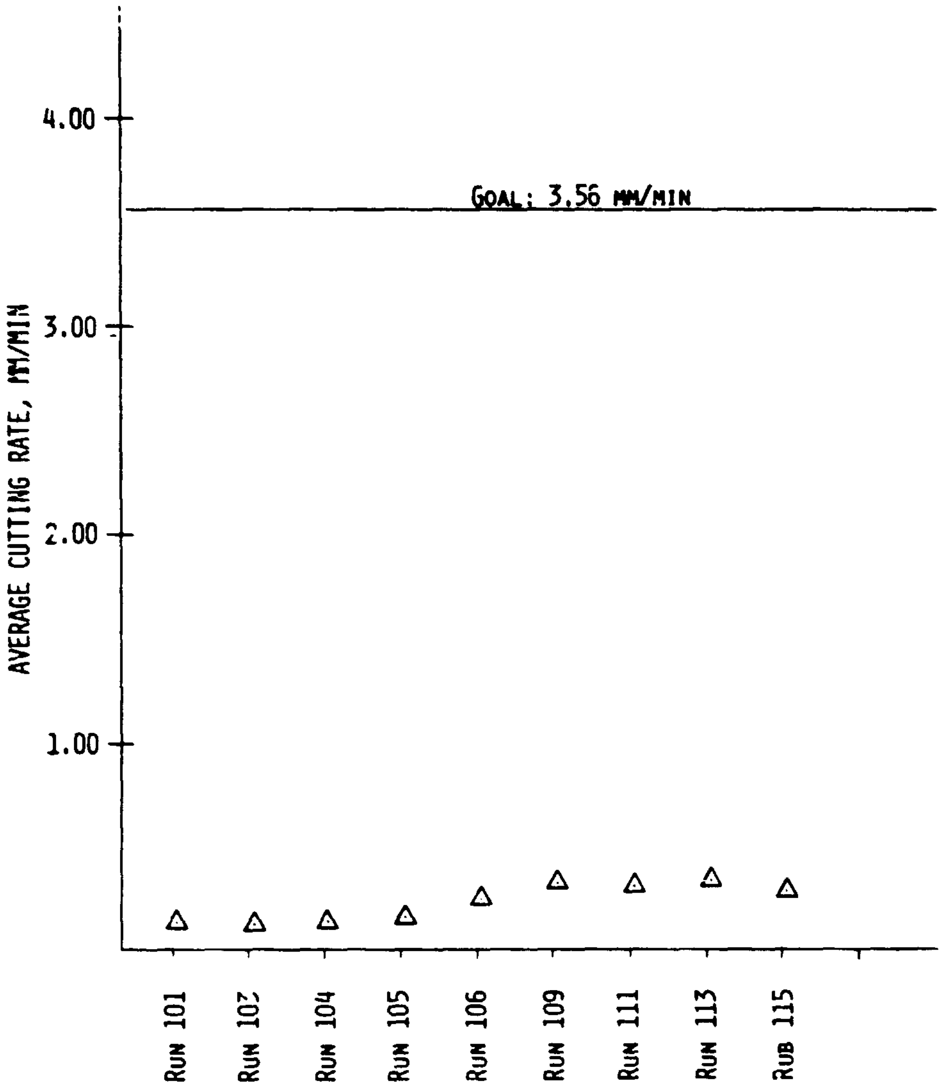

Conclusions

WITH THE HIGH MATERIALS COST ASSOCIATED WITH THE MBS TECHNOLOGY A CUTTING RATE OF $1M^2$/HR. IS NECESSARY.

BASED UPON THE RESEARCH PERFORMED THUS FAR, IT WOULD BE NECESSARY TO SUSTAIN A CUTTING RATE OF 3.5 MM/MIN.

THE CURRENT TECHNOLOGY IS NOT CAPABLE OF MEETING THIS CRITERIA.

ADVANCED CZOCHRALSKI INGOT GROWTH

KAYEX CORP.

ADVANCED CZOCHRALSKI INGOT GROWTH	KAYEX CORPORATION APRIL 22, 1982
GOALS:	**STATUS:**
GROWTH OF 150 KG OF INGOTS FROM ONE CRUCIBLE USING PERIODIC MELT REPLENISHMENT	ONE 150 KG RUN PERFORMED DURING THIS CONTRACT
DIAMETER 15 CM	ACHIEVED
THROUGHPUT - 2.5 KG/HR	1.46 KG/HR, 150 KG RUN
RECHARGE MELTING RATE 25 KG/HR	14.3 KG/HR
AFTER-GROWTH YIELD 90%	ACHIEVED; 52% MONO, BALANCE POLY
MICROPROCESSOR CONTROLS PLUS IMPROVED SENSORS FOR: MELT TEMPERATURE, DIAMETER, MELT LEVEL	CONSTRUCTED, INTERFACED & DEMONSTRATED
PROTOTYPE EQUIPMENT FOR HIGH VOLUME PRODUCTION, TRANSFERABLE TO INDUSTRY	JPL MOD 2000 → CG6000

RLL 4/22/82

ADVANCED CZOCHRALSKI INGOT GROWTH	KAYEX CORPORATION APRIL 22, 1982
APPROACH:	**STATUS:**
CONSTRUCT AN IMPROVED CRYSTAL GROWER HAVING THE PERFORMANCE REQUIRED TO ACHIEVE GOALS	INGOT SIZE ACHIEVED, BUT NOT THROUGHPUT
CONSTRUCT AN AUTOMATED SYSTEM WHICH WILL OFFER RELIABLE PERFORMANCE LEADING TO IMPROVED YIELDS AND REDUCED LABOR COST	SYSTEM OPERATIONAL - INSUFFICIENT DATA TO CONFIRM YIELD & LABOR
CONDUCT PROCESS DEVELOPMENT ON LARGE SIZE CRYSTAL GROWTH, MELT REPLENISHMENT AND IMPROVED THROUGHPUT AND YIELDS	INGOT SIZE 6" DIA x 37-1/2 KG ACHIEVED THROUGHPUT BELOW TARGET
CONDUCT PARALLEL ANALYTICAL PROGRAM TO HELP UNDERSTAND THE PROCESS	FURNACE GAS ANALYSES CRUCIBLE DEVITRIFICATION STUDY SOLAR CELL FAB AND TEST

RLL 4/22/82

ORIGINAL PAGE IS
OF POOR QUALITY

Program Plan, Revision 2

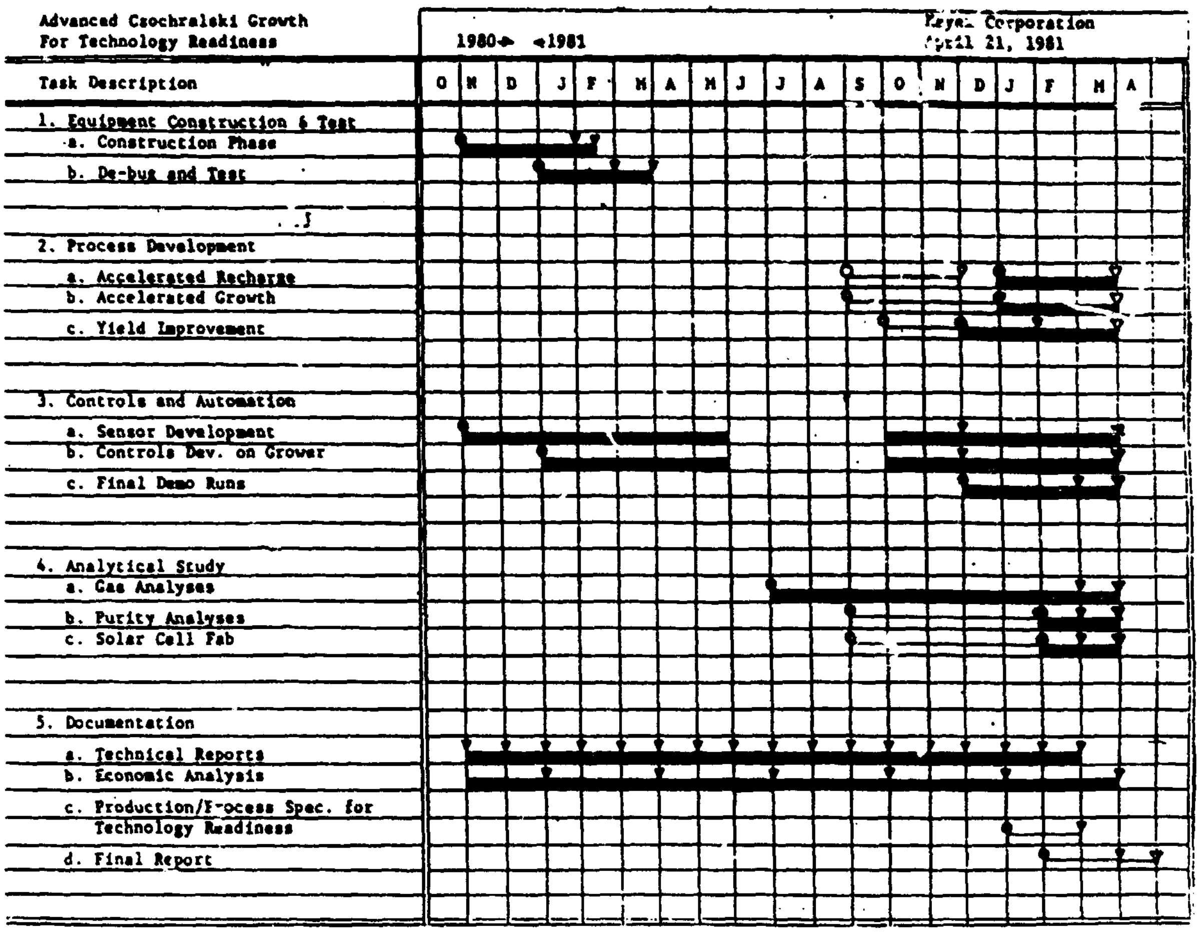

Program Plan

THE PROGRAM PLAN CONSISTS OF, FIRST, A CONSTRUCTION PHASE, WHICH WAS COMPLETED IN THE FIRST FIVE MONTHS.

A PARALLEL SENSOR DEVELOPMENT PROGRAM WAS CARRIED OUT INITIALLY ON A SECOND COMMERCIAL MACHINE AND, SUBSEQUENTLY, THE SENSORS WERE INTERFACED TO THE JPL FACILITY.

FOR A PERIOD OF TIME IN LATE 1981, VERY LITTLE EFFORT WAS EXPENDED, EXCEPT FOR THE CONTINUED DEVELOPMENT OF THE GAS ANALYSIS SYSTEM.

FOR THE LAST SEVERAL MONTHS, THE EFFORT WAS REDIRECTED THROUGH A TDM TO EMPHASIZE PROCESS UNDERSTANDING RATHER THAN EXTENSIVE DEMONSTRATION OF 150 KG RUNS.

THE EXPERIMENTAL WORK IS NOW COMPLETE AND THE FINAL DOCUMENTATION IS IN PROCESS.

Solar Efficiency vs Kilograms Grown

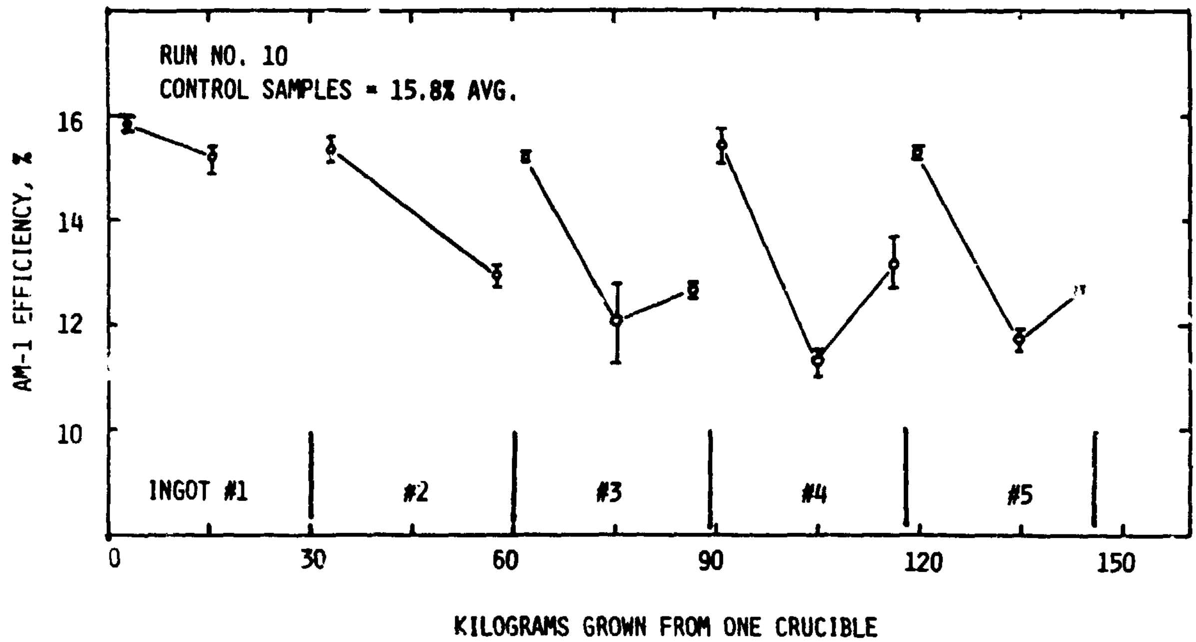

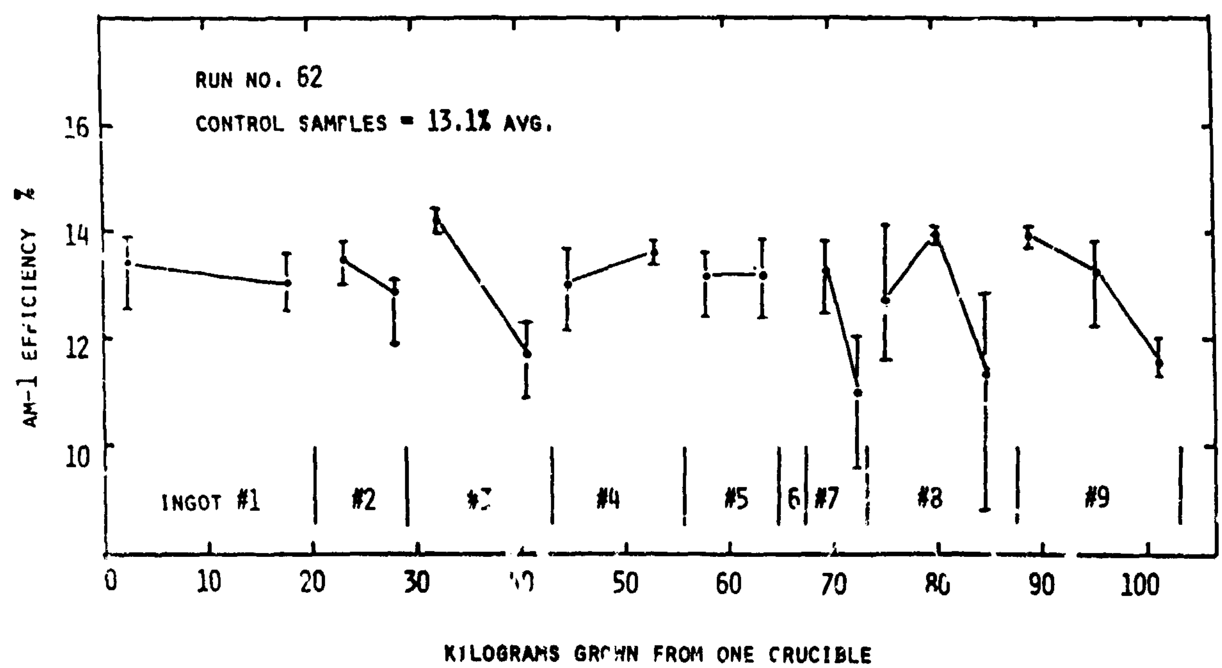

ADVANCED CZOCHRALSKI INGOT GROWTH

KAYEX CORPORATION
DOE/JPL 955733

PROBLEMS - CONCERNS

PROBLEM AREA	APPROACH
• YIELD OF MONOCRYSTAL, LOWER EFFICIENCY OF POLY MATERIAL	• STUDY STRUCTURE LOSS MECHANISMS, PRIMARILY MELT CONTAMINATION - CRUCIBLE DISSOLUTION - CRUCIBLE DEVITRIFICATION - GAS AMBIENT PURITY & FLOW
• THROUGHPUT AS RELATED TO RATE LIMITING FACTORS	• IMPROVE HOT ZONE DESIGN
- MELTING RATE	- FURTHER WORK WITH RADIATION SHIELDING
- CORKSCREWING	- TEMPERATURE PROFILING OF MELT
- STABILIZATION OF MELT TEMPERATURE	- IMPROVED TUNING OF MICROPROCESSOR TO SPEED UP STABILIZATION, SEEDING AND NECKING

ADVANCED CZOCHRALSKI
ENERGY DISPERSIVE X-RAY ANALYSIS OF ROSETTE DEFECTS
ON INNER SURFACE OF USED CRUCIBLE

1. COMPOSITION AT RIM OF DEFECT

ELEMENT	ATOMIC WEIGHT PERCENT	ATOMIC PERCENT	OXIDE FORMULA	OXIDE PERCENT
Si	87.39	89.92	SiO_2	91.53
S	1.97	1.78	SO_3	2.52
Cl	6.15	5.01	Cl	3.11
K	2.91	2.15	K_2O	1.75
Ca	1.58	1.14	CaO	1.09

2. COMPOSITION OF CENTER OF DEFECT AND BULK SiO_2 GLASS CONTAINED NO DETECTABLE IMPURITIES.

RLL 4/21/82

CO and H_2 vs Run Time

IN AN ATTEMPT TO UNDERSTAND THE MECHANISM OF STRUCTURE LOSS, WE HAVE CONSTRUCTED A DEVICE WHICH SAMPLES AND ANALYZES THE GROWER EXHAUST GAS FOR CARBON MONOXIDE, HYDROGEN, AND WATER. IF CARBON IS CONTAMINATING THE MELT, IT WILL BE CONCENTRATED IN THE RESIDUAL MELT AND COULD LEAD SUBSEQUENTLY TO SILICON CARBIDE PRECIPITATION, AS MORE AND MORE CRYSTALS ARE GROWN.

CARBON MONOXIDE HAS BEEN FOUND IN SURPRISINGLY HIGH CONCENTRATIONS, AND IS A FUNCTION OF TEMPERATURE. APPROXIMATELY 5000 PPM ARE SEEN DURING MELTDOWN.

LARGE-AREA SILICON SHEET TASK

MATERIAL CHARACTERIZATION

CORNELL UNIVERSITY

<table>
<tr><td>TECHNOLOGY
LARGE AREA SILICON SHEET - ANALYSIS</td><td>REPORT DATE
April 17, 1982</td></tr>
<tr><td>APPROACH
• Optical Microscopy and Etching.
• Transmission Electron Microscopy
• Electron beam Induced Current Microscopy
• Chemical Analysis (e^-, ion, neutron, mass spec).

CONTRACTOR
Cornell University/Material Science

GOALS
• Characterize structure and chemical composition of point, line and planar defects in un-processed LASS material.
• Characterize structure and chemical composition of point, line and planar defects in processed LASS material.
• Evaluate crystal growth/defect relation
• Evaluate processing/defect relation.</td><td rowspan="1">STATUS
• EFG
TEM and STEM analysis of defects in processed EFG completed. Chemical make up of large precipitates identified.
• WEB
RT EBIC of processed WEB completed. Temperature dependent EBIC being carried out to determine local energy levels. Rutherford backscattering completed.
• HEM
Optical Microscopy and etching completed EBIC completed.
• <u>NEW ANALYTICAL TOOLS ADDED SINCE LAST PI</u>
1) JEOL 200 CX STEM with EDX
2) Temperature dependent EBIC
3) General Ionix Accelerator for back-scattering analysis.</td></tr>
</table>

Coherent Twins

- 60° rotation on (111) plane
  - perfect first nearest neighbor fit

- Periodicity of three
  - SIGMA 3 boundary

- Small deviations from ideal twin are accomodated by DSC dislocations

  $$b = (a/6)\ 112$$

  These dislocations are the analogue of complete dislocations in small angle grain boundaries.

- Dislocations are necessarily associated with a step in the boundary
  - presents possibility to study effects of jogs.

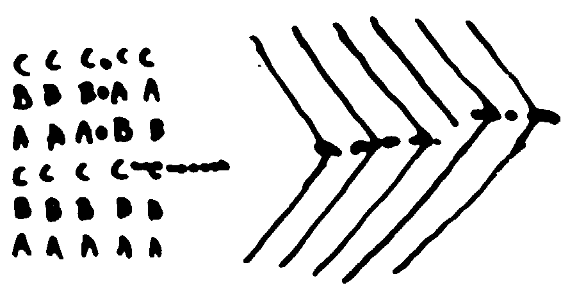

Twist Boundaries

Network of screw dislocations

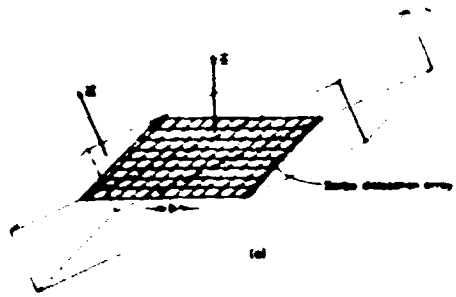

On $(\bar{1}11)$ dislocations react to form hexagonal networks - low angle - twin relation.

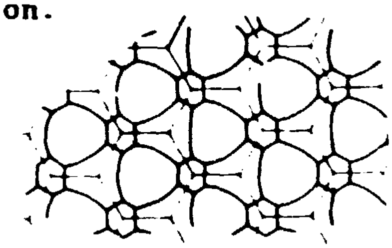

Hornstra, J.
1959

Physica 25
409-472

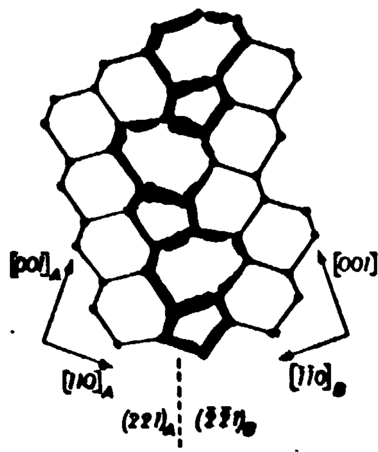

Fig. 6. Symmetrical tilt boundary with $\theta_1 = 38°57'$ and zig-zag arrangement of dislocations.

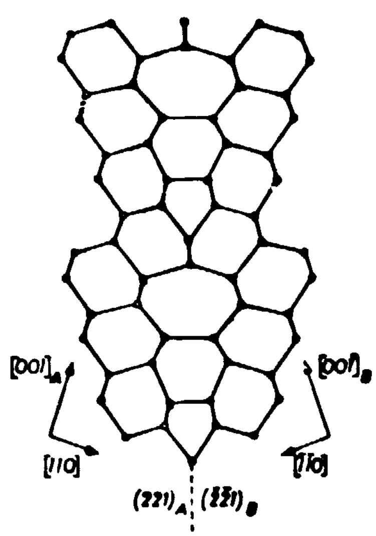

Fig. 7. As Fig. 6 but with overlapping dislocations, thus forming double dislocations.

For [redacted] ($\theta_1 = 31°35' = \arccos 23/27$) the model [redacted]. Thus,

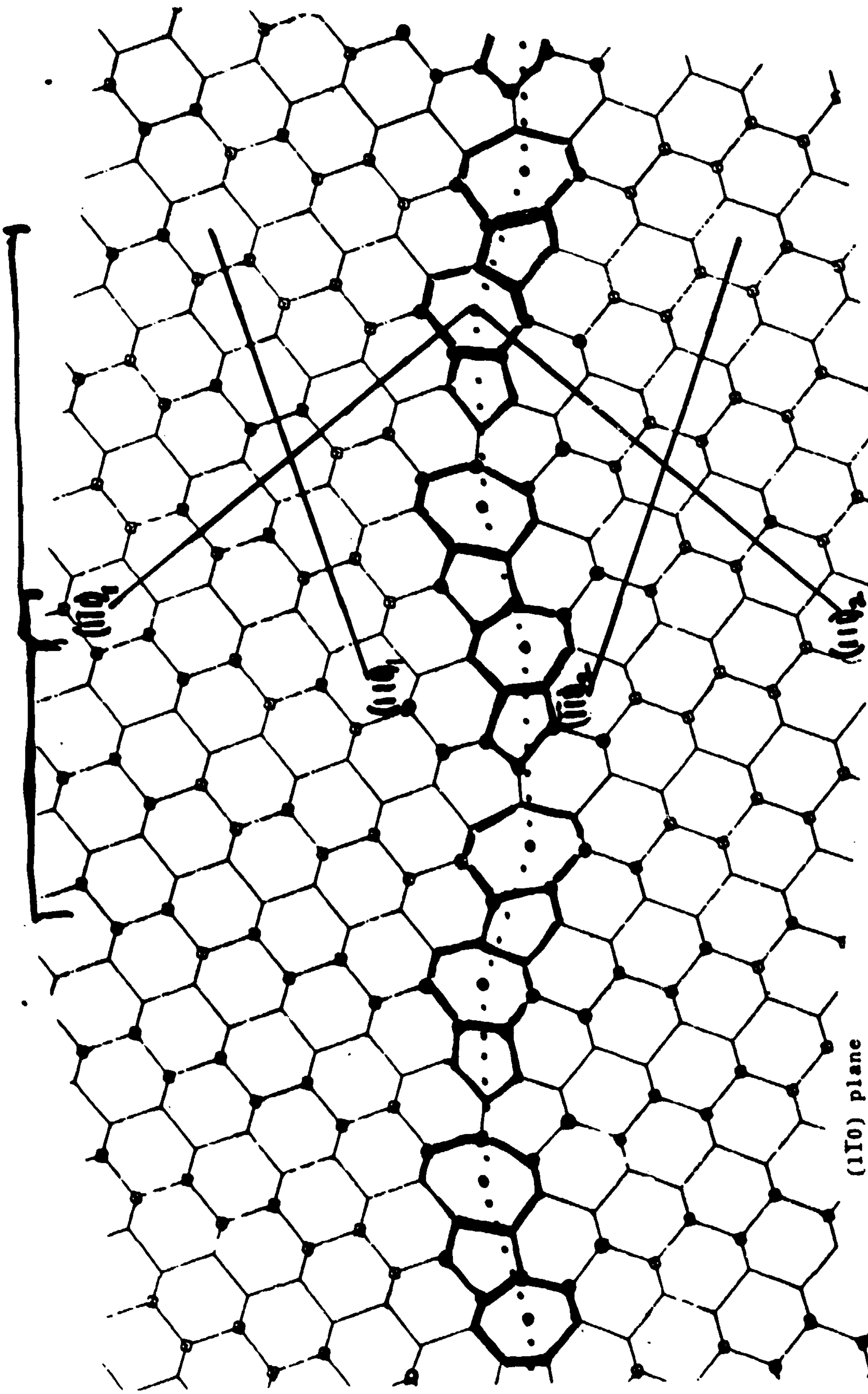

Proposed model for a $\Sigma = 5$, $\theta = 31.58^{\circ}$/ $[1\bar{1}0]_{1/2}$

GBP = $(552)_1$; $(\bar{5}\bar{5}2)_2$

ORIGINAL PAGE IS
OF POOR QUALITY

Hornstra, J.
1959

Physica 25
409-422

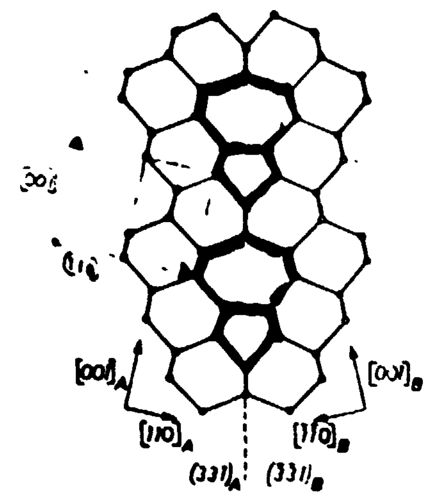

Fig. 5. Projection on (1$\bar{1}$0) of a symmetrical tilt boundary with tilt axis [110], angle of tilt θ_1 = 26°32′ and median plane (110). The height of the atoms above the plane of projection is expressed in $z = \frac{1}{4}a\sqrt{2}$, where a is the lattice constant.

53

J. Phys. Chem. Solids Pergamon Press 1958. Vol. 5, pp. 129-141.

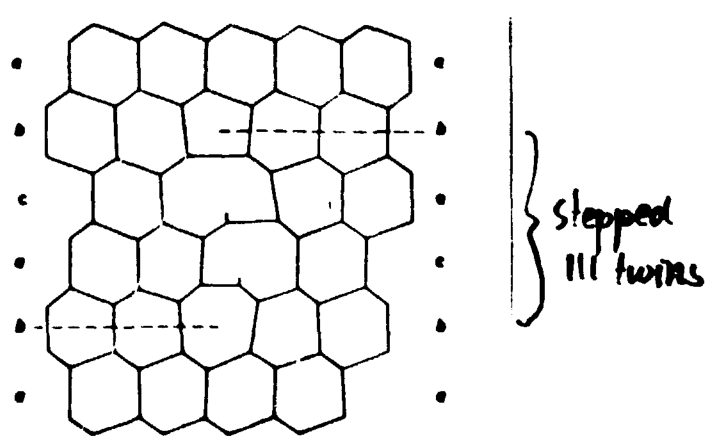

8. DISLOCATIONS AND TWIN BOUNDARIES

As has been shown in Fig. 13(c), a shift of the twin boundary involves a partial dislocation. A shift of one (double) atomic plane involves a partial of type I, a shift of two planes one of type II, a shift of three planes, however, involves a lattice defect of a different kind. The possible structure of it is shown in Fig. 19(a) for the diamond lattice and in Fig 19(b) for the f.c.c. lattice. It is no dislocation as its Burgers vector is zero.

Summary

SIGMA = 3

- o BOUNDARY PER SE NOT ELECTRICALLY ACTIVE
- o ELECTRICAL ACTIVITY CORRELATES WITH PRESENCE OF PARTIAL DISLOCATIONS.
- o PARTIAL DISLOCATIONS SHOW ENHANCED ACTIVITY COMPATIBLE WITH JOG MODEL
- o EVIDENCE FOR KINK ACTIVITY FROM CURVED PARTIALS.

SIGMA = 9

- o 111/115 TWIN SHARES HABIT PLANE WITH FIRST ORDER TWIN - FREQUENTLY MIS-IDENTIFIED AS THE LATTER.
- o ELECTRICAL ACTIVITY COMPATIBLE WITH BROKEN BOND MODEL.
- o ALTERNATING SECTIONS GIVE DOT-LIKE EBIC CONTRAST SIMILAR TO PARTIAL DISLOCATIONS IN FIRST ORDER TWINS.

SIGMA = 27

- o CHARACTER OF BOUNDARY DEPENDS ON BOUNDARY PLANE VARIES OVER SHORT DISTANCES (0.1 um).
- o UNSYMMETRIC GBP CORRELATED TO DISSOCIATED BOUNDARIES:

  SIGMA27 = SIGMA9 + SIGMA 3
- o MICROFACETTING IN ACCORDANCE WITH HORNSTRA.
- o UNDISSOCIATED BOUNDARY ON SYMMETRIC GBP HAS STRUCTURE OF 5 and 7 MEMBERED RINGS SHOULD LEAD TO GAP STATES.

Summary of Sigma = 27

- Undissociated 255/255 is symmetric. and located on second highest density CSL (highest 115/115)

- Dissociated section is un-symmetric.
  Components :Symmetric SIGMA 9 112/112
  (2 nd highest after 111/115)

- Largest facet is SIGMA 3 111/111 coherent twin

- Other facet probably 111/115

- 3 Step periodicity correlated to stacking sequence - Hornstra model of atomistic faceting. (Brockman).

Techniques

EBIC

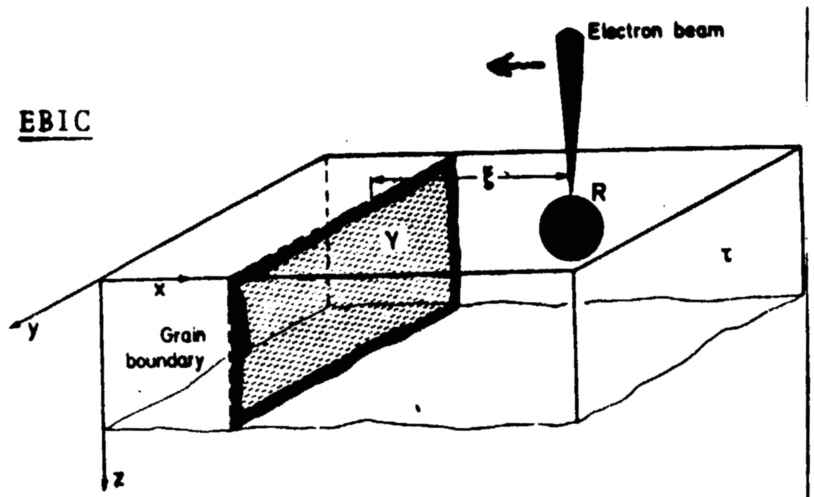

EBIC contrast of grain boundaries can be calculated by solving the 3-D diffusion equation under the following assumptions (J.Marek)

- o ∞ recombination velocity at the boundary plane
- o $R_p \gg$ depletion layer thickness.

Typical operation conditions for 10 cm Si

$d \approx 1\mu m$

$R_p \approx 6\mu m$ (30 Kev)

Maximum contrast when $R_p \approx L$.

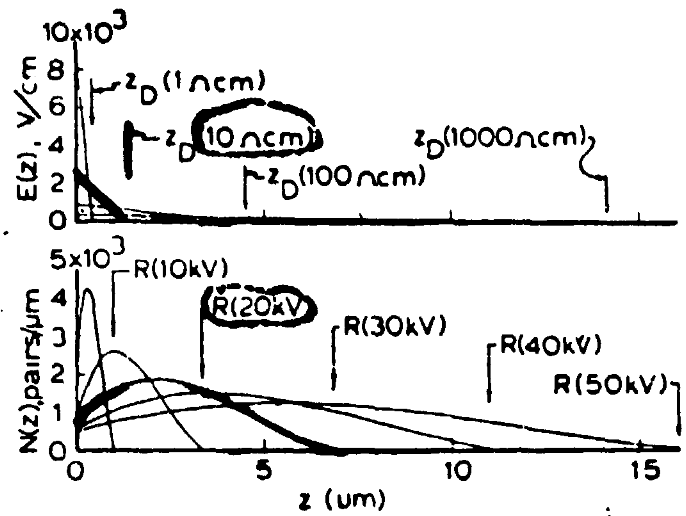

After Leamy et al.

$$R = \alpha E^{1.75}$$

Recent results indicate α may be twice as high as indicated above.

ORIGINAL PAGE IS OF POOR QUALITY

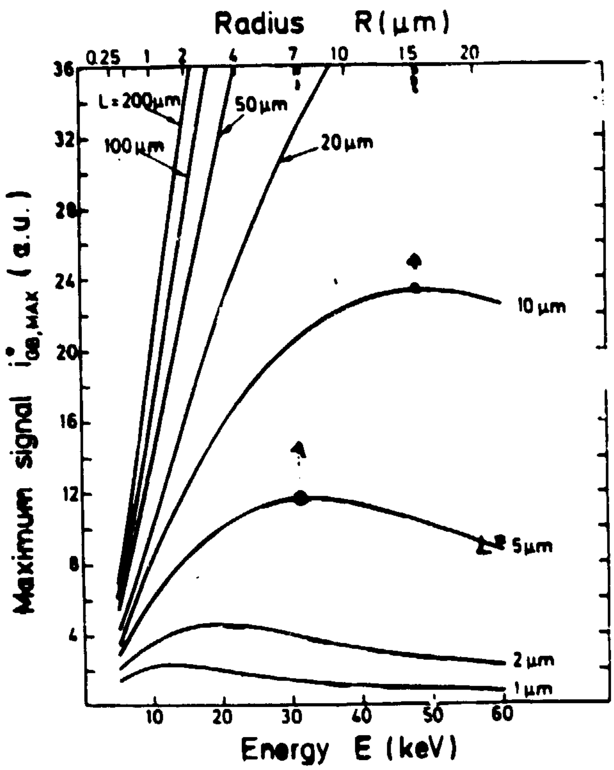

J.Marek

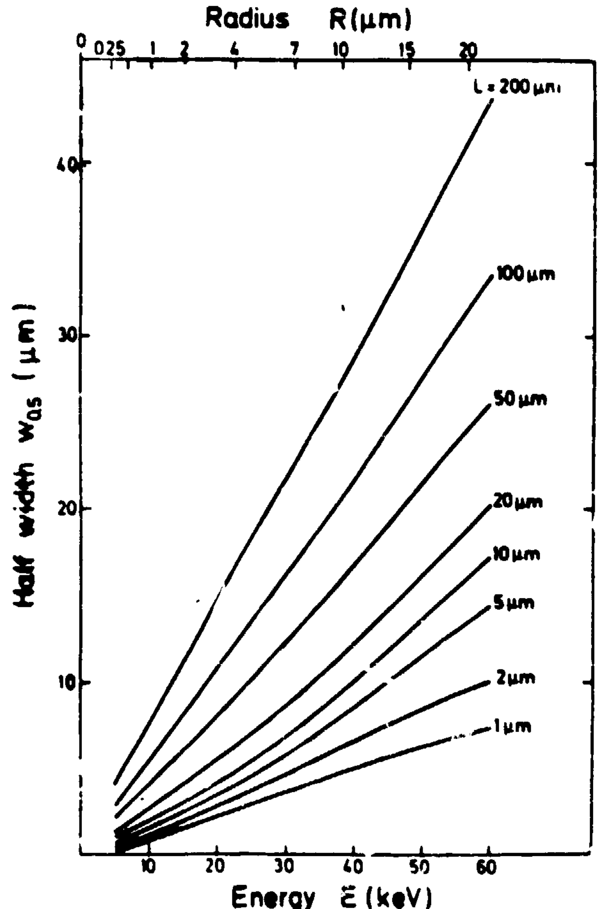

J.Marek

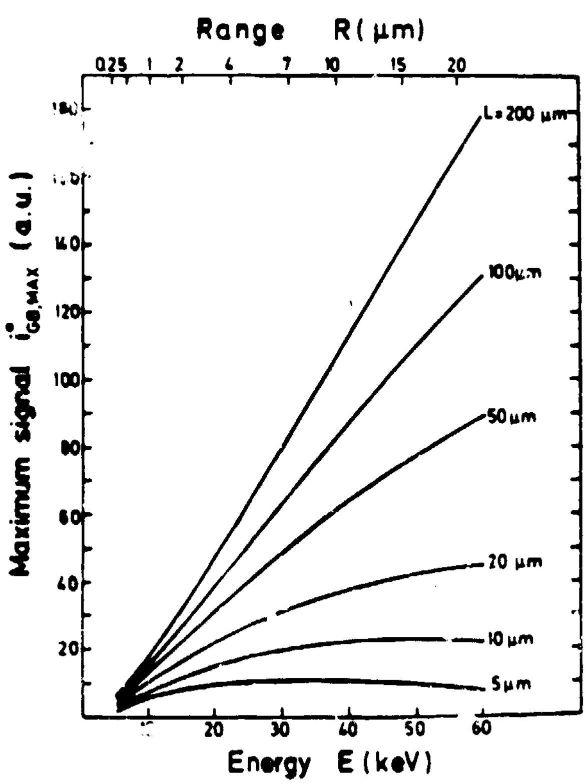

J.Marek

ORIGINAL PAGE IS
OF POOR QUALITY

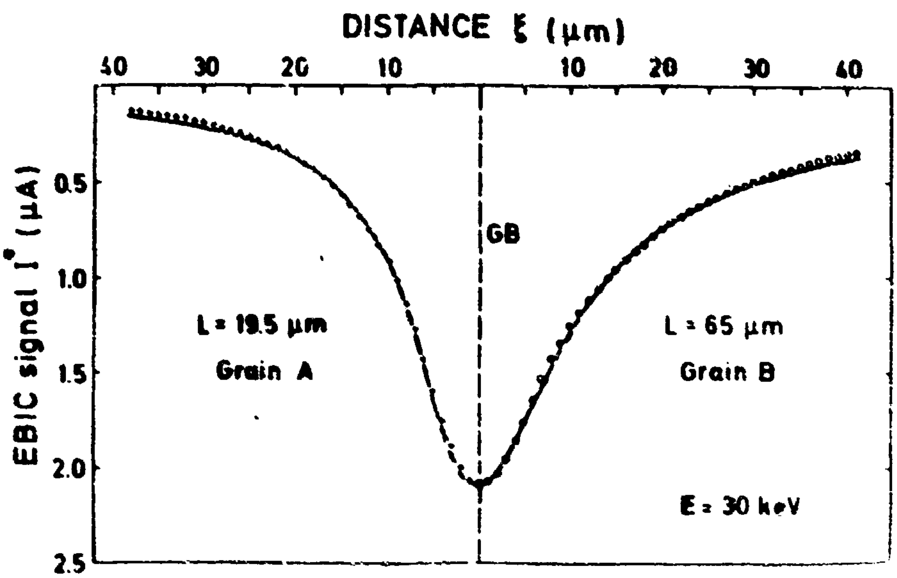

J.Marek

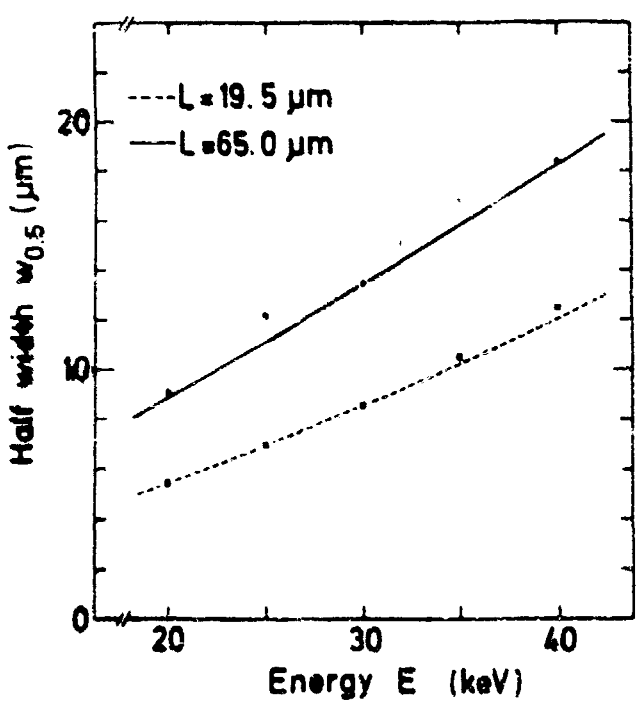

J.Marek

Web

- Contains one or several twin planes in center plane of ribbon

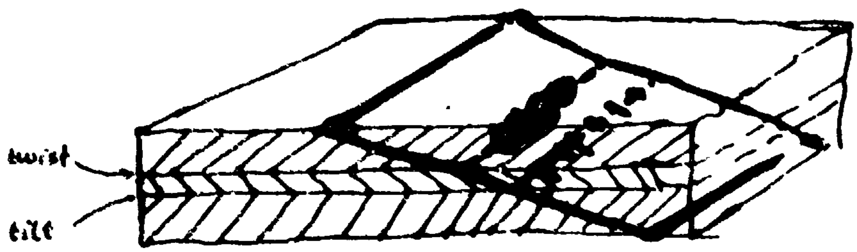

- Shallow bevel allows EBIC imaging of dislocation network on these twins

- Rotational misfit of seconds of arc results in sufficiently large spacing to be resolved by EBIC.

ORIGINAL PAGE IS
OF POOR QUALITY

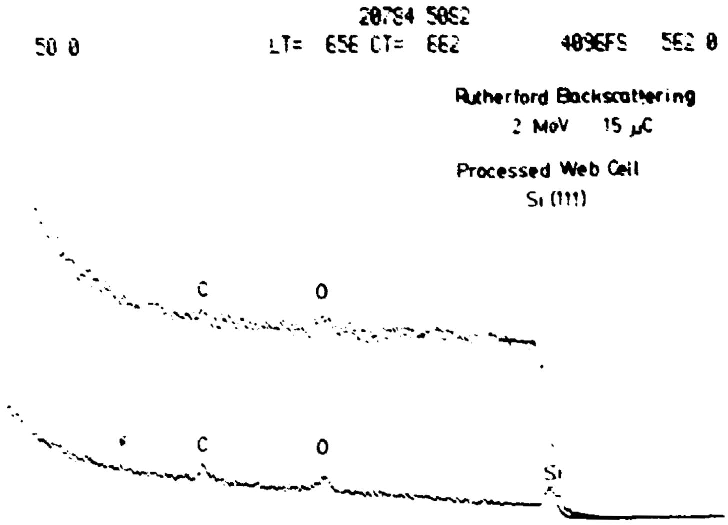

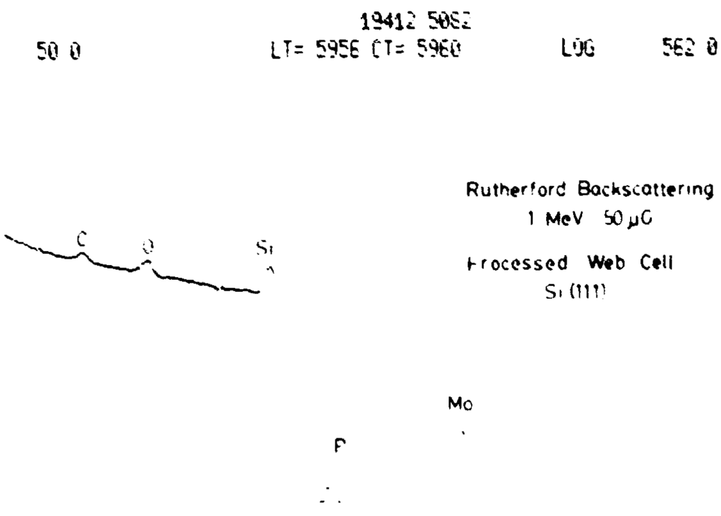

Problems and Concerns

- Statistics of Results .

Time and manpower restrictions confine analysis to a few specimen of a given material. Thus, some caution must be exercised when applying results to the population as a whole, especially for materials in which the crystal growth and processing techniques are continuously refined.

GRAIN BOUNDARY INVESTIGATION

JET PROPULSION LABORATORY

L.J. Cheng

Participants

LI-JEN CHENG

GERRY CROTTY

TAHER DAUD

KATHY DUMAS

SANDY HYLAND

TOM MacCONNELL

RINDGE SHIMA

CHIN-MIIN SHYU

KATE STIKA

Objective

TO DEVELOP BETTER POLYCRYSTALLINE SILICON SOLAR CELLS THROUGH BETTER UNDERSTANDING OF THE BEHAVIOR OF GRAIN BOUNDARIES IN SILICON

Approach

EXPERIMENTAL STUDIES ON SAMPLES OF

- LARGE GRAIN SILICON INGOTS (WACKER, SEMIX, AND HEM)
- CZ BICRYSTALS WITH CONTROLLED LATTICE MISMATCH

Subjects Under Study

- BICRYSTAL GROWTH
- ELECTRONIC TRANSPORT PHENOMENA
  - POTENTIAL BARRIER
  - CARRIER RECOMBINATION
  - TRAPPING STATES
- ATOMIC TRANSPORT PHENOMENA
  - ENHANCED DIFFUSION OF IMPURITIES
  - IMPURITY GETTERING
- EFFECTS ON SOLAR CELL PERFORMANCE

Energy-Band Diagram at Boundary Region for p-Type Si

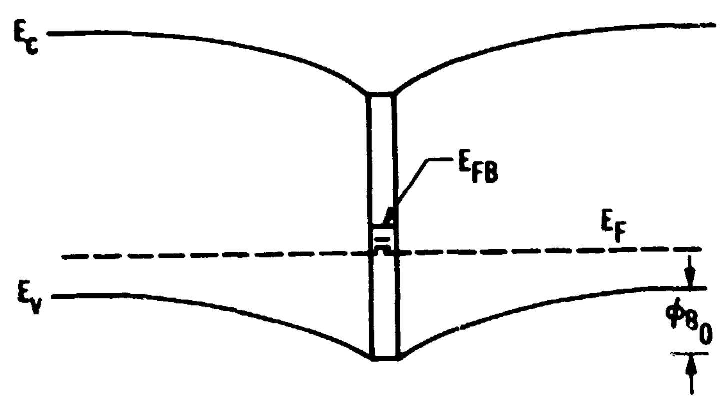

$$\phi_{B_0} = E_A + T\frac{\partial \phi_{B_0}}{\partial T} \qquad Q = \frac{\epsilon_0 \epsilon N_A}{C_0}$$

$$\phi_{B_0} = \frac{eQ^2}{8\epsilon_0 \epsilon N_A} \qquad Q = \int_{E_{FB}}^{E_F} d(E, \sigma)dE$$

Experimental Arrangement for Zero-Bias Conductance Measurements

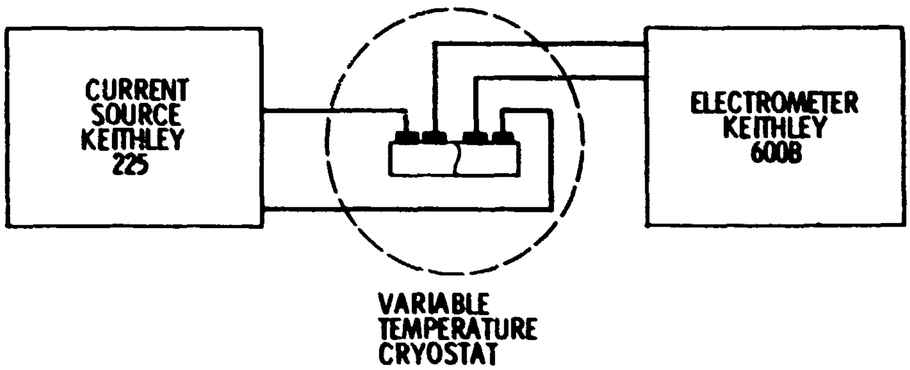

Temperature Dependence

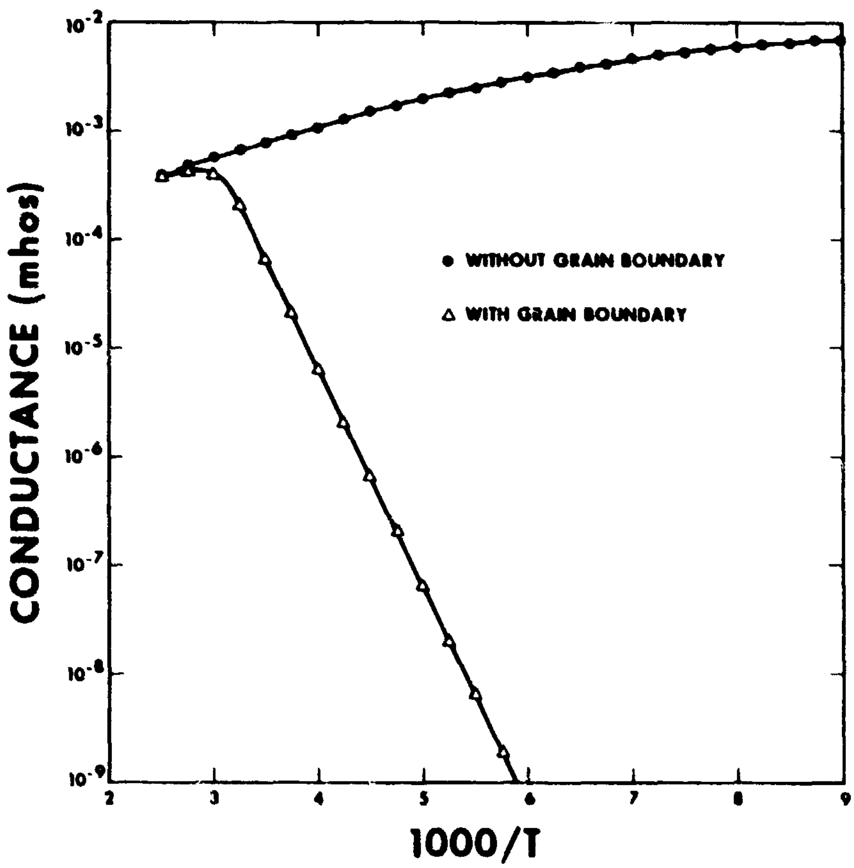

ORIGINAL PAGE IS
OF POOR QUALITY

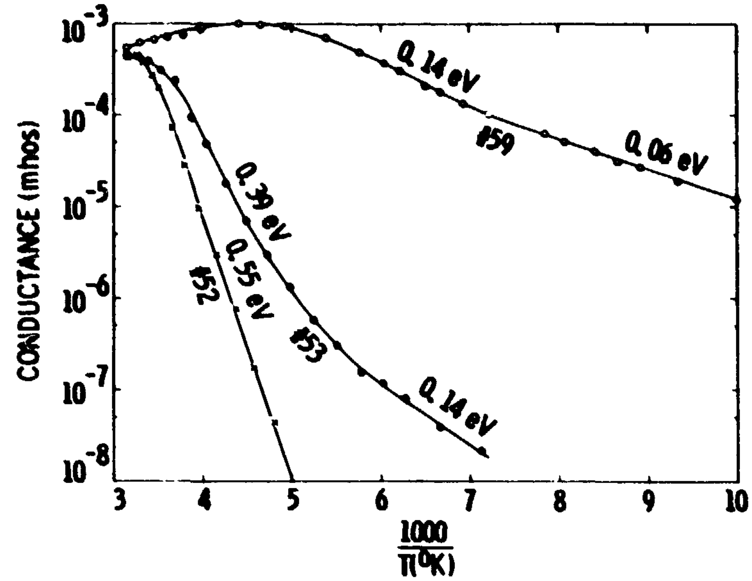

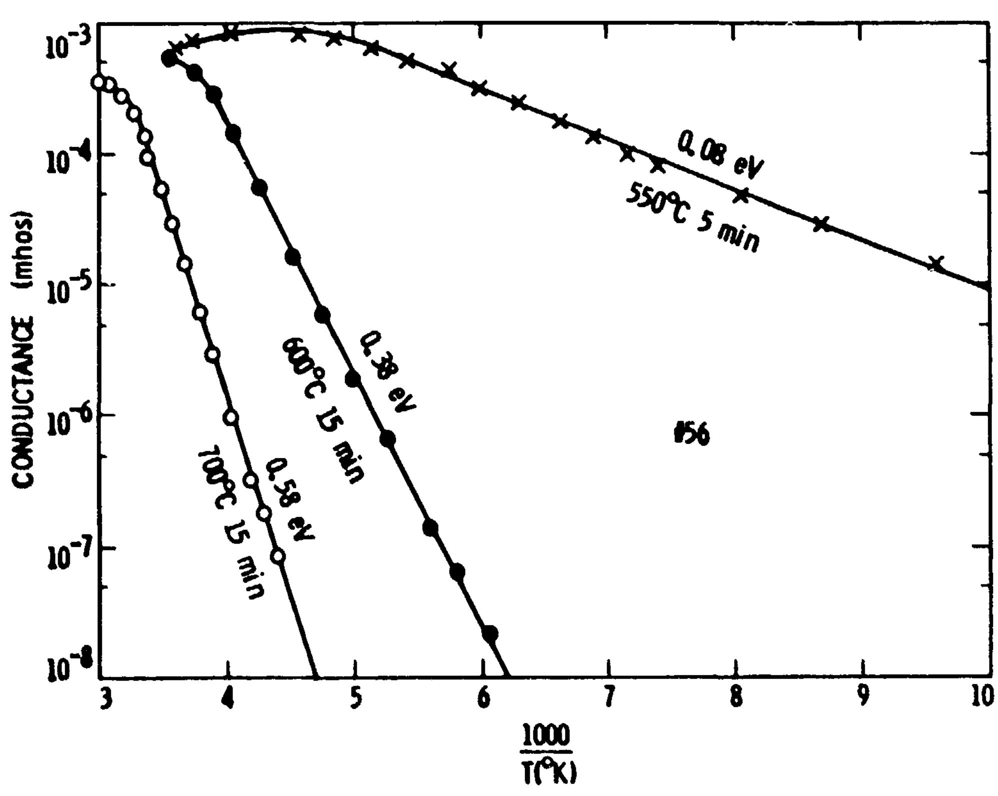

ORIGINAL PAGE IS OF POOR QUALITY

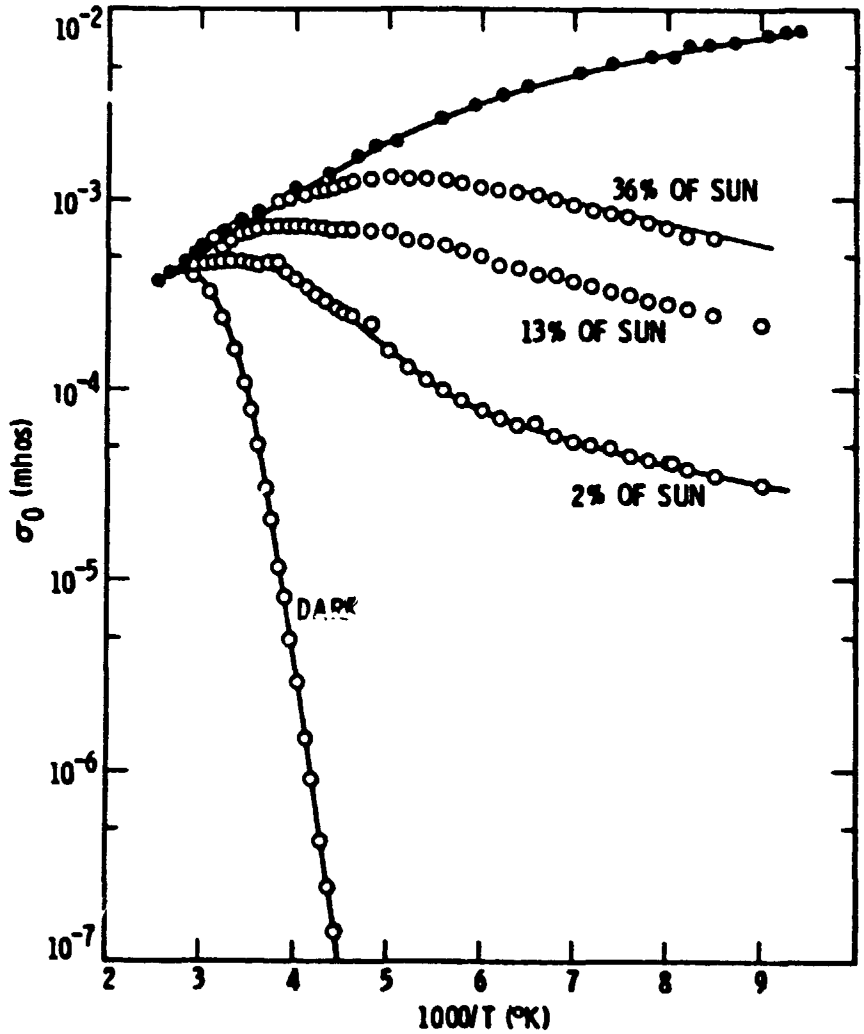

Potential Barrier

RESULTS:

- CONSIDERABLE VARIATION IN E_A ALONG GRAIN BOUNDARIES, PRESUMABLY DUE TO VARIATION OF LOCAL DISORDERS
- INCREASE OF E_A WITH ANNEALING TEMPERATURE, LIKELY DUE TO LOCAL DEFECT CHANGES AND IMPURITY GETTERING
- DECREASE OF ϕ_B WITH LIGHT INTENSITY, CAUSED BY MINORITY CARRIER TRAPPING

ORIGINAL PAGE IS
OF POOR QUALITY

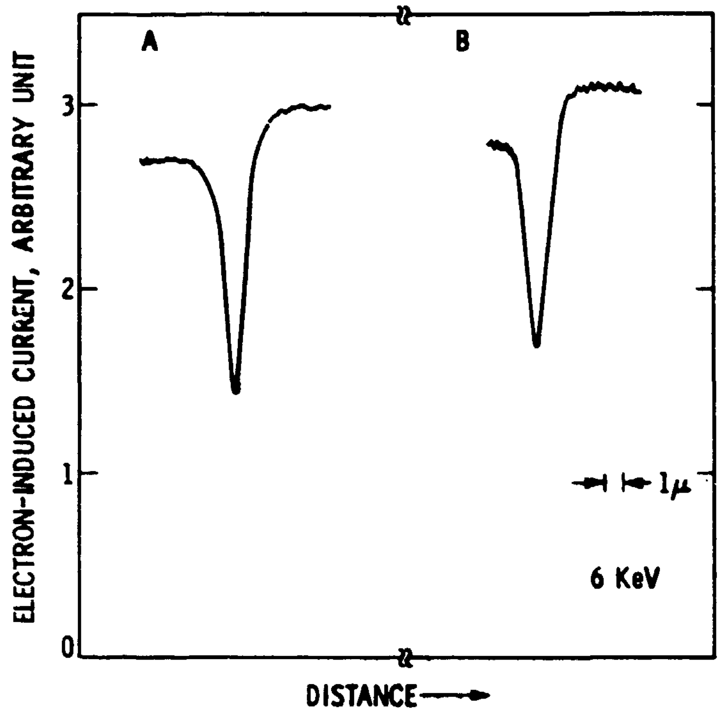

Experimental Arrangement for Photoconductivity Measurements

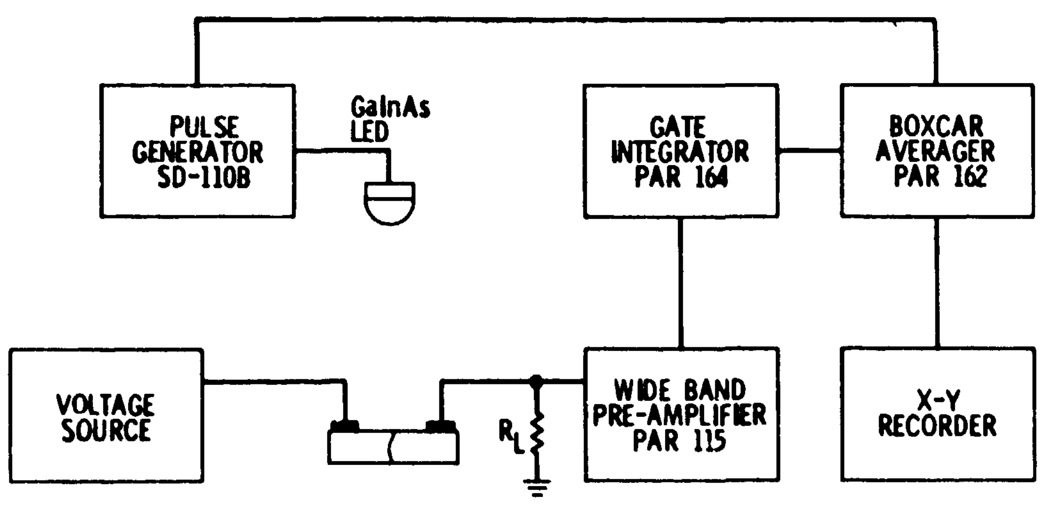

Light Effects on Grain Boundary Properties

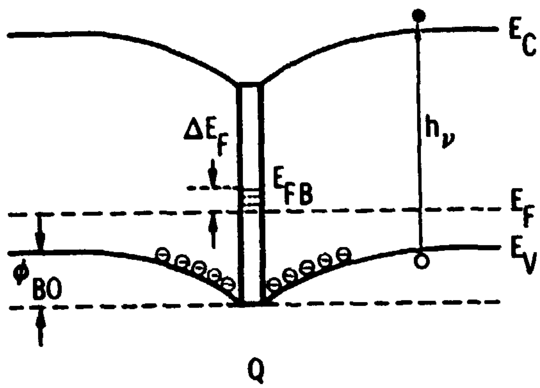

- DECREASE OF Q
- INCREASE OF G_0
- CREATION OF CARRIER RECOMBINATION CURRENT

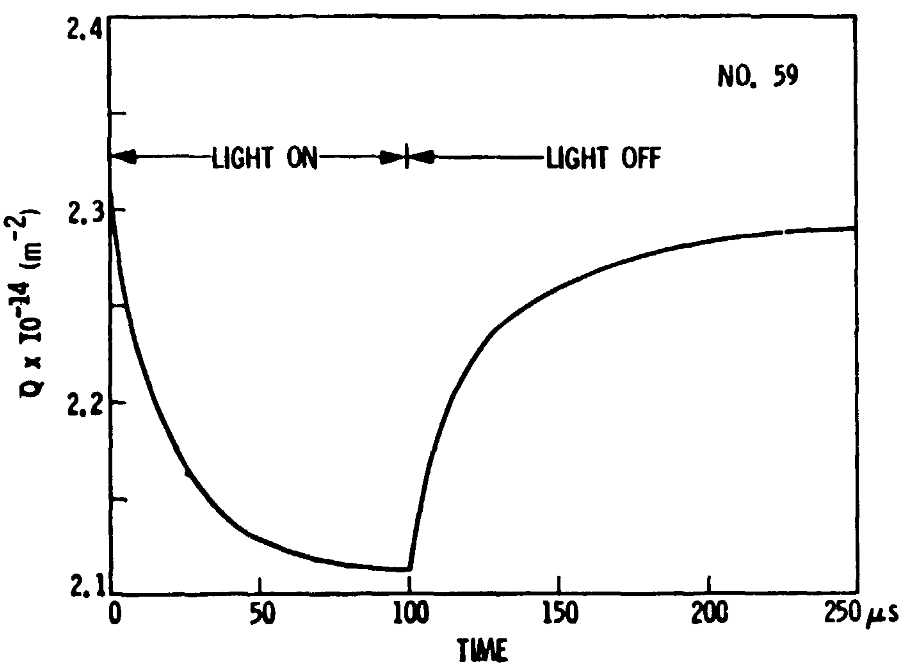

UNDER ILLUMINATION,

$$\frac{dQ}{dt} = J_{maj} - J_{min}$$

$(J_{maj} = J_{min}$ AT THE EQUILIBRIUM)

AND, IN THE DARK AFTER THE LIGHT IS OFF,

$$\frac{dQ}{dt} = J_{maj}'$$

WHERE

$$J_{maj} = (2cA - B)\exp(-(E_F + \phi_{B0})/kT)$$

$$J_{min} = \frac{D_e}{e L_e}(n_\infty - n_0)$$

RECOMBINATION VELOCITY AT THE GRAIN BOUNDARY

$$S = \frac{J_{min}}{e\, n_0}$$

Electrical Properties of Grain Boundaries

Sample No.	E_a (eV)	G_0 (mho/m^2)	ϕ_{B0} (eV)	Q ($/m^2$)	I*	S (m/s)
51	0.55	5.98×10^{2}	0.12	5.66×10^{14}	0.66I	2.5
					I	6.4
59	0.10	2.45×10^{3}	0.02	2.22×10^{14}	I	0.88
					1.8I	1.09

*I = Light intensity which creates an equilibrium minority carrier density of 1.08×10^{18} electrons/m^3 in the bulk of the sample.

Recombination Velocity

RESULTS:

- DEVELOPED A TECHNIQUE USING PHOTOCONDUCTIVITY IN CONJUNCTION WITH ϕ_{BO} (D) AND Q(D) MEASUREMENTS FOR THE MEASUREMENT OF MINORITY CARRIER RECOMBINATION VELOCITY AT THE GRAIN BOUNDARY

- OBSERVED INCREASES OF S WITH BOUNDARY STATE DENSITY AND LIGHT INTENSITY

Experimental Arrangement for DLTS Measurements

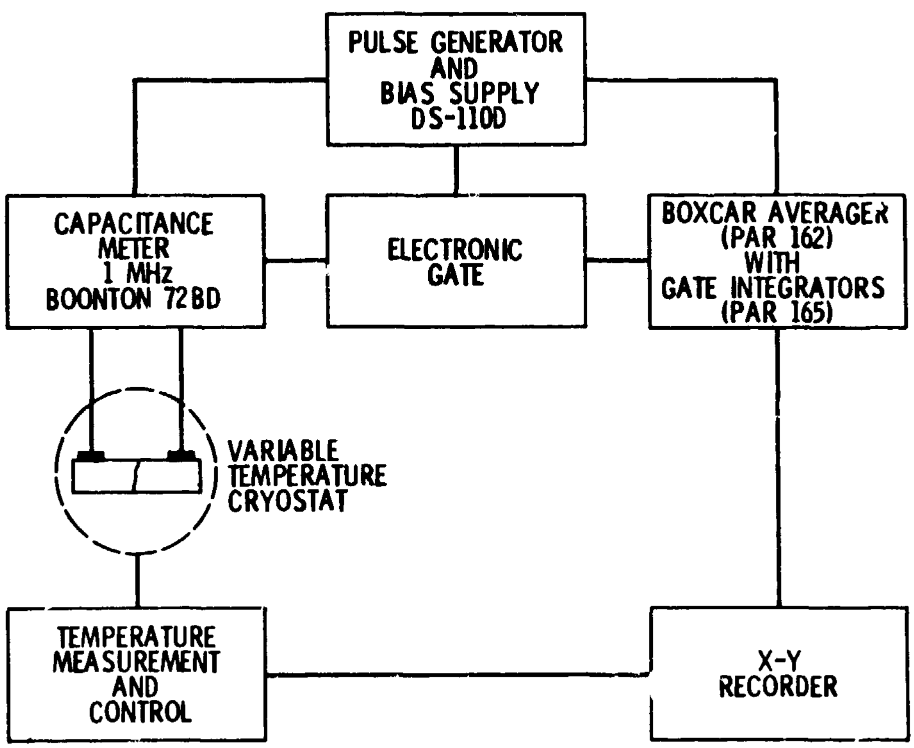

Pulse Width Dependence

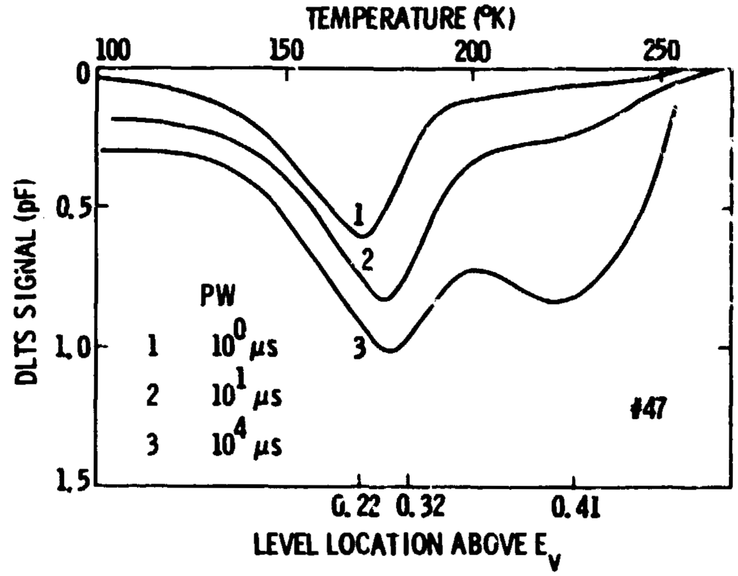

Distribution of the Density of States

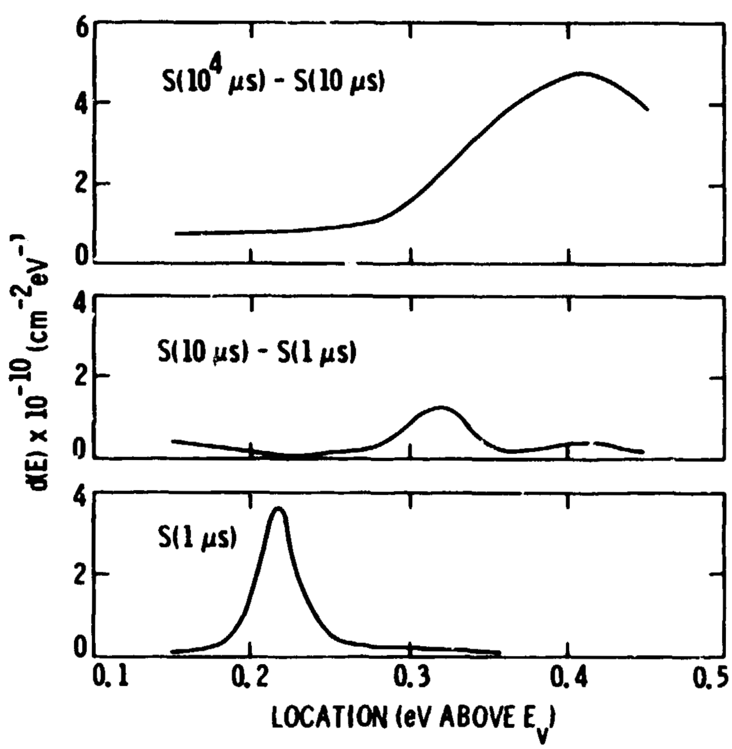

Electronic States

RESULTS:

- DEMONSTRATED THE APPLICATION OF DEEP LEVEL TRANSIENT SPECTROSCOPY (DLTS) IN THE STUDY OF ELECTRONIC STATES AT GRAIN BOUNDARIES OF SILICON
- OBSERVED A TREND THAT THE DENSITY OF GRAIN BOUNDARY STATES IS GENERALLY INCREASING WITH THE DISTANCE FROM THE EDGES OF THE BAND GAP. HOWEVER, THE DETAILS VARY CONSIDERABLY FROM SAMPLE TO SAMPLE WHICH CAN BE ATTRIBUTED TO LOCAL VARIATION OF DISORDERS

Cross Section of Phosphorus-Diffused Polycrystalline Silicon

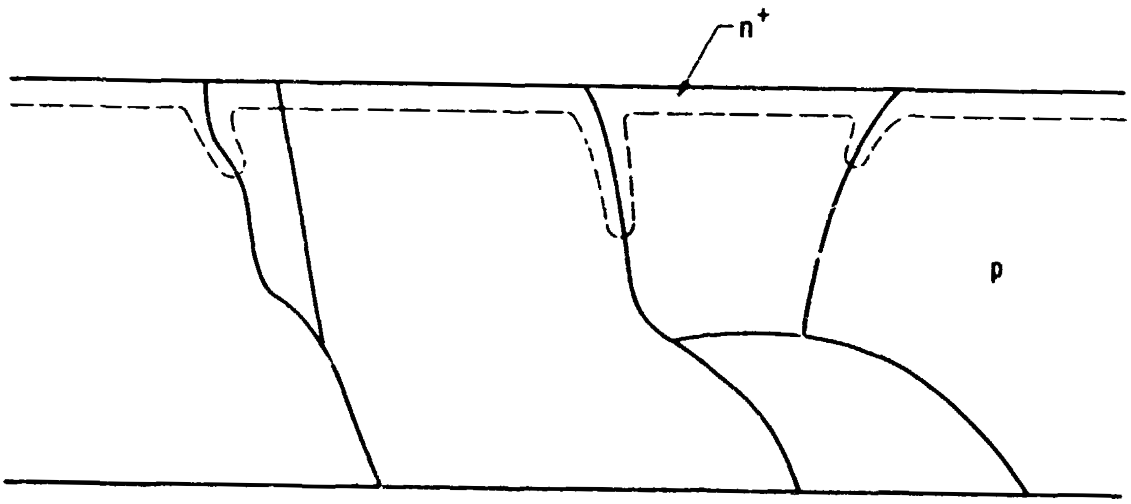

Cross Section of Grooved Sample at Grain Boundary

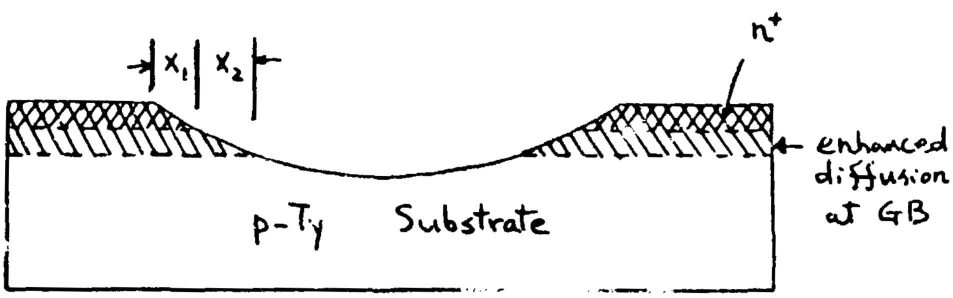

Staining ! F with light

Enhanced Diffusion of Phosphorus

GROOVED AND STAINED

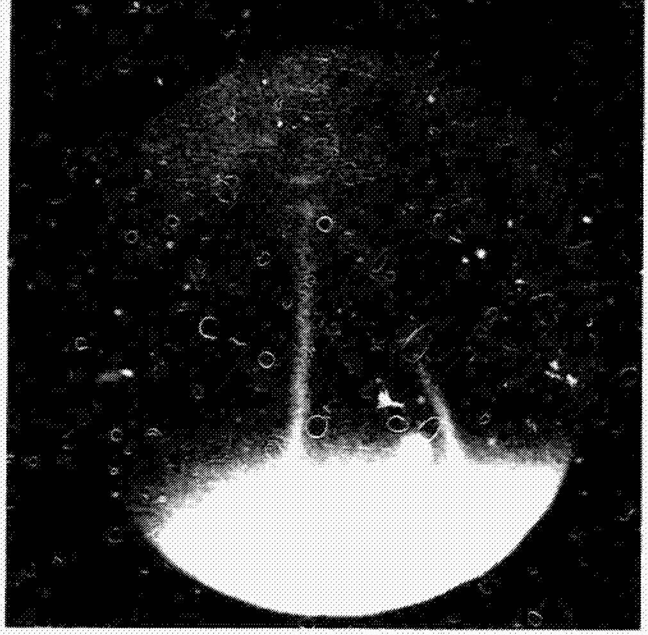

SiP^- ION IMAGE

Grooved and Stained

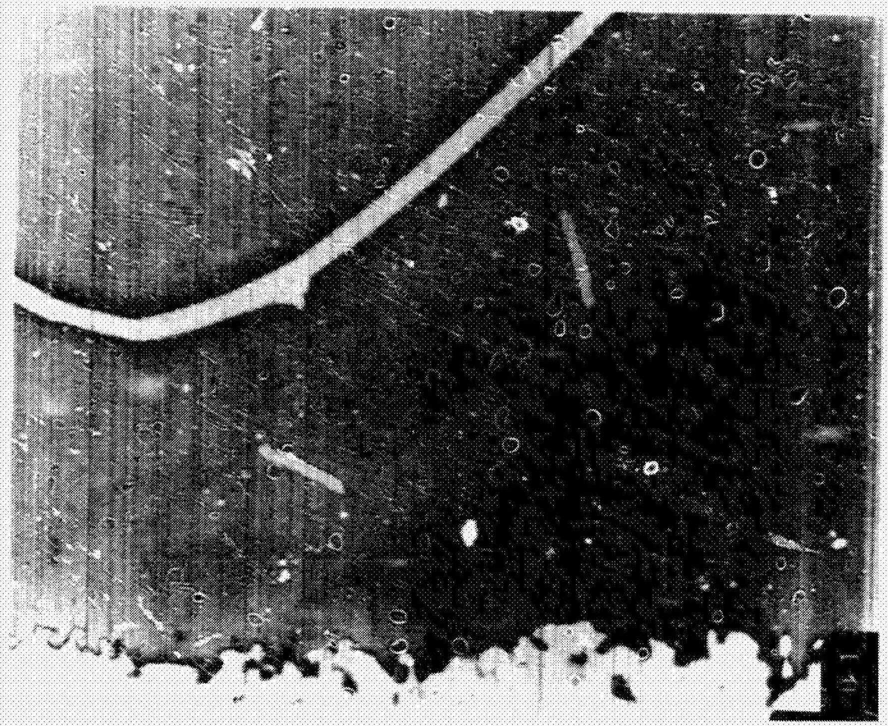

Sirtl-Etched

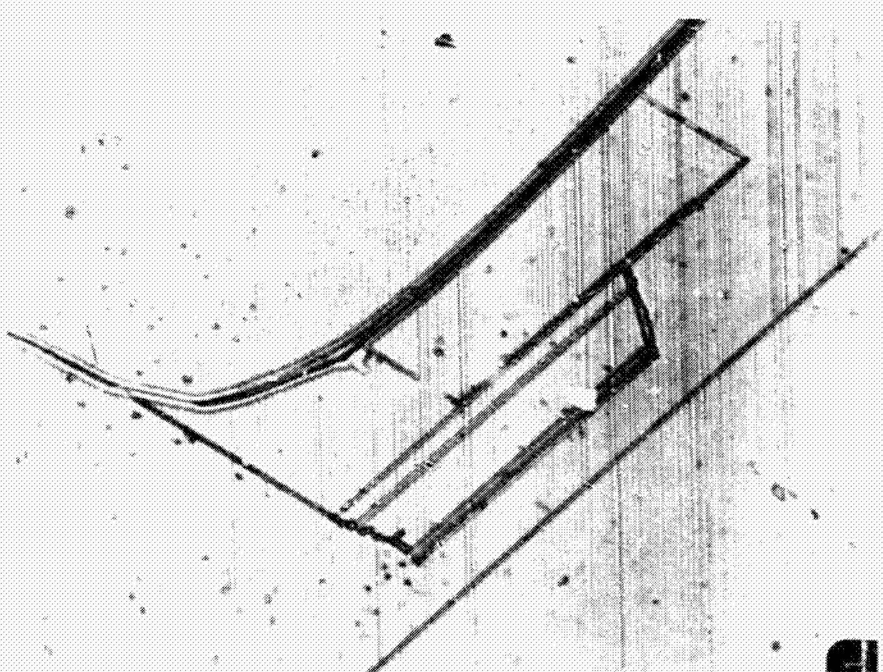

EBIC

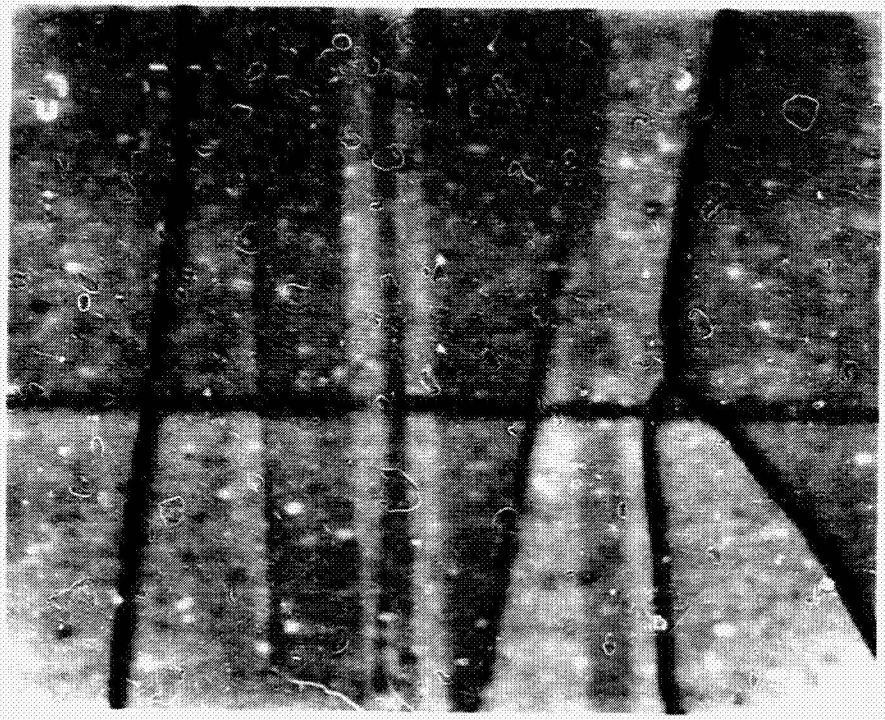

Grooved and Stained

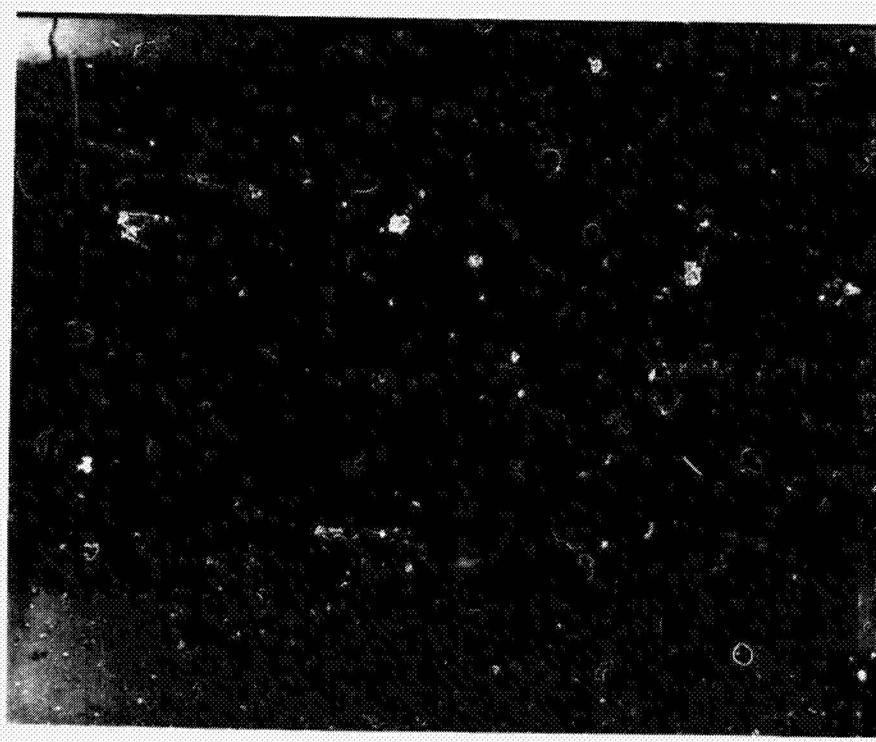

Depth of Diffused Regions at Grain Boundaries

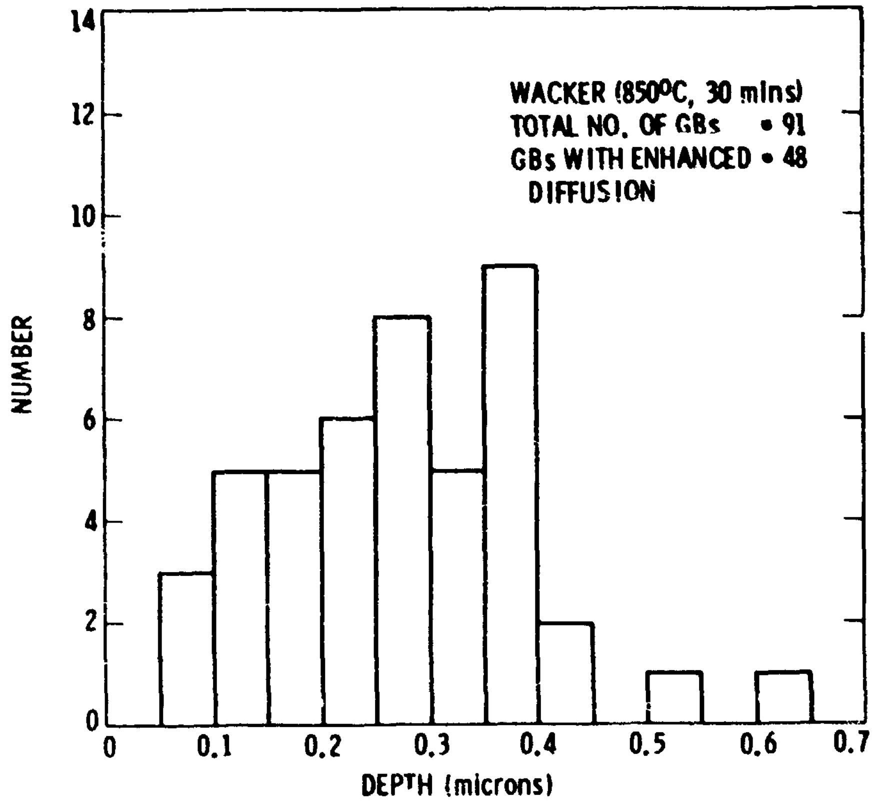

Enhanced Diffusion of Phosphorus

RESULTS:

- THE GROOVING AND STAINING TECHNIQUE IS A SUITABLE METHOD FOR THE OBSERVATION OF ENHANCED DIFFUSION OF PHOSPHOROUS AT GRAIN BOUNDARIES IN SILICON
- THE ENHANCED DIFFUSION OCCURS ONLY AT "HIGH-ORDER" GRAIN BOUNDARIES, GENERALLY ASSOCIATED WITH HIGH CARRIER RECOMBINATION
- THE DEPTH OF THE ENHANCED DIFFUSION VARIES DRASTICALLY FROM BOUNDARY TO BOUNDARY, WHICH MAKES THE QUANTITATIVE MEASUREMENT DIFFICULT UNLESS THE GRAIN BOUNDARY IS WELL CHARACTERIZED

Present Activities and Plans

- DENSITY OF STATES, RECOMBINATION VELOCITY, AND BARRIER HEIGHT AS FUNCTIONS OF LATTICE MISMATCH AND PROCESS PARAMETERS (INCLUDING PASSIVATION)
- QUANTITATIVE STUDIES ON ENHANCED DIFFUSION OF PHOSPHOROUS
- IMPURITY BEHAVIOR (e.g., CARBON, AND OXYGEN)
- EFFECTS ON SOLAR CELL PERFORMANCE

ORIGINAL PAGE IS
OF POOR QUALITY

STUDY OF ABRASIVE-WEAR RATE OF SILICON

UNIVERSITY OF ILLINOIS AT CHICAGO

J. Clark
D.S. Lim
S. Danyluk

TECHNOLOGY	REPORT DATE
Materials Properties Modification	April 22, 1982
APPROACH An experimental program is carried out to study the fundamental mechanisms of abrasion and wear, and deformation of silicon by a single crystal diamond in various fluid environments. **CONTRACTOR** University of Illnois at Chicago **GOALS** Develop a model for surface-mechanical property modification of silicon under the influences of fluid environments	**STATUS** The abrasion rate and depth of damage of (100) and (111) p-type silicon in three fluid environments has been determined. The surface deformation mechanism was found to change when the fluid was varied. The diamond geometry affects the wear rate. There appears to be a correlation between the wear rate and the dielectric constant of the fluid. The brittle lateral crack model does not appear to describe the wear rates measured.

Introduction

Optical and scanning electron microscopy are used to determine the wear rate and deformation mechanism of diamond abrading (100) and (111) Cz silicon in water, ethanol and acetone. A multi-scratch experiment is used to determine the effects of normal force on the abrading diamond and fluid on the abrasion rate and depth of damage. These results are compared with a lateral crack model of abrasion of brittle materials.

Variables

Fluid, Temperature, Voltage, Photo-Irradiation, Normal Force (F_N), Orientation, Abrasion Speed.

Data

Groove depth vs. variables, SEM of groove surface, depth of damage.

Analysis

Stress analysis, depth of damage, lateral crack model.

Summary of Results

1. Wear rate varies by ~100% (acetone; ethanol; water).
2. Depth of damage larger for water than ethanol.
3. (100) and (111) wear rates are different.
4. Dielectric constant of the fluid related to the silicon hardness.
5. Lateral crack model describes wear rate when $F_N \gtrsim 60$ g.

ORIGINAL PAGE IS
OF POOR QUALITY

Changes in Surface Hardness of Silicon

Reference	Effect	Percent Softening	Comments
Kuczynski and Hochman	Photon irradiation	70% softening	Intensity and surface preparation important; microhardness test
Ablova	H_2O adsorption	Softening	Surface preparation and impurity content important; microhardness test
Westbrook and Gilman	Potential between indenter and crystal	60% softening	Disappeared at elevated temperatures; microhardness test
Yost and Williams	NaCl and $Na_4P_2O_7$	50-80% softening depending on concentration	Zeta-potential measurements of crushed silicon
Cuthrell	CCl_4 and H_2O adsorption	Not determined	Adsorption changed mode of drilling
This work	H_2O, ethanol, acetone adsorption	Up to 70% softening dependent on type of fluid and F_N	Pyramid diamond scratch test

ORIGINAL PAGE IS
OF POOR QUALITY

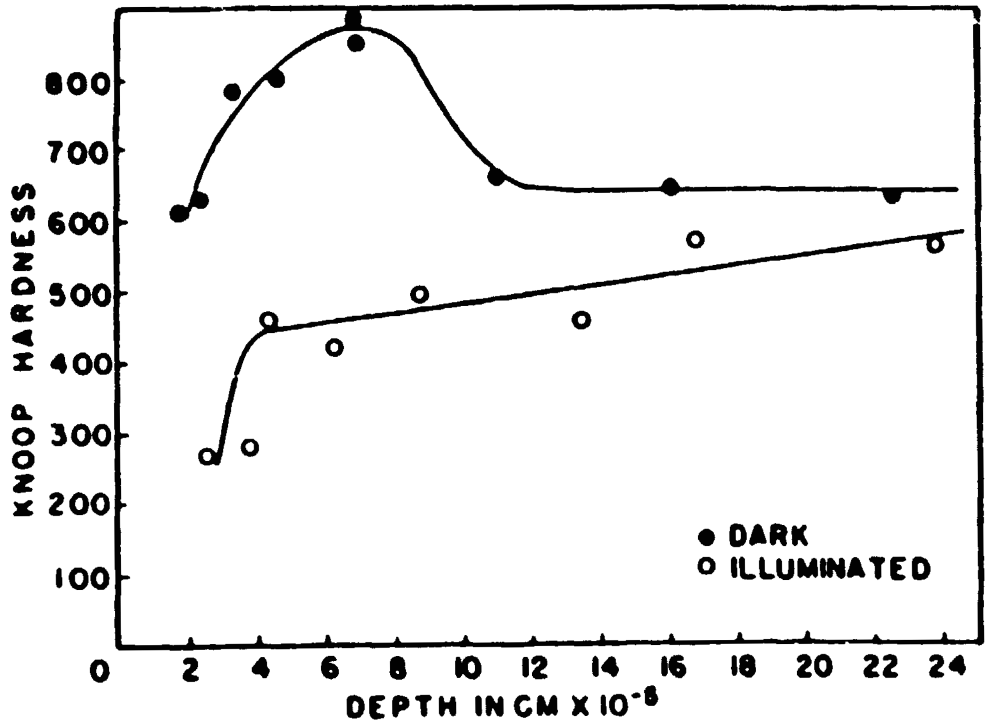

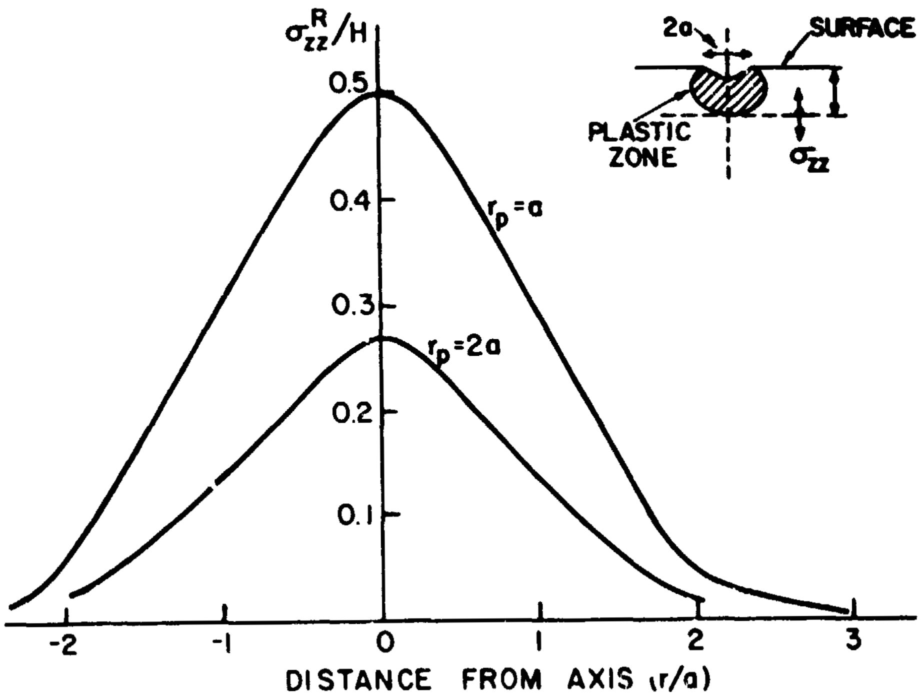

The spatial dependence of the residual tensile stress along a plane through the intersection of the plastic zone with the penetration axis: the stresses were estimated from an analytic elastic/plastic solution for a spherical cavity and an elastic solution for a half space.

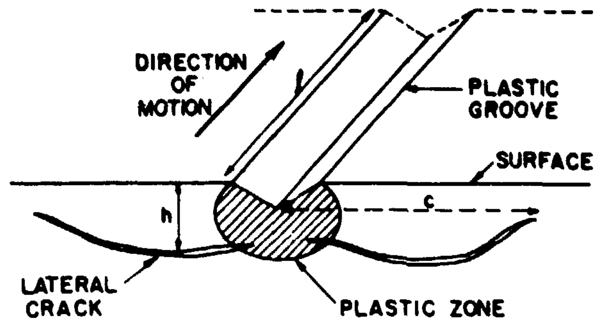
DIRECTION
OF
MOTION
PLASTIC
GROOVE
SURFACE
h
c
LATERAL
CRACK
PLASTIC ZONE

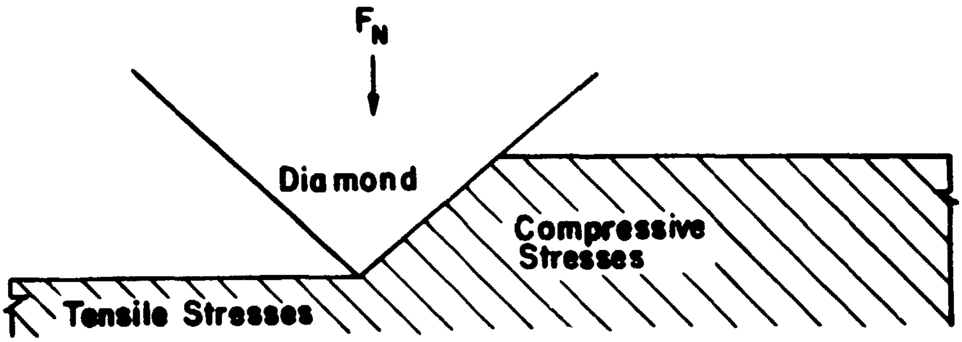
F
N
Diamond
Compressive
Stresses
Tensile Stresses

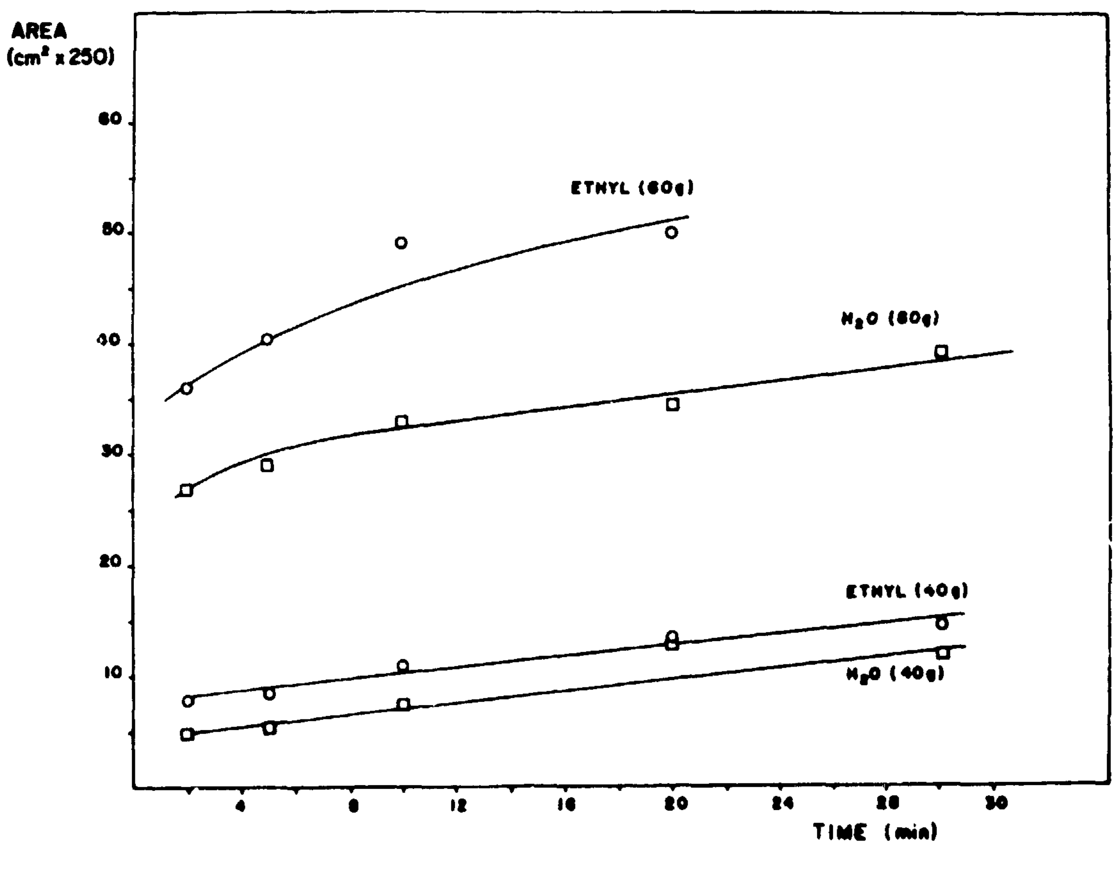
AREA
(cm² x 250)
60
50
40
30
20
10
ETHYL (60g)
H₂O (60g)
ETHYL (40g)
H₂O (40g)
4
8
12
16
20
24
28
TIME (min)

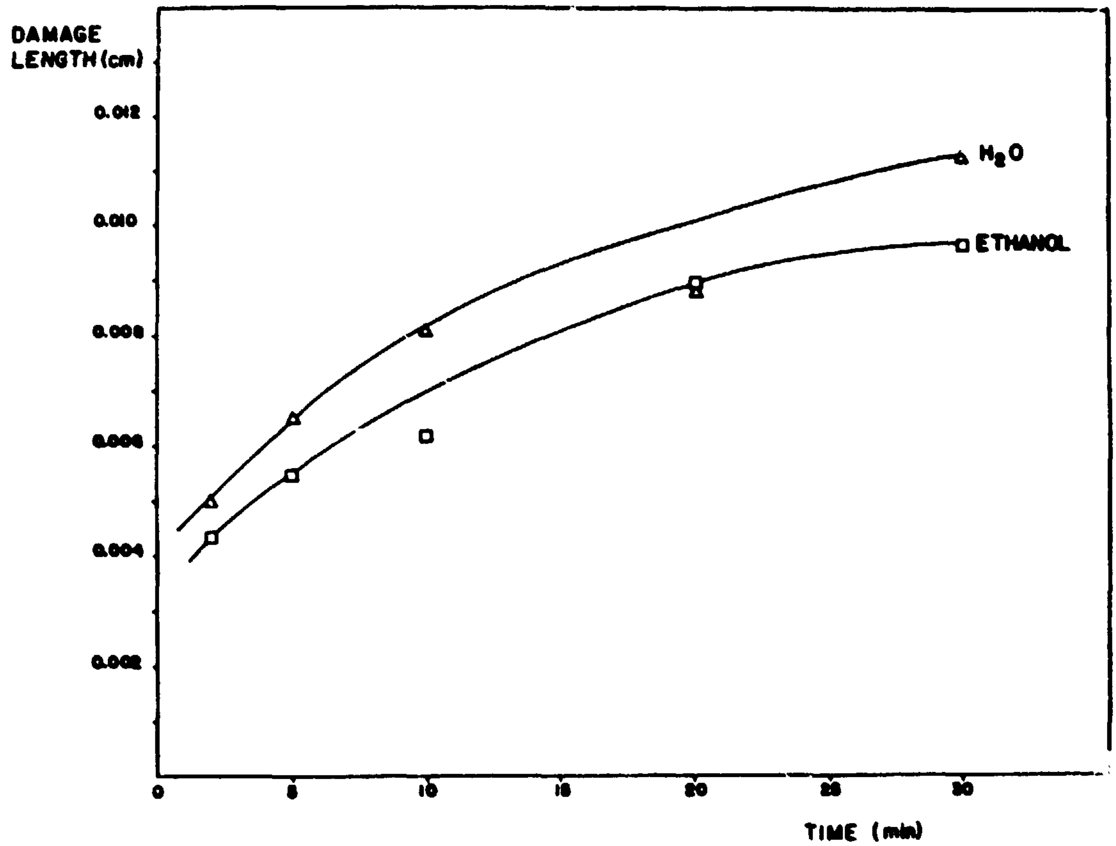
DAMAGE
LENGTH (cm)
0.012
0.010
0.008
0.006
0.004
0.002
H_2O
ETHANOL
0
5
10
15
20
25
30
TIME (min)

Depth of Damage From Single Scratch Abrasion on Silicon

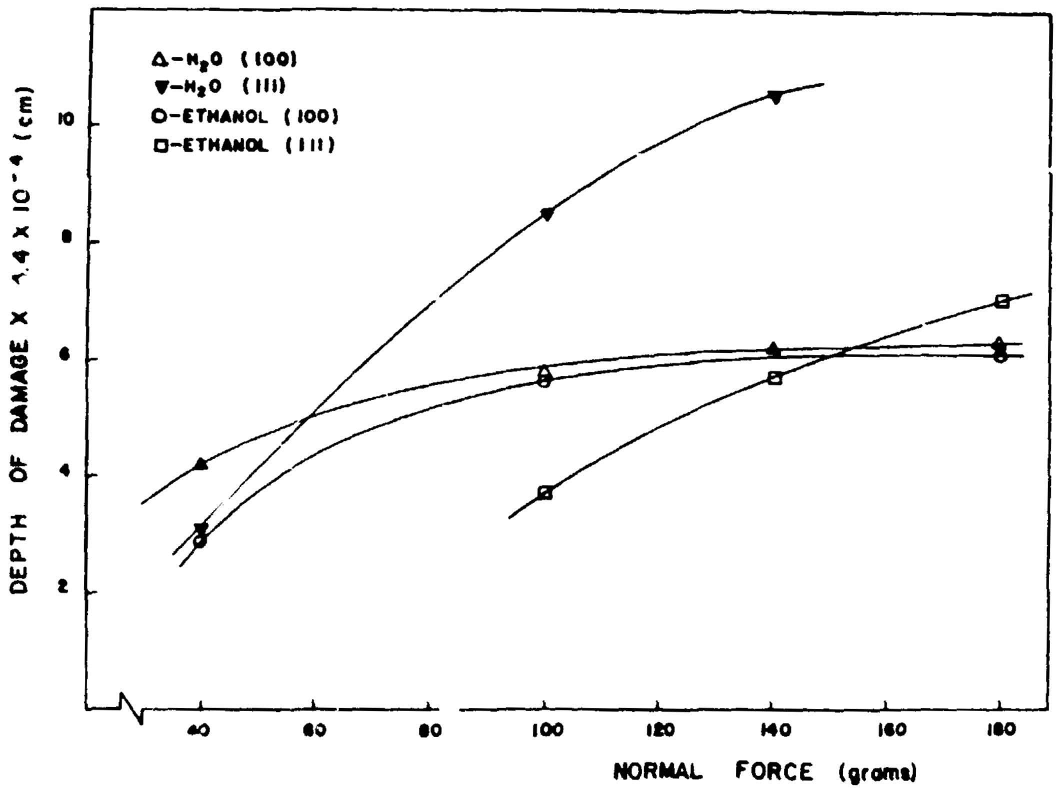

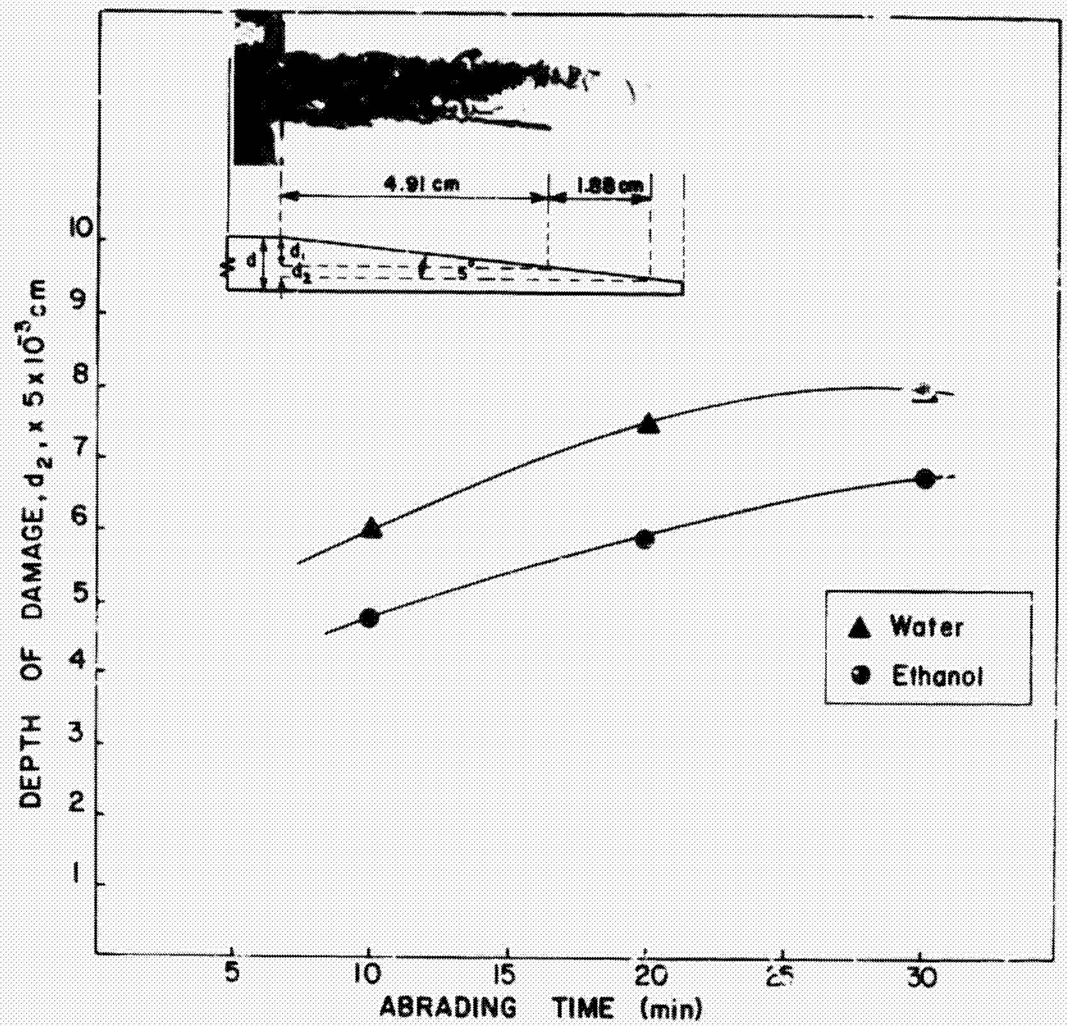

Depth of Damage in (100) p-Type Silicon Formed by a Diamond at Room Temperature vs Abrasion Time (min.). The Fluid Environment Was Varied. The Normal Force Was F_N = 40 g.

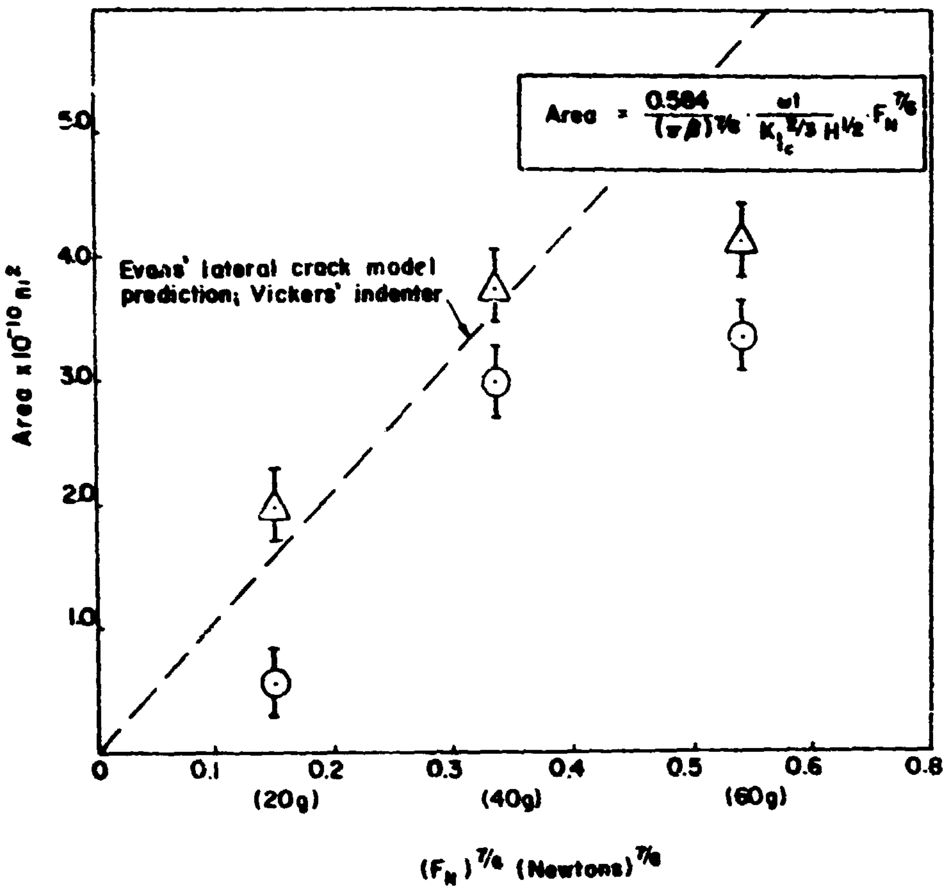

Problems and Concerns

The diamond geometry changes during the abrasion experiments due to microcracking at the diamond surface.

The diamond vibration must be stabilized.

The temperature at point of contact between the diamond and the silicon is unknown.

SOLAR CELL FABRICATION AND ANALYSIS

APPLIED SOLAR ENERGY CORP.

TECHNOLOGY	REPORT DATE
SOLAR CELL FABRICATION & ANALYSIS	APRIL 22, 1982
APPROACH 1) FABRICATION OF SOLAR CELLS BY BASELINE & ADVANCED PROCESSES POSSIBLY INCLUDING GETTERING AND ANNEALING. 2) ANALYSIS USING DARK AND LIGHT I-V, DIFFUSION LENGTH MEASUREMENTS, SPECTRAL RESPONSE. **CONTRACTOR** APPLIED SOLAR ENERGY CORPORATION	**STATUS**
GOALS 1) AN UNDERSTANDING OF THE MECHANISMS THAT LIMIT THE EFFICIENCIES OF SOLAR CELLS MADE FROM VARIOUS SILICON SHEETS. 2) AN UNDERSTANDING OF THE EFFECT ON SOLAR CELL EFFICIENCY OF VARIATIONS IN GROWTH PARAMETERS.	

1. EFG (MOBILE TYCO)

   10 CM WIDE MATERIAL GROWN WITH OR WITHOUT CO_2.

2. UCP (SEMIX)

   HIGH EFFICIENCY PROCESS ON MATERIAL FROM INGOT 5464-13C.
   MORE SEVERE GETTERING ON MATERIAL FROM INGOT 5464-13C.
   10 CM X 10 CM CELLS ON MATERIAL FROM RANDOM SOURCES.

3. HEM (CRYSTAL SYSTEM)
   MORE SEVERE GETTERING ON MATERIAL FROM INGOTS 4141C AND 4148.

Summary of Solar Cells Made From EFG 17-200 Series

		Voc (mV)	Jsc (mA/cm)	OFF (%)	(%)	REMARKS
17-200-1A (4 CELLS)	AVE.	495	22.5	71	7.9	CO_2 OFF
	S.D.	±10	±1.5	±4	±.7	
	RANGE	480-504	20.2-23.6	65-73	7.1-8.6	
17-200-113 (2 CELLS)	AVE.	515	23.0	76	9.0	CO_2 ON
	S.D.	±7	±1.2	±1	±.5	
	RANGE	510-520	22.1-23.8	75-77	8.6-9.3	
17-200-1D (3 CELLS)	AVE.	529	24.2	74	9.4	
	S.D.	±5	±.2	±3	±.4	
	RANGE	524-534	24.0-24.3	70-76	9.0-9.7	
17-202-1C (4 CELLS)	AVE.	505	22.6	73	8.3	
	S.D.	±17	±1.6	±1	±.9	
	RANGE	486-516	20.8-24.2	72-74	7.4-9.2	
17-203-1D (2 CELLS)	AVE.	499	21.0	73	7.7	
	S.D.	±1	±.3	±1	±.3	
	RANGE	498-500	20.8-21.?	72-74	7.5-7.9	
17-203-1E (2 CELLS)	AVE.	487	19.8	71	6.9	
	S.D.	±7	±1.4	±4	±.2	
	RANGE	482-492	18.8-20.8	68-74	6.7-7.0	
ACCUMULATIVE AVE OF "CO_2 ON" CELLS (13 CELLS)		508	22.4	73	8.4	

C2 CONTROL (4 CELLS)	AVE.	583	27.9	78	12.6
	S.D.	±2	±.4	±1	±.2
	RANGE	580-584	27.4-28.3	77-7S	12.3-12.9

ORIGINAL PAGE IS
OF POOR QUALITY

Summary of Solar Cells Made From 17-175 Series

		VOC (mV)	Jsc (mA/cm)	CFF (%)	(%)	REMARKS
17-175-1A-2 (7 CELLS)	AVE	519	21.2	72	7.9	CO_2 OFF
	S.D.	±8	±1.15	5	±.8	
	RANGE	504-530	19.8-22.8	62-75	6.4-9.0	
17-175-1A-6 (5 CELLS)	AVE	493	20.1	61	6.2	
	S.D.	±34	±1.2	±16	±2.1	
	RANGE	434-518	19.4-21.8	61-74	2.7-8.3	
ACCUMULATIVE AVERAGE OF "CO_2 OFF" CELLS (12 CELLS)		508	20.7	67	7.2	
17-175-1E-52 (8 CELLS)	AVE	539	22.3	73	8.9	CO_2 ON
	S.D.	±12	±2.1	±3	±1.1	
	RANGE	516-554	19.3-24.7	68-77	7.0-10.[illegible]	
17-175-1E-56 (6 CELLS)	AVE	505	21.3	59	6.4	
	S.D.	+40.4	+2.4	+15	+2.2	
	RANGE	432-546	17.6-22.6	35-70	3.4-9.1	
ACCUMULATIVE AVERAGE OF "CO_2 ON" CELLS (14 CELLS)		524	21.9	67	7.8	

CZ CONTROL (4 CELLS)	AVE	585	28.2	75	12.4
	S.D.	±2	±.6	±3	±.4
	RANGE	582-586	27.5-28.9	71-78	12.0-12.7

Distribution of J_{SC} on EFG Ribbon 17-175-1E-52

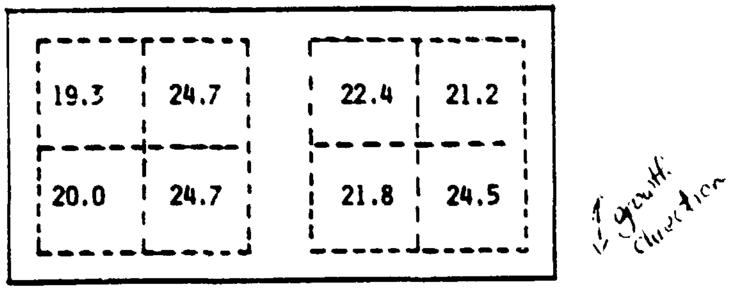

UCP Ingot No. 5848-13C

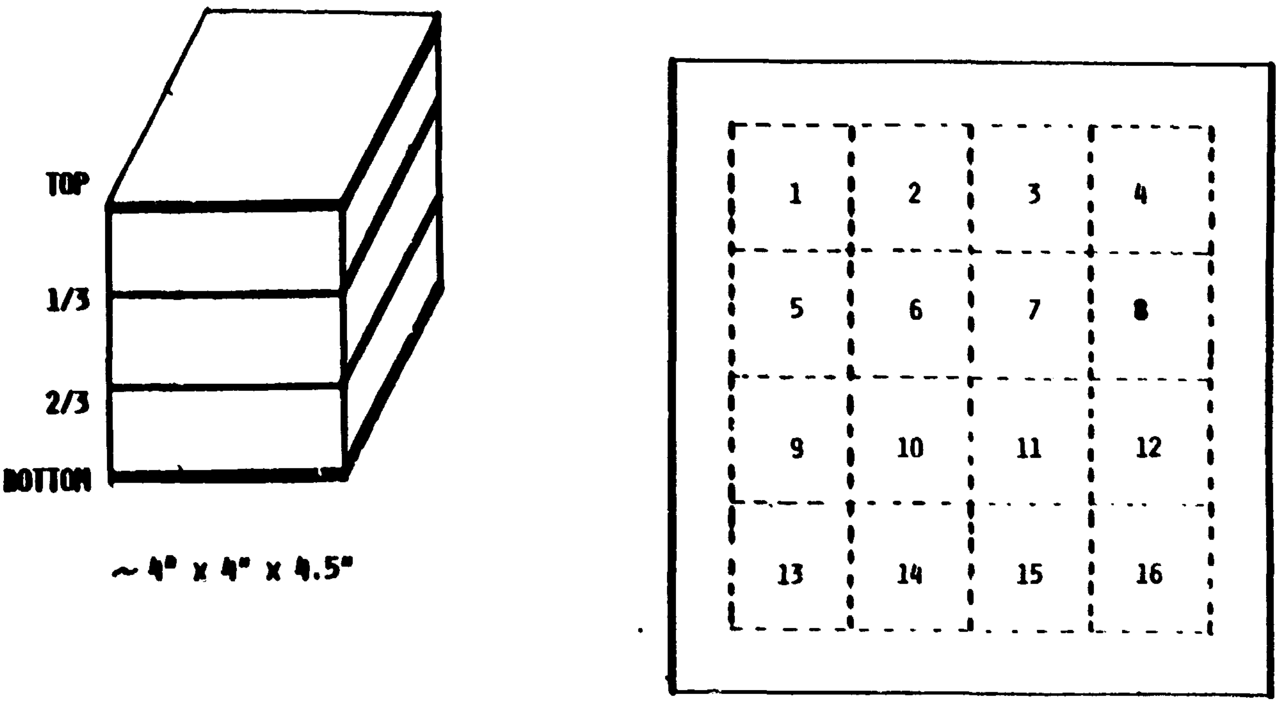

THE CELL'S # AND THEIR RELATIONS TO THE ORIENTATION OF THE QUARTER INGOT ARE MARKED

ORIGINAL PAGE IS
OF POOR QUALITY

Average Efficiency of Different Layers of Ingot 5840-13C

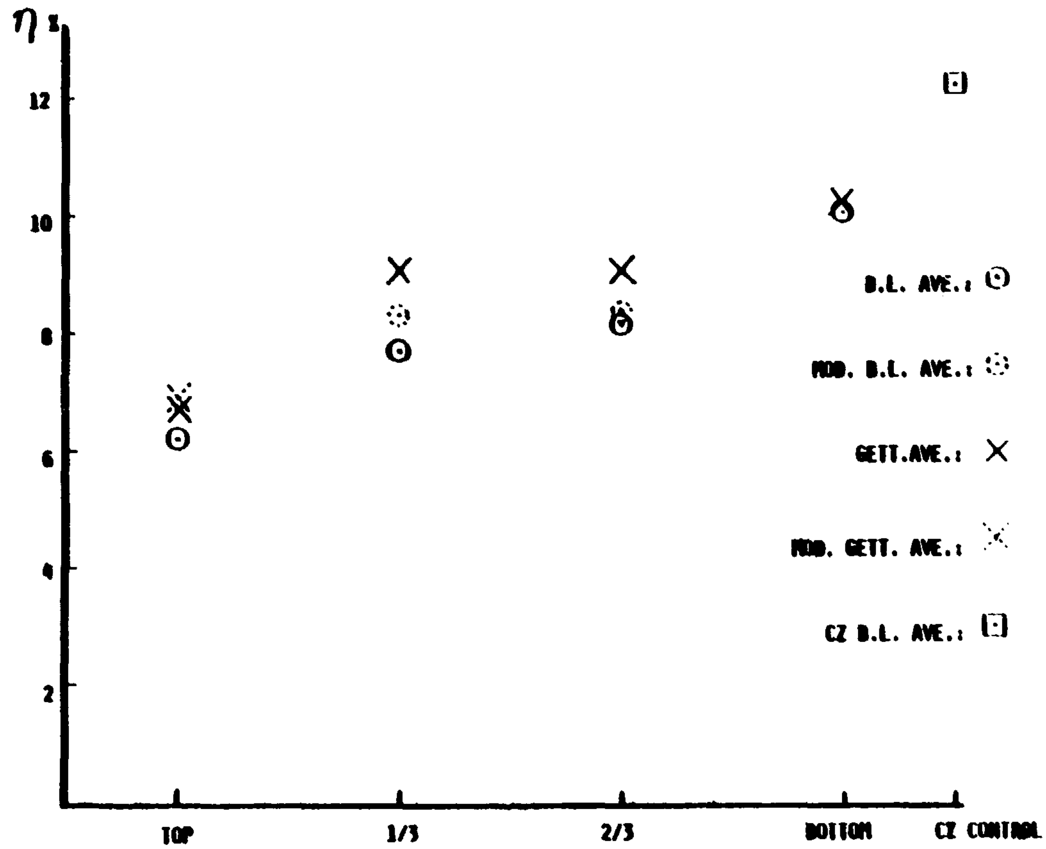

Summary of SJ, BSF and MLAR Cells From UCP Ingot 5848-13C

		Voc (mV)	Jsc (mA/cm^2)	CFF (%)	η (%)
Evaporated Al BSF (UCP - 12 Cells)	A.V.	561	28.7	76	12.2
	S.D.	6	0.6	4	0.8
	RANGE	550-570	27.4-29.4	62-79	9.9-13.1
CZ Control (3 Cells)	A.V.	593	32.6	78	15.1
	S.D.	1	0.2	1	0.2
	RANGE	592-594	32.4-32.8	77-79	14.9-15.3

Average J_{SC} of Different Layers, Ingot 5848-18C

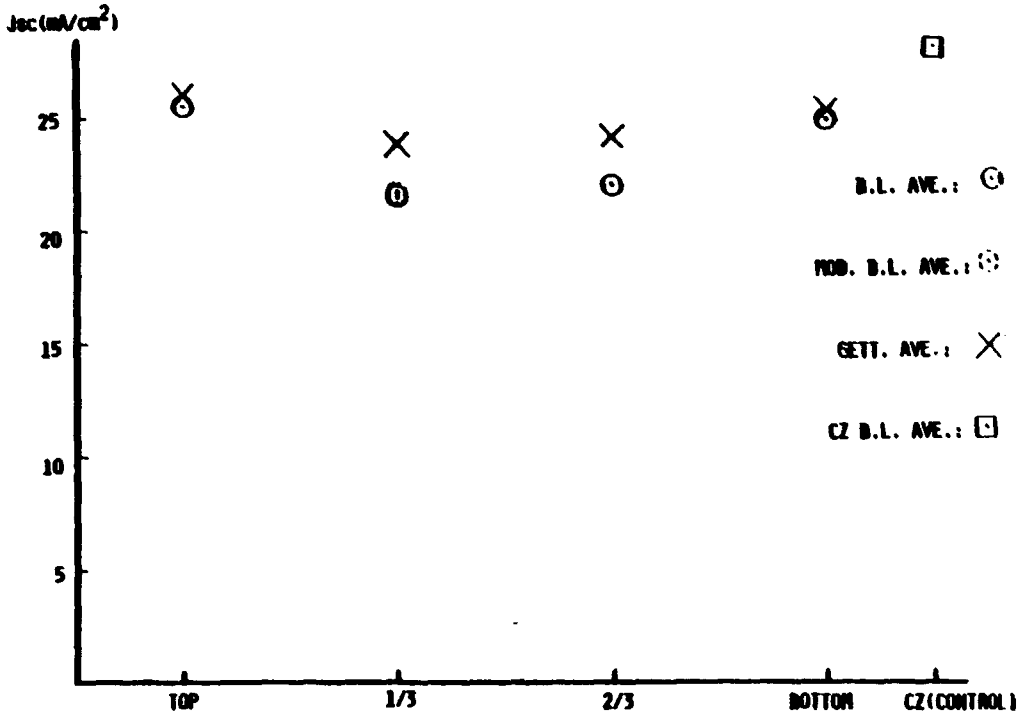

Summary of J_{SC} From Cells From More Severe Gettering Tests (UCP Ingot No. 5848-13C)

Gettering Treatment	Wafer	Ave. Jsc (mA/cm^2)	Jsc* of The Cell Covered With SiO_2
None	1/3	22.5	-
	2/3	23.7	-
875°C ½ Hr.	1/3	24.6	24.7
	2/3	24.3	24.8
875°C 1 Hr.	1/3	25.5	25.2
	2/3	26.3	24.4
950°C 1 Hr.	1/3	27.0	24.8
	2/3	26.3	25.9
CZ Control (No Treatment)		28.5	-
1050°C 1 Hr.	1/3	26.2	25.9
CZ Control (No Treatment)		28.2	-

*Jsc of the cell covered with CVD SiO_2 during gettering diffusion.

Results of Light-Bias Minority Carrier Diffusion Length Study on Getter

PROCESS	CELLS #	L_{D1} (μm) D.C. DARK	L_{D2} (μm) 0.05 SUN	L_{D3} (μm) 1 SUN	L_{D4} (μm) DARK AFTER LIGHT TURN OFF
BASELINE	2-1	11	16	17	12
8.75°C 1/2 Hr GETTERING	2-4 2-8*	29 29	44 40	60	30
875°C 1 HR GETTERING	2-13 2-9*	159 100	65 60	72	140
950°C 1 HR GETTERING	2-12 2-15*	182 107	89 49	72	167
1050°C 1 HR GETTERING	2-12 2-9*	212 135	116 62	69 81	244 117
CZ CONTROL	1	150	152	156	137

* CELLS WERE COVERED WITH SiO_2 DURING GETTERING DIFFUSION.

Summary of Results From 10 x 10 UCP Cells From Random Sources

	Voc (mV)	Jsc (mA/cm²)	CFF (%)	(%)
AVE.	553	26.9	72	10.8
S.D.	6	.9	1	.5
RANGE	546-558	25.2-27.6	72-74	10.0-11.3

AREA = 98 cm²   NO. OF CELLS = 6

Comparison of J_{sc} From HEM Cells Gettered for 1 h at 1050°C With HEM Baseline Cell From Corresponding Area

INGOT #	BASELINE Jsc	GETTER Jsc
41-41C	25.6	26.3
41-48	27.6	28.1